



UvA-DARE (Digital Academic Repository)

A Review on Melt-Spun Biodegradable Fibers

Naeimirad, M.; Krins, B.; Gruter, G.-J.M.

DOI

[10.3390/su151914474](https://doi.org/10.3390/su151914474)

Publication date

2023

Document Version

Final published version

Published in

Sustainability (Switzerland)

License

CC BY

[Link to publication](#)

Citation for published version (APA):

Naeimirad, M., Krins, B., & Gruter, G.-JM. (2023). A Review on Melt-Spun Biodegradable Fibers. *Sustainability (Switzerland)*, 15(19), Article 14474. <https://doi.org/10.3390/su151914474>

General rights

It is not permitted to download or to forward/distribute the text or part of it without the consent of the author(s) and/or copyright holder(s), other than for strictly personal, individual use, unless the work is under an open content license (like Creative Commons).

Disclaimer/Complaints regulations

If you believe that digital publication of certain material infringes any of your rights or (privacy) interests, please let the Library know, stating your reasons. In case of a legitimate complaint, the Library will make the material inaccessible and/or remove it from the website. Please Ask the Library: <https://uba.uva.nl/en/contact>, or a letter to: Library of the University of Amsterdam, Secretariat, Singel 425, 1012 WP Amsterdam, The Netherlands. You will be contacted as soon as possible.

Review

A Review on Melt-Spun Biodegradable Fibers

Mohammadreza Naeimirad ^{1,2,*} , Bas Krins ¹ and Gert-Jan M. Gruter ^{2,3} 

¹ Senbis Polymer Innovations B.V., Eerste Bokslootweg 17, 7821 AT Emmen, The Netherlands; b.krins@senbis.com

² Industrial Sustainable Chemistry, Universiteit van Amsterdam, Science Park 904, 1098 XH Amsterdam, The Netherlands; g.j.m.gruter@uva.nl

³ Avantium N.V., Zekeringstraat 29, 1014 BV Amsterdam, The Netherlands

* Correspondence: m.naeimirad@senbis.com

Abstract: The growing awareness of environmental issues and the pursuit of sustainable materials have sparked a substantial surge in research focused on biodegradable materials, including fibers. Within a spectrum of fabrication techniques, melt-spinning has emerged as an eco-friendly and scalable method for making fibers from biodegradable plastics (preferably bio-based), intended for various applications. This paper provides a comprehensive overview of the advancements in the realm of melt-spun biodegradable fibers. It delves into global concerns related to micro- and nanoplastics (MNPs) and introduces the concept of biodegradable fibers. The literature review on melt-spun biodegradable monofilaments and multifilaments unveils a diverse range of polymers and copolymers that have been subjected to testing and characterization for their processing capabilities and the performance of the resultant fibers, particularly from mechanical, thermal, and biodegradation perspectives. The paper discusses the impact of different factors such as polymer structure, processing parameters, and environmental conditions on the ultimate properties, encompassing spinnability, mechanical and thermal performance, and biodegradation, with schematic correlations provided. Additionally, the manuscript touches upon applications in sectors such as clothing, technical textiles, agriculture, biomedical applications, and environmental remediation. It also spotlights the challenges encountered in the commercialization of these fibers, addresses potential solutions, and outlines future prospects. Finally, by shedding light on the latest developments, challenges, and opportunities in the field, this review endeavors to stimulate further innovation and adoption of biodegradable fibers. It seeks to unlock their potential and contribute to the realization of a more environmentally conscious society.

Keywords: bio-based polymers; fiber melt-spinning; microplastics; biodegradation; sustainability; mechanical properties



Citation: Naeimirad, M.; Krins, B.; Gruter, G.-J.M. A Review on Melt-Spun Biodegradable Fibers. *Sustainability* **2023**, *15*, 14474. <https://doi.org/10.3390/su151914474>

Academic Editor: Kavita Mathur

Received: 20 August 2023

Revised: 25 September 2023

Accepted: 29 September 2023

Published: 4 October 2023



Copyright: © 2023 by the authors. Licensee MDPI, Basel, Switzerland. This article is an open access article distributed under the terms and conditions of the Creative Commons Attribution (CC BY) license (<https://creativecommons.org/licenses/by/4.0/>).

1. Introduction

Nowadays, plastic products have become an indispensable part of our daily lives, possessing a wide range of properties that vary from flexibility to rigidity, permeability to impermeability, and hydrophilicity to hydrophobicity. These properties are determined by the composition of the polymer's repeating units, commonly referred to as the chemical backbone. Plastics play a crucial role in promoting sustainability on various fronts. For instance, the utilization of lightweight plastic materials enhances fuel efficiency in automobiles and aircraft; plastic insulators contribute to energy conservation; and plastic food packaging extends the shelf-life of products, thereby reducing food waste [1]. The remarkable success and continuous expansion of the plastic industry can be attributed to its affordability, durability, favorable strength-to-weight ratios, and the convenience it brings to our everyday lives [2]. Moreover, the plastic industry serves as a significant source of employment, with over 1.6 million individuals employed within the sector across the European Union, resulting in a turnover of 360 billion Euros in 2018 [3]. However,

the extensive production and accumulation of plastics have led to severe environmental issues. The annual global production of plastic exceeds 380 million tons (excluding 110 million tons of fibers and also thermoset resins and rubbers), increasing at a rate of 4% each year [4]. Consequently, between 1950 and 2015, a staggering 6300 million tons of plastic waste were generated [5]. This implies that the production of 500 million tons of plastics is obtained from approximately 4–8% of global oil consumption—1000 million tons of oil (500 million tons of C/H in the product and 500 million tons of energy required for the production) [6]. In 2050, this will be threefold, and plastic production will go over 1 billion tons [7,8]. Presently, it is estimated that a minimum of eight million tons of plastic find their way into the ocean annually [9]. In 2010 alone, between 4.6 and 12.7 million tons of plastic waste produced by 192 coastal countries ended up in the ocean, with single-use plastics constituting half of the marine pollutants found on beaches [10]. According to the European Commission, approximately 1.5–4% of the total global plastic production enters the ocean every year [9]. Furthermore, a significant portion of plastic waste, approximately 79%, has not undergone recycling, resulting in an alarming volume of discarded plastic [5]. While these sustainable routes are still under consideration for social acceptance [11], shockingly, an estimated 31.9 million metric tons of plastic products make their way into the total environment annually [12].

Various end-of-life scenarios exist for plastic materials, including mechanical recycling [13], chemical recycling (hydrolysis, glycolysis, methanolysis, thermolysis, and pyrolysis) [14], biological recycling [15], composting, biodegradation, incineration (accounting for 40% in the EU), and landfilling (representing 27% in the EU) [3]. However, landfilling and incineration of conventional plastics present several environmental concerns [16]. Incineration, while reducing the need for landfilling and enabling energy recovery, must comply with environmental regulations outlined in the EU Hazardous Waste Incineration Directive 2000/76/EC [17]. In Europe, for instance, approximately 25.8 million tons of post-consumer plastic waste are generated annually, with 30% being recycled and 40% destined for incineration [18]. Plastic products can contribute to litter, leading to the release of micro- and nanoplastics (MNPs) [19–21] into the oceans and aquaculture [22], then posing potential risks to human health when they enter the lungs [23] or bloodstream [24]. Additionally, plastics contribute to climate change by emitting greenhouse gases (GHGs) during the extraction and processing of fossil resources. As mentioned, plastic production alone consumes approximately 5–7% of the global oil supply and emitted over 850 million tons of CO₂ in 2019. However, tripling global plastic production by 2050 will result in more than 50% contribution to greenhouse gas emissions (GHGe) if oil-based feedstock is still the major portion [25]. Addressing these challenges has become a priority for major global entities, including the United Nations Environment Assembly Programme (UNEA-5.2) [20], particularly for action against microplastics in oceans [26], the World Economic Forum (WEF) [27], the World Health Organization, and the European Union (EU) [18,28]. Meanwhile, the European Bioplastics Association is releasing statistical data about bio-based and biodegradable polymers every year [29].

Arikan and Özsoy [30] highlighted several environmental and economic issues resulting from the widespread use of plastics, such as landfill problems, plastic accumulation in oceans, incineration, non-degradability, durability, and economic concerns related to crude oil competition and energy security. Therefore, it is crucial to minimize the environmental impacts of plastics by transitioning to circular and sustainable plastic systems [31]. Spierling et al. [32] suggested that shifting around 66% (approximately 220 million tons based on 2017 estimates) of plastic production to bio-based materials could potentially save 241–316 million tons of CO₂-equivalents annually. Consequently, the development of bio-based and biodegradable plastics has emerged as a topic of interest for creating future materials capable of replacing conventional plastics in various sustainable applications. Meanwhile, the circular economy approach, including chemical and mechanical recycling of thermoplastic bio-based polymers, also deserves attention. Different sectors within the plastics industry, including the fiber and textile sectors, are striving to embrace this green

transition. It is good to know that bio-based and biodegradable textiles have a long history as cellulosic (cotton) and protein (wool) fibers [33].

Historically, non-fiber plastics have been dominated by polyethylene (PE; 36.4%), polypropylene (PP; 21%), and polyvinyl chloride (PVC; 12%) since 1950. In contrast, the fiber market is largely dominated by polyethylene terephthalate (PET; 60%). In 2015, the largest plastic volumes in global commercial sectors were in packaging (35.9%), construction (16.0%), textiles (14.5%), and consumer goods (10.3%) [5]. Furthermore, global fiber production reached 111 million metric tons, having doubled over the past 20 years [34]. Figure 1 illustrates the distribution of plastics in the different sectors and their respective plastic waste management approaches thus far.

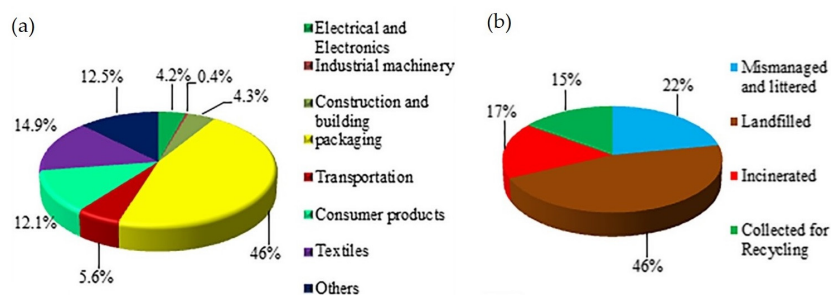


Figure 1. (a) Plastic consumption in various sectors; and (b) Plastic waste management in the world [35]. Reprinted with permission from the publisher.

The aforementioned pie charts show that textiles account for 14.9% of global plastic production, with a significant portion of PET (70% of 80 million tons produced annually) being used for fiber and yarn production. However, only 15% of plastic products are collected for recycling. The small size and high aspect ratio of single fibers released from textiles, including microplastics and microfibers, make them particularly hazardous. Detecting and efficiently collecting these microplastics, especially microfibers, from the oceans is not possible. Floating microplastics in coastal areas can reach counts of 103 to 104 per m^3 . This lack of efficient removal methods is concerning because these floating microplastics accumulate pollutants and transport them through ocean currents. Persistent organic pollutants (POPs) bind to the surface of plastic debris in the marine environment [36]. Systematic studies [37–40] indicate that microfibers released from textiles, particularly polyester (PET), pose a significant concern. The release of microfibers during washing can range from 210 to 72,000 microplastic fibers per gram of textile, with median fiber lengths ranging from 165 to 841 μm . So far, more than 20,000 fibers per day were carried downstream by the river, while up to 213,200 fibers per square kilometer were detected drifting on the ocean's surface [41]. These microfibers contribute to marine contamination, often referred to as “plastic soup” with press releases highlighting their contribution of about 35% reported by Statista [42], Reuters [43], The Guardian [44], the European Environment Agency [45,46], and elsewhere [22,47–49]. Meanwhile, shedding from face masks has become a big source of microfibers, particularly during the COVID-19 period [50]. Artificial turfs are also mentioned as a source of fibrous microplastics [41]. Although a green transition via bio-based plastics or renewable materials may reduce greenhouse gas emissions (GHGe) [21], whose quantification will require Life Cycle Assessment (LCA) [51], the microplastic problems still remain challenging. The global crisis in terms of plastic littering will furthermore force a transition towards materials that will not linger in nature but will degrade over time in case they inadvertently end up in nature [52,53]. Biodegradation of fibrous products is under consideration for making more sustainable clothing and textiles, which is reviewed elsewhere [34,54,55]. Here it was suggested that the raw materials for textiles should be made renewable or easily recyclable with little or no concern for the environment, and later on it was concluded that concerns about untraceable fiber plastics can be solved by using biodegradable fibers, which is in line with the statement by the Narayan group for intro-

ducing biodegradable plastics as a solution for environmental pollution by conventional plastics, either non-degradable or renewable [56].

Polylactic acid (PLA), polyhydroxyalkanoates (PHAs), thermoplastic starch (TPS), polybutylene adipate terephthalate (PBAT), polybutylene succinate (PBS), and polycaprolactone (PCL) are typically considered biodegradable thermoplastics that are produced on an industrial scale [7]. However, their commodity applications are limited by their poor physical properties and a low glass transition temperature (T_g) and melting temperature (T_m)—for the majority of biodegradable polymers with lower crystallinity—for the replacement of fossil-based counterparts, such as PET.

All in all, bio-based alternatives to petroleum-derived polymers can mitigate climate change, while biodegradable polymers are needed to tackle the issues caused by their extensive use and improper disposal [57]. The textile industry has also embraced the adoption of bio-based and biodegradable polymers, with the textile market projected to grow at a CAGR of 12% over the next decade [31]. The clothing sector is expected to play a dominant role in this market. Therefore, biodegradable plastics are the best option when the product or litter is unintentionally fate-in-nature. Aerobic or anaerobic digestion and composting are the routes of final utilization [58].

Numerous review articles have been published about bio-based and biodegradable polymers [7,30,59–66], making biocomposites [31,67,68], fibrous products [54,69–71] biomedical applications [69,70,72], and their biodegradation [63,73]. Rosenboom et al. [1] from the Langer group reviewed the advantages and challenges of bio-based plastics in transitioning towards a circular economy, emphasizing the lower carbon footprint and favorable material properties of bio-based plastics compared to fossil-based plastics. They also highlighted the importance of essential regulations and financial incentives to scale up bio-based and biodegradable plastics from niche polymers to large-scale market applications with a truly sustainable impact. In another recent review, Motlounq et al. [31] provided a general overview of biodegradable polymers, including fibers, with a focus on processing and mechanical properties. However, this review had limited coverage of biodegradation in various environments and other applications. Patti et al. [40] reviewed bio-based and biodegradable alternatives in the textile value chain to tackle GHGe and microplastic problems, respectively. There is still much room for extensive research on biodegradation and other applications of biodegradable polymers.

Meanwhile, melt-spinning is a widely used, sustainable, and cost-effective method for producing man-made fibers and filament yarns from thermoplastic polymers. The process (Figure 2) involves feeding polymer pellets or chips into a single screw extruder, where they are melted and pressurized. In some cases, masterbatches can be added through a side extruder for specific applications such as dope-dyed yarns [54,74]. A melt pump ensures a consistent throughput rate. The spin pack, which includes polymer filtering and distribution components as well as the spinneret, is responsible for forming the filaments with the desired characteristics such as number and cross-section. It is crucial to design the extrusion and spinning lines in a way that prevents melt stagnation, which can lead to polymer degradation and intermittent discharge. After leaving the spinneret, the extruded strands are either directed into a quenching chamber or a water bath to solidify. The filaments undergo cooling and are then subjected to drawing to induce or enhance crystallinity, either online or offline, using several godets (cold or hot). Heating the godets or guiding the filaments over hot plates or through stretching ovens can enhance their drawability. Finally, the filaments are wound onto bobbins using a winder or collected to be cut into staple fibers [54].

Melt-spinning is considered more economical and sustainable compared to other spinning methods such as dry-spinning and wet-spinning. Dry-spinning and wet-spinning have lower production speeds and involve the use of chemical solvents, which are not environmentally friendly [75]. Moreover, these methods can result in surface pores and voids. Therefore, melt-spun fibers have significant potential to replace conventional fiber in various applications where biodegradability is important [31].

The physiochemical properties of synthesized biodegradable polymers and their effect on biodegradation are areas of ongoing investigation. Considering the influence of processing parameters on the structure and performance of man-made fibers, along with the end-of-life environment affecting biodegradation routes and rates, designing biodegradable polymers becomes a challenge. Optimizing both physiochemical properties and biodegradability is crucial. A deeper understanding of the relationship between polymer structure and biodegradation will aid in the development of new biodegradable polymers and end products by modifying relevant processing-related properties. This concept contributes to a better comprehension of the polymer's structure-property relationship [76–78].

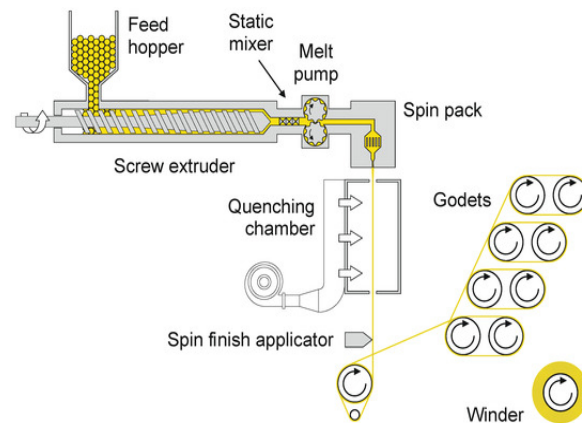


Figure 2. Sketch of a conventional melt-spinning-drawing-winding (SDW) pilot line [54]. Reprinted with permission.

To the best of our knowledge, while biodegradable polymers (particularly bio-based) are a hot topic among researchers and Non-Governmental Organizations (NGOs) aiming for a sustainable world, and the current state of biodegradable fibers presents an exciting opportunity for both the scientific community and public society, there is currently no comprehensive review specifically focusing on recent developments in man-made biodegradable fibers produced through melt-spinning. Previous reviews, such as the one by Mochizuki et al. [79] on biodegradable thermoplastic polymers and fibers, date back to 1995. Therefore, this article aims to provide a review of the recent advances in melt-spun biodegradable fibers to contribute to global sustainability goals and inspire further research and innovation in the field of biodegradable fibers and sustainable textile products (Figure 3).

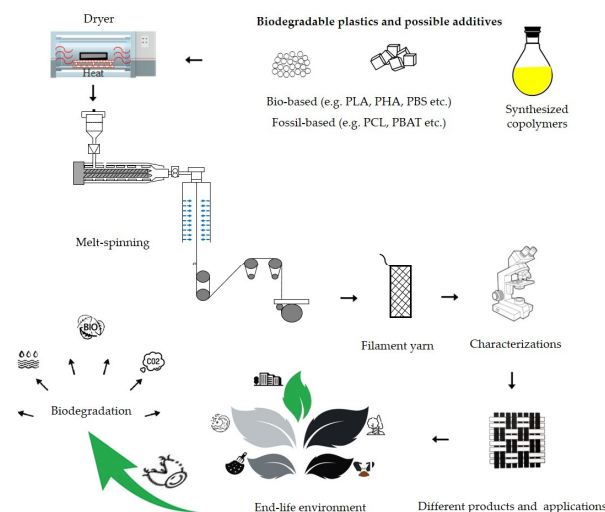


Figure 3. Schematic overview on melt-spun biodegradable fibers.

2. Bio-Based and Biodegradable Plastics

The demand for bio-based polymers and their use in more sustainable products, including fibers and textiles, is driven by both market demand and legislative intentions. When considering sustainability, two main subsectors are relevant: bio-based polymers and biodegradable polymers (some polymers can be both). Bio-based polymers are derived from natural resources such as starch (e.g., thermoplastic starch) or cellulose (e.g., cellulose acetate) and polyhydroxyalkanoates (PHAs) or can be produced from bio-based monomers (e.g., bio-PE, PLA, PBS, PBAT, etc.), while biodegradable polymers are designed to naturally break down and be utilized in the environment through biotic or abiotic processes, regardless of whether they are derived from synthetic or biomass feedstock [53,80].

Currently, the production of bio-based and biodegradable plastics is around 2.2 million tons per year, and its expansion is considered part of future circular economies, aligning with the United Nations' Sustainable Development Goals and EU legislation [81]. These initiatives aim to shift away from fossil resources, introduce new recycling or degradation pathways, and reduce the use of toxic reagents and solvents in production processes. However, it should be noted that bio-based plastics are not automatically more sustainable than fossil-based plastics. While using renewable resources can help reduce carbon emissions, other factors throughout the life cycle can influence the overall sustainability of the materials [1,53]. The Langer group has identified five main challenges in the implementation of bio-based plastics, known as the "5Es": Economics, Efficiency, End-of-life, Education, and Ethics. However, depending on the type of bio-based plastics, they can offer improved circularity by utilizing renewable (non-fossil) resources, reducing carbon footprints, providing biodegradability as an alternative end-of-life option, and offering improved material properties [1].

The specific physicochemical, biological, and degradation properties of biodegradable polymers make them attractive for various applications, including fibers and textiles [7]. As environmental concerns related to plastic accumulation and landfill waste continue to grow, extensive research is being conducted to find possible solutions. These polymers can be classified into two main categories based on whether their starting materials are derived from petroleum or non-petroleum sources. Moreover, recent advances in polymer synthesis enable the production of polymers with diverse characteristics. Among petroleum-based biodegradable polymers, particular attention has been given to aliphatic/aromatic copolymers that combine the biodegradability of aliphatic units with the beneficial physical properties of aromatic units [82].

According to Figure 4, there are various examples of biodegradable polymers, regardless of whether they are derived from fossil or bio-based sources (considering composting as a human-driven process for utilization). For instance, polylactic acid (PLA) is only compostable, while polyhydroxyalkanoates (PHAs), plasticized thermoplastic starch (TPS), polybutylene succinate (PBS), polycaprolactone (PCL), and polyglycolic acid (PGA) are biodegradable. Meanwhile, polyurethanes are generally less biodegradable due to the strength of the urethane bonds. However, fungi and certain soil bacteria can assist in hydrolyzing the ester groups within polyester-containing polyurethane [83]. Additionally, less degradable monomers such as terephthalates can be made more degradable through copolymerization with more hydrolysable, hydrophilic, and less crystalline co-polymers, as observed in poly(butylene-*co*-adipate terephthalate) (PBAT) [84]. The subsequent sections will discuss other biodegradable copolymers, including poly(lactic-*co*-glycolic acid) (PLGA), poly(butylene succinate-*co*-butylene adipate) (PBSA), poly(butylene succinate-*co*-terephthalate) (PBST), polybutylene-*co*-ethylene succinate-*co*-adipate (PBEAS), poly(butylene terephthalate-*co*-succinate-*co*-adipate) (PBTSA), and poly(isosorbide-*co*-hexylene) oxalate polyester (PIHO).

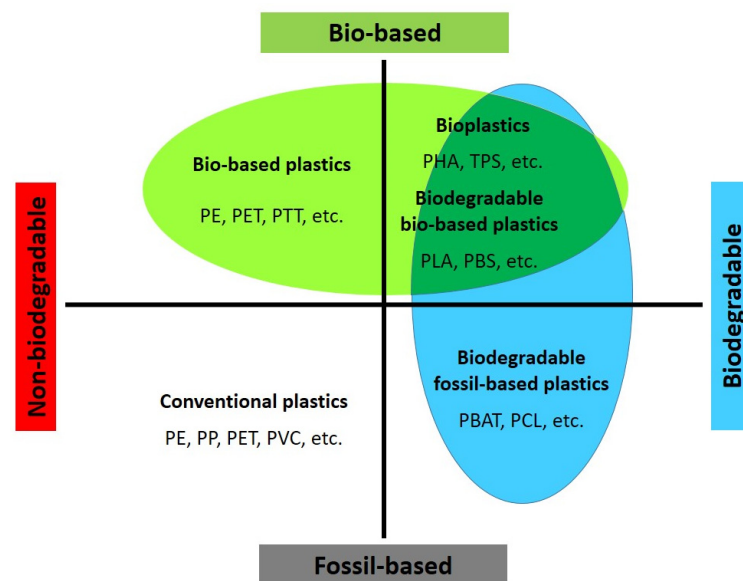


Figure 4. Classification of different plastics. Adapted from [6,64,80].

2.1. Biodegradable Thermoplastic Polymers

2.1.1. PLA

PLA (polylactic acid) is an aliphatic polyester and one of the most competitively priced bio-based plastics, with a production capacity exceeding 250,000 tons per year. It is typically produced through the ring-opening polymerization of lactide (the cyclic dimer of lactic acid). PLAs can be made from monomers with two isomers of lactic acid (L-lactic acid) or (D-lactic acid) which will result in PLLA, PDLA, or a copolymer (PLDLA). In general, D-content will reduce crystallinity. Table 1 provides a summary of its chemical structure and general properties. Although PLA can exhibit optical clarity and has been used as a substitute for polyolefin films and polystyrene foams, including in single-use items, it tends to be brittle and slow to crystallize. Therefore, modifications and blending with other bio-based/biodegradable polymers or the use of nucleation agents are often necessary [85].

PLA has high crystallinity, which contributes to its favorable properties for various applications. However, it is only compostable within 6 months at temperatures higher than its T_g , typically at around 58 °C in industrial composting conditions. At ambient temperature, PLA degrades very slowly in soil and water, with estimates suggesting that complete degradation could take several years depending on the environment [86,87].

Since its industrial production began in the 1990s, PLA has gradually gained popularity as a commodity thermoplastic, expanding into more diverse applications, including the textile sector, due to its significant drop in price [88]. Consequently, PLA has become the most common bio-based and biodegradable (compostable) material used for melt-spun bio-based polymer fibers. Its high crystallinity, better mechanical properties, and lower thermal degradation compared to other biodegradable polymers make it suitable for numerous applications. Melt-spinning of PLA fibers has been employed for a long time, with take-up speeds reaching up to 5000 m/min [89]. It is considered the most promising sustainable and biodegradable fiber to replace PET in textile products [75]. The development of PLA fiber structure during the melt-spinning process is presented in a chapter by Roungpaisan et al. [90].

When PLA polymer is hydrolyzed to a molecular weight (MW) below 10,000 Mn, it can be broken down by bacteria and fungi into carbon dioxide and water. Hydrolysis is a time-consuming process that can be accelerated by high temperatures, such as those found in industrial composting. Teijin Frontier has recently introduced a biodegradation accelerator to expedite hydrolysis, leading to faster degradation in oceans, rivers, and soil [91]. Thanks to large-scale manufacturers such as TotalEnergiesCorbion (Luminy®) and NatureWorks (Ingeo™), PLA remains the most promising bio-based and biodegradable

(compostable) polymer for textile applications. For more information on PLA production and its application in fibers and textiles, further reviews can be found elsewhere [75,92].

2.1.2. PHAs

PHAs (polyhydroxyalkanoates) are a family of emerging biodegradable aliphatic polyesters with a projected annual market volume of over 100,000 tons in the near future. PHA production can be accomplished through the process of microbial fermentation using bacterial strains [93], such as *Pseudomonas* and *Ralstonia*, as well as algae. Subsequent extraction of PHAs is performed to isolate the polymer. These microorganisms possess the remarkable ability to store PHA within their cells, reaching levels of up to 80% of their cell volume. A key advantage of the biological PHA production process is its ability to utilize diverse carbon-rich feedstocks, including low-cost food residues and liquefied plastic waste, thereby enhancing circularity [7]. PHAs, composed of (R)-3-hydroxyalkanoic acids, are a class of non-toxic, biodegradable, and biocompatible polyesters that closely resemble petrochemical plastics in their thermoplastic properties [25,94]. The physical characteristics of PHAs vary due to the diverse compositions of their monomers, enabling them to cater to a wide range of applications. Based on the length of the PHA monomer's carbon chain, PHAs are classified as short-chain length (scl) PHAs (consisting of 4 or 5 carbons) or medium-chain length (mcl) PHAs (consisting of 6–14 carbons). The properties of PHAs, such as degree of crystallinity, T_m , and T_g , heavily rely on the monomer composition, which, in turn, is influenced by factors such as the organism, growth conditions, and polymer extraction method. While sclPHA exhibits properties closer to conventional plastics such as polypropylene, mclPHA displays more elastomeric properties [7]. Poly-3-hydroxybutyrate (PHB) is the most extensively studied PHA polymer, characterized by its brittle and highly crystalline nature akin to polypropylene. However, to tailor the thermal and mechanical properties of PHAs, copolymerization is often employed [80,95]. For instance, the copolymer poly-3-hydroxybutyrate-co-3-hydroxyvalerate (PHBV) is more desirable than the PHB homopolymer due to its lower melting temperature, reduced crystallinity, and improved processability [80,96,97]. Thus, by adjusting the chain length of the repeat unit, introducing side chain functionalities, and varying the comonomer composition, the material properties of PHAs can be finely tuned to yield co-polymers with diverse characteristics. These range from rigid and brittle poly(3-hydroxybutyrate) (PHB) to softer and more flexible poly(3-hydroxybutyrate-co-3-hydroxyhexanoate) (PHBH) [7]. Among the most promising PHAs, polyhydroxybutyrates (PHBs) have gained widespread recognition and demonstrate significant potential for replacing conventional plastics [36]. PHAs possess appealing properties that make them suitable as a source material for bio-based plastics, either as direct replacements for petroleum-derived plastics or as blends with some other polymers. In addition to their application in the textile industry, PHAs also exhibit favorable barrier properties that make them suitable for replacing bulk packaging materials such as PE and PP [94].

The biodegradation efficiency of PHAs and their biological resources make them highly valuable for replacing traditional plastics [98]. In the marine environment, PHAs were found to biodegrade at an average rate of 0.04–0.09 mg/day/cm², suggesting that it would take approximately 1.5 to 3.5 years for a PHA water bottle to be completely decomposed [99].

The mechanical properties of PHAs are influenced by factors such as MW, side chain length, monomer type, and ratio. The interaction of these variables can affect the T_g and T_m , as well as the crystallinity (stiffness/flexibility) of the polymers [96]. PHBs, for example, exhibit instability near their melting point of 160–180 °C, with a T_g of 0–5 °C. Thermal degradation occurs around 170 °C, leading to reduced molecular weight [100]. The mechanical properties of specific PHA polymers are influenced by the metabolic pathways, enzymes of the bacterial strain, and substrate utilization [70]. The superior biocompatibility and biodegradability of PHAs compared to synthetic biodegradable polymers make them highly promising for various fiber applications, particularly in biomedicine [69,70].

However, purification, high cost, limited mechanical performance, and thermal instability, resulting in molecular weight reduction and a limited processing window, remain significant barriers for PHAs. Consequently, the complex crystallization behavior of PHAs, their thermal instability, and the associated challenges in spinning procedures continue to be areas of active research [70]. Further information on PHAs, such as capable microorganisms for fermentation, carbon feedstock substrates, PHA accumulation rates, chemical structures, polymer properties, and applications, is reviewed elsewhere [36], including their industrialization opportunities [101], and application in the medical sector [70].

Currently, PHAs hold a small market share (due to their costly production, purification steps, low processability, and thermal degradation), with a production volume of 25,200 tons in 2019, accounting for 1.2% of the overall bio-based plastic market and representing a 1.7-fold decrease compared to the previous year [7]. However, they have an increasing demand outlook. Known manufacturers of PHAs include Biomer, Kaneka, Danimer, Tianan, BluePHA, CJ CheilJedang, Mango Materials, Newlight, Paques Biomaterials, and Mitsubishi, while more industrializations are elaborated by GO!PHA and ARENA elsewhere [101].

2.1.3. TPS

TPS (thermoplastic plasticized starch) is a biodegradable polymer derived from starch, which is typically sourced from corn, potatoes, or other plant materials. It has emerged as an environmentally friendly alternative to petroleum-based plastics. However, when it comes to melt-spinning, TPS faces certain challenges. One significant limitation is its relatively low melt strength and poor processability at high temperatures. TPS tends to degrade and undergo thermal decomposition before it can be effectively melt-spun into fibers. Its narrow processing window and propensity for viscosity reduction and chain scission during melt processing can result in suboptimal mechanical properties and limited control over fiber diameter and properties. Although, with an optimal ratio of the components (amylose and amylopectin), the processability can be improved to some extent, multifilament yarn melt-spinning is far from being achieved. To address these limitations, various approaches have been explored, such as incorporating additives or other polymers into TPS or modifying the starch structure [102], to enhance its melt-spinnability and performance in fiber production [103–105].

TPS is produced on a large scale worldwide, and companies such as Novamont, Roquette, and Polyscope Polymers are among the manufacturers of this product.

2.1.4. PBS

PBS (polybutylene succinate) is an aliphatic copolyester with longer hydrocarbon repeat units, resulting in a more flexible molecular structure compared to PLA. This gives PBS distinct material properties, such as a low T_g and high elongation at break (>500%), making it more similar to polyolefins. While PBS is typically synthesized from non-renewable feedstock, it can also be produced from renewable sources, resulting in Bio-PBS. For instance, succinic acid, one of the monomers used in PBS production, can be obtained through the fermentation of sugars, while butanediol can be obtained by succinic acid hydrogenation [106] or derived from hydrocracking starches and sugars [107]. Studies have shown that PBS particles can undergo significant mineralization (over 90%) within 200 days under industrial composting conditions. However, limited mineralization was observed in a 6-month incubation at 25 °C [108,109]. One challenge of using PBS in textile applications is its sub-zero glass transition temperature and low melting point. More information about PBS can be found elsewhere [110].

The industrial production of PBS, including bio-based PBS derived from sugarcane, cassava, and corn, has been in progress since 2017, reflecting the shift towards sustainable, bio-based, and biodegradable plastic alternatives. Mitsubishi Chemical Corporation and Dongguan Green Earth Plastics are among the manufacturers of PBS.

2.1.5. PCL

PCL (polycaprolactone) is an aliphatic polyester of synthetic origin that has gained considerable attention in recent times. It is produced by ring-opening polymerization of ϵ -caprolactone, a cyclic monomer. Catalysts such as stannous octoate are utilized to initiate the polymerization process, and low-molecular-weight alcohols can be employed to control the polymer's molecular weight. The resulting molecular weight, molecular weight distribution, end group composition, and chemical structure of PCL copolymers can be influenced by various mechanisms such as anionic, cationic, coordination, and radical polymerization. The average molecular weight of PCL samples typically falls within the range of 3000 to 100,000 g/mol, and classification based on molecular weight is common practice. PCL exhibits semi-crystalline characteristics, with a melting point ranging from 59 to 64 °C and a T_g of -60 °C. What makes PCL highly versatile is its ease of modification in terms of physical, chemical, and mechanical properties. This can be achieved through copolymerization or blending with other polymers [111]. Numerous research groups have conducted investigations on the melt-spinning of PCL fibers, employing various processing conditions [112–116].

PCL is biodegradable under anaerobic conditions, although at a slower rate compared to PHA [117]. It is worth noting that PCL has a very low melting point. However, it is widely utilized in medical applications, such as sutures, under the trade name Monocryl™. Companies such as Perstorp and Daicel offer PCL in their product portfolios, marketed under the commercial names Capa®, and Daltoplast®, respectively.

2.1.6. PGA

PGA (polyglycolic acid) is the simplest aliphatic polyester derived from glycolic acid through a ring-opening polymerization process (glycolide). It is well-known for its high strength, excellent biocompatibility, and biodegradability, making it suitable for a wide range of applications. One notable application of PGA is in fiber production. PGA fibers exhibit exceptional tensile strength and find uses in various industries, including medical, textile, and packaging. In the medical field, PGA fibers are commonly used for sutures, providing temporary support during wound healing before naturally degrading over time. The packaging industry utilizes PGA for applications that require high-strength and biodegradable characteristics. PGA fibers offer a unique combination of strength, biocompatibility, and biodegradability, making them an appealing choice for applications that prioritize sustainability and performance. PGA undergoes complete degradation through hydrolysis (both enzymatic and non-enzymatic). This interesting polymer provides a high crystallization rate and content (even higher than PLA) and fast biodegradation (even faster than PCL and PHA) at the same time. PGA provides a fast biodegradation rate (due to hydrolysis), high mechanical properties (due to in-order structure and high crystallization), and biocompatibility for the spun fibers. It is also interesting that PGA is not soluble in most organic solvents, including chloroform, and needs fluorinated solvents such as HFIP. Furthermore, PGA has excellent barrier properties [118]. However, due to its relatively low T_g (35–40 °C), stiffness or brittleness, high relative density (1.53), and fast hydrolysis, it may not be very suitable for all textile products [119,120]. The history of fiber spinning and the biodegradation assessment of PGA dates back more than 30 years [121]. Details about polymerization, possible copolymers, different properties, and potential applications of PGA are reviewed elsewhere [122,123]. Companies such as Kureha, Shenzhen Polymtek Biomaterial, Durect, and Zhejiang Hisun Biomaterials provide PGA for various applications.

2.1.7. PLGA

PLGA (poly(lactic-co-glycolic acid)) is a copolymer of PGA synthesized through ring-opening polymerization of lactide and glycolide cyclic diesters. The copolymerization process allows for the adjustment of the ratio between lactide and glycolide, providing control over the material's properties, such as crystallization, hydrolysis, biodegradation rate, mechanical strength, and hydrophilicity [119,120]. PLGA has found wide-ranging

applications in the form of fibers. Various techniques, such as electrospinning, melt-spinning, or wet-spinning, can be employed to produce PLGA fibers, resulting in different fiber morphologies and mechanical characteristics. PLGA fibers have been utilized in diverse applications, including drug delivery, tissue engineering, wound dressings, tissue suturing, and biosensing. The versatility and biocompatibility of PLGA make it a promising material for fabricating fibers with tailored properties for a wide range of biomedical and pharmaceutical applications [124]. Recent research is also exploring the synthesis of PLGA from CO₂ and its barrier properties [119]. Companies such as Evonik, Akina, and Mitsui are involved in the production of PLGA.

2.1.8. PBAT

PBAT (poly(butylene adipate-*co*-terephthalate)) is a biodegradable copolymer synthesized through the polymerization of the three monomers or from PBA with dimethyl terephthalate (DMT) and 1,4-butanediol (BDO) monomers [125]. These copolymerization processes result in a material that combines the flexibility of butylene adipate with the strength and rigidity of butylene terephthalate. PBAT exhibits excellent biodegradability under appropriate conditions. PBAT fibers have gained attention in various applications due to their unique properties. Techniques such as melt-spinning can be used to produce PBAT fibers, allowing for the fabrication of fibers with different morphologies and mechanical characteristics. PBAT applications include fibers, nonwovens, packaging, and hygiene products. The flexibility, biodegradability, and tunable properties of PBAT fibers make them a promising choice for sustainable and eco-friendly fiber applications. PBAT exhibits elastic properties with a low modulus and high recoverability due to its hard-soft segment chemical structure. However, the T_m of PBAT is around 100 °C, which may be a limiting factor for certain applications [126]. Commercial products such as Ecoflex[®] from BASF, Mater-Bi[®] from Novamont, and Ecoworld[®] from JinHui Zhaolong High Technology are available on the market. Rodenburg was also reported as a manufacturer of PBAT in the past [82]. The FDCA analog PBAF is also under development [127,128].

2.1.9. PBSA

PBSA (poly(butylene succinate-*co*-adipate)) is a copolymer synthesized through the polymerization of succinate and PBA. The specific parameters of the copolymerization process can be adjusted to control the material's properties, such as mechanical strength, thermal stability, and biodegradability. PBSA can also be used for fiber production. The combination of biodegradability, mechanical performance, and processability makes PBSA fibers an attractive option for sustainable approaches [129]. Manufacturers such as Mitsubishi, BASF, and Tianjin GreenBio Materials produce PBSA for various applications.

2.1.10. PBST

PBST (poly(butylene succinate-*co*-terephthalate)) is a versatile biodegradable copolymer that offers unique properties and finds diverse applications in the field of fibers. It is synthesized through the copolymerization of butylene succinate and terephthalate monomers. By combining the desirable traits of polybutylene succinate and terephthalate, PBST exhibits enhanced mechanical strength, thermal stability, and biodegradability. Melt-spun PBST fibers can be produced with different morphologies and mechanical properties, making them suitable for a variety of applications. In industries such as textiles, PBST fibers serve as an eco-friendly alternative, meeting the increasing demand for sustainable materials in today's world [129]. Companies such as Novament, Meredian, Sinopec Yizheng, and Lotte Chemicals are some examples of sources for PBST.

2.1.11. PBEAS

PBEAS (poly(butylene-*co*-ethylene adipate-*co*-terephthalate)) is a copolymer synthesized through the copolymerization of butylene, ethylene, adipic-, and succinic acid monomers. This combination of monomers results in a copolymer with a balance of

flexibility, mechanical strength, and biodegradability. PBEAS fibers have been reported in monofilament and multifilament topologies, although the presence of block copolymers can interfere with the process due to their high elastic behavior. The low melting point of PBEAS can also present a challenge for certain applications. Nevertheless, PBEAS fibers have been considered in some reports for their potential in the green transition of the textile sector [129,130]. Information on specific manufacturers of PBEAS is limited; however, some examples are Shenzhen Esun Industrial, Tianjin GreenBio Materials, and Zhejiang Hisun Biomaterials.

2.1.12. PB TSA

PB TSA (poly(butylene terephthalate-*co*-succinate-*co*-adipate)) is a complex copolymer composed of BDO, TA, SA, and AA monomers. It is a less commonly known biodegradable copolymer compared to others, and most of the research on PB TSA is reported in laboratory-scale studies. The ratio of aliphatic units to aromatic units in PB TSA was designed to be around 1:1 in these studies [131], with a heat of fusion (ΔH_m) of 145 J/g [82]. The mole fraction of butylene terephthalate (BT) units in PB TSA terpolymer, as determined by ¹H NMR (nuclear magnetic resonance), is reported to be 48 mol% [82].

2.1.13. PIHO

PISOX, or PIHO (polyisobutide-*co*-1,6-hexanediol oxalate), is a biodegradable copolymer derived from isobutide and 1,6-hexanediol, with oxalate linking the two diols. Isobutide is a biobased compound derived from sorbitol (hydrogenated glucose). PISOX exhibits properties such as good thermal stability, mechanical strength, and biodegradability, making it suitable for various applications. The presence of oxalate linkages in the polymer structure enables its biodegradation by enzymatic and non-enzymatic hydrolysis, which can occur in various environmental conditions.

Research and development efforts have been conducted to explore the potential of PISOX as a biodegradable copolymer. For example, Gert-Jan Gruter's group has developed novel high- T_g PISOX-HDO copolyesters with high thermal and mechanical performance along with a fast degradation rate in soil and marine environments. They observed relatively fast non-enzymatic hydrolysis of polyoxalates as a contributor to the fast biodegradation. It was also shown that the enzymatic hydrolysis of the constituting monomers is the rate-determining step in this biodegradation mechanism. The combination of high T_g (>100 °C) and fast biodegradability makes PISOX-HDO copolyester suitable for short-term applications that demand strong mechanical and physical properties while also being environmentally friendly [63,108,120].

Some other new polymers and copolymers such as polydioxanone (PDO), polyglycolic acid-*co*- ϵ -caprolactone (PGC), polyglycolic acid-*co*-trimethylene carbonate (PGTMC), poly-lactic acid-glycolic acid-*co*- ϵ -caprolactone (PLGC), poly-lactic acid-glycolic acid-*co*-trimethylene carbonate (PLGT), and polyglycolic acid-*co*- γ -butyrolactone (PGB) were reported recently [122].

Furthermore, in addition to copolymerization processes that allow molecular-level design, some commercial compounds/blends are available that manufacturers try to adjust to certain properties, including a balance between processability, mechanical/thermal performance, and biodegradation.

2.2. Biodegradation

Biodegradable plastics undergo biodegradation in three steps: disintegration, depolymerization, and assimilation and mineralization by microorganisms. Abiotic factors such as heat, light, mechanical stress, and moisture directly impact the first two steps and indirectly affect the third step. Biotic factors, such as microorganisms (type and quantity), through their enzymatic actions, can directly influence all three steps. Biodegradable condensation polymers break down into oligomers and monomers, which microorganisms utilize as substrates for metabolism and growth [108,120]. Hydrolysis is the rate-limiting

step for polyester biodegradation, and microbial activity inhibition also plays a significant role [63,120].

Depolymerization, specifically the hydrolysis of ester bonds at room temperature in soil, is a crucial prerequisite for mineralization, which involves the microbial utilization of polymer carbon. Physical processes aid depolymerization by facilitating fragmentation and reducing particle size. Amorphization of crystalline structures in semi-crystalline plastics through processes such as micronization or extrusion can indeed increase their susceptibility to enzymatic degradation. Hydrolysis is faster in accessible amorphous regions of the polymer, particularly aliphatic esters, and can be enhanced by microbial enzymes, acids, or bases [132].

Photodegradation, induced by UV light or oxygen, breaks tertiary and aromatic C–C bonds, resulting in brittle and discolored materials. This process can be further enhanced by incorporating metallic catalysts into the polymer. Oxo-degradation, triggered by metals, leads to fragmentation into microplastics and incomplete digestion, which is why it has been restricted [1]. Additionally, the biodegradation cycle consists of three phases: lag, biodegradation, and plateau.

It is worth mentioning that biodegradation is a surface action. The rate of biodegradation is highly dependent on the chemical structure of the polymer, stabilizing additives, product geometry (particularly size and surface area), surrounding conditions (e.g., the presence of water and oxygen), and the availability of microorganisms. Complete biodegradation or mineralization in a specific environment is influenced by characteristics such as crystallinity, as well as the presence of additives such as plasticizers and environmental factors such as temperature, moisture, pH, and the presence of suitable microorganisms [133].

Certifications and labels are used to identify biodegradable materials, often based on industrial standards discussed elsewhere [134], like EN 13432 [135] or ASTM D6400 [136]. For example, the “industrial” sub-label for compostability is based on tests specified in these standards, evaluating biodegradation, disintegration, toxicity, and heavy metal content [137].

While PLA is considered compostable, minimal degradation has been observed at ambient temperatures in seawater and soil. This discrepancy can be explained by the more favorable conditions for PLA biodegradation in industrial composting, including higher temperatures (58 °C; close to PLAs T_g), higher microbial concentrations, and increased moisture content compared to the natural environment [138]. It should be noted that the intensity of degradation varies across different end-life environments, including industrial composting, home composting, soil, water, and marine environments [139].

2.3. Bio-Based and Biodegradable Plastics Market

While bio-based and biodegradable plastics remain a niche market with only 2.22 million tons in 2022 (0.5% of total plastic production), there is a movement towards their wider deployment. The global biodegradable plastics market is projected to reach USD6.73 billion by 2025, up from USD3.02 billion in 2018 [140]. Meanwhile, PHAs and PLA are reported to be the main contributors to the growth of bio-based biodegradable plastics [4]. They have a share of 3.9% and 20.7% of the bio-based plastic market, respectively. However, bio-based plastics are associated with disadvantages such as high cost, uneconomic feasibility, brittleness, low thermal properties and instabilities, and hydrophilic nature [36]. Therefore, some materials are stuck in the research and development stages [141].

Table 1. Chemical structure and some properties of biodegradable/compostable polymers that have been used for melt-spinning so far.

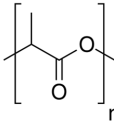
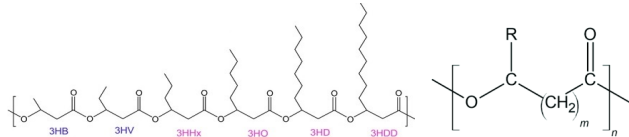
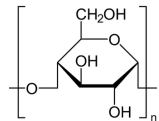
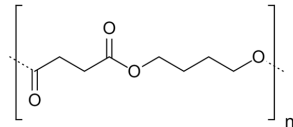
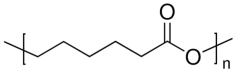
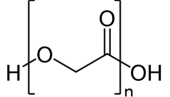
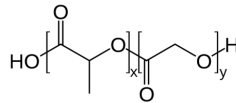
No	Polymer	Chemical Structure	Main Properties
1	PLA		Melting point = 160–180 °C Glass transition = 55–60 °C Density = 1.25 g/cm ³ MW range = 20,000–200,000 g/mol or Daltons Biodegradation ¹ : Industrial compostable (<6 months)
2	PHAs		Melting point = 140–171 °C Glass transition = 4 °C Density = 1.25 g/cm ³ MW range = 10,000–1000,000 g/mol Biodegradation: Marine degradable (<12 months)
3	TPS		Melting point = 150–170 °C Glass transition = 50–80 °C Density = 1.2–1.6 g/cm ³ MW range = 10,000–500,000 g/mol Biodegradation: Marine degradable (<12 months)
4	PBS		Melting point = 110–120 °C Glass transition = -32 °C Density = 1.00 g/cm ³ MW range = 10,000–200,000 g/mole Biodegradation: Soil degradable (<24 months)
5	PCL		Melting point = 60 °C Glass transition = -72 °C Density = 1.12 g/cm ³ MW range = 3000 to 100,000 g/mol Biodegradation: Marine degradable (<6 months)
6	PGA		Melting point = 225–230 °C Glass transition = 35–40 °C Density = 1.53 g/cm ³ MW range = 10,000–300,000 g/mole Biodegradation: Marine and soil degradable (<3 months)
7	PLGA	 mechanical strength (a significant increase of 78%)	Melting point = 262 °C Glass transition = 40–55 °C Density = 1.3 g/cm ³ MW range = 10,000–110,000 g/mol Biodegradation: Marine and soil degradable (<6 months when G/L > 1)

Table 1. Cont.

No	Polymer	Chemical Structure	Main Properties
8	PBAT		Melting point = 120 °C Glass transition = -28 °C Density = 1.26 g/cm ³ MW range = 10,000 to 300,000 g/mol Biodegradation: Soil degradable (<24 months)
9	PBSA		Melting point = 112 °C Glass transition = -38 °C Density = 1.25 g/cm ³ MW range = 10,000 to 100,000 g/mol Biodegradation: Soil degradable (<12 months)
10	PBST		Melting point = 115 °C Glass transition = 40 °C Density = 1.26 g/cm ³ MW range = 10,000 to 200,000 g/mol Biodegradation: Soil degradable (<12 months)
11	PBEAS		Melting point = 50–60 °C Glass transition = -15 °C Density = 1.2 g/cm ³ MW range = 10,000 to 100,000 g/mol Biodegradation: Soil degradable (<12 months)
12	PBTSA		Melting point = 150–200 °C Glass transition = 30–70 °C Density = 1.2–1.4 g/cm ³ MW range = 20,000 to 100,000 g/mol Biodegradation: Soil degradable (<12 months)
13	PIHO		Melting point = N/A Glass transition = 103 °C Density = 1.38 g/cm ³ MW range = 10,000 to 100,000 g/mol Biodegradation: Marine and soil degradable (<6 months)

¹ Here the environment with the minimum intensity (that biopolymer is degradable) is mentioned. However, biodegradation time depends on several factors of the product, e.g., the specific composition of the material, the molecular weight, the specific surface area or size, and environmental conditions such as temperature, moisture content, and existing microorganisms.

3. Melt-Spun Biodegradable Fibers

The melt-spinning process can involve monocomponent, bicomponent, or multicomponent fibers with different cross-sections and configurations, which are discussed in detail elsewhere [54,142]. However, there are challenges associated with the melt-spinning of biodegradable polymers, including low crystallization rates, thermal degradation, and a limited processing temperature window during extrusion [143]. Nevertheless, biodegradable polymers such as PLA, PBS, PHB, PCL, PBAT, and others have garnered significant interest for the production of melt-spun biodegradable fibers for various applications [31]. Recent studies have focused on melt-spinning these biodegradable polymers and characterizing the spun fibers, as discussed in the following sections.

3.1. Monocomponent Filaments and Fibers

Using only one polymer without compounding or additive through a plant with one extruder or piston-cylinder setup is the first approach for making thermoplastic fibers. Numerous studies have focused on investigating the impact of processing conditions on the properties of melt-spun biodegradable fibers [54]. For example, Schick et al. [87] compared PBS, PBAT, and TPS with PP as a reference material through melt-spinning, achieving benchmark tenacities of over 500 mN/tex for PP, while PBS and PBAT exhibited only 100 mN/tex. This study revealed higher crystallinity for PBS yarns (70%) compared to PBAT (14%). Meanwhile, TPS was found to be unsuitable for yarn production. By optimizing the process, the tenacity of home-compostable bio-based polymers can potentially be improved, making them suitable for applications that require moderate mechanical properties.

Park et al. [144] investigated the effects of spinning speed and heat treatment on the mechanical properties and biodegradability of melt-spun PLA fibers. They suggested optimal spinning process conditions that provided a suitable range of tenacity and biodegradability in textile fibers. They performed trials with a take-up speed of 2000–4000 m/min and heat-treated the yarns. Biodegradability was estimated from the decreases in breaking stress, weight loss, and degree of crystallinity after soil burial [145,146]. Ali et al. [147] examined the correlation between the spinning process and fiber characteristics by analyzing the structure and properties of PLA fibers produced at various spinning speeds. Chirag et al. [148] conducted a similar study investigating the relationship between the spinning process and the properties of the resulting fibers. This study found that utilizing a low melt extruder temperature (220 °C), high throughput (0.6 g per hole per minute-GHM), high take-up speed (1500 m/min), high drawing temperature (75 °C), and the maximum achievable draw ratio led to the highest tenacity among the fibers studied. However, this approach also resulted in significant process-induced thermal degradation. This investigation was extensively covered in a Ph.D. thesis [149]. Schmack et al. [150] conducted high-speed melt-spinning-drawing experiments (2000–6000 m/min) using a spinneret with 12 orifices 300 µm in diameter for PLA fibers produced through reactive extrusion polymerization. They characterized the physical, thermal, and hydrolytic degradation properties of the fibers. The highest achieved tensile strength was 430 MPa, with a modulus of 6 GPa for the sample drawn at the maximum ratio of 6. They also examined five other PLA samples with varying D-lactide contents (1–8%) and different tactics. The fibers spun at the highest speed from PLA with 1% D content and drawn at the maximum ratio exhibited the highest tensile properties, with a tenacity of 300 MPa, an elongation at break of 30%, and a tensile modulus of 6.8 GPa. Conversely, the PLA sample with 8% D content demonstrated the poorest spinnability [151]. In a similar study by Takasaki et al. [152], monofilament melt-spinning of PLA with D contents of 1.5%, 8.1%, and 16.4% demonstrated the ability to accommodate filaments spun from low-D content polymers even at speeds of up to 10,000 m/min. These filaments exhibited higher orientation, crystallinity (45%), and mechanical properties (570 MPa strength and 5.9 GPa modulus). PLA fibers with high D content remained amorphous until the highest examined take-up velocities showed a lower intention to crystallize.

Yuan et al. [153] utilized a micro-extruder with a 1 mm diameter die to produce monofilaments from PLLA, using three different grades with varying molecular weights. Subsequently, hot drawing was performed. The findings indicated a significant decrease in the viscosity-average molecular weight of PLLA, ranging from 13.1% to 19.5% during pulverization and from 39.0% to 69.0% during melt extrusion. The final PLLA fibers, with diameters ranging from 110 μm to 160 μm , exhibited tensile strengths between 300 MPa and 600 MPa. Nishimura et al. [154] achieved a PLLA fiber with a tensile strength of 810 MPa through melt-spinning, coupled with two steps of drawing at a draw ratio of 18 in hot water. Even after the fiber was exposed to the environment for 1 year, the surface remained smooth, and the tensile strength did not experience a significant decline. Hydrolysis tests demonstrated that the fiber was not susceptible to non-enzymatic hydrolysis after 1 month of immersion in a buffer solution at 37 $^{\circ}\text{C}$, but rapid hydrolysis occurred above 60 $^{\circ}\text{C}$, highlighting the effectiveness of surpassing the T_g . SEM observations revealed a regular pattern of cracks oriented vertically to the fiber axis, indicating the development of a highly ordered structure aligned with the fiber axis. In a different approach, Paakinaho et al. [155] employed PLDLA copolymer (with a ratio of 96/4 L/D) to produce melt-spun fibers. Two different dies, 8-filament (\varnothing 0.4 mm) and 12-filament (\varnothing 0.2 mm), were used during melt-spinning, followed by hot drawing. This study investigated the effects of molecular weight and melt processing on the hydrolytic degradation of the fibers through *in vitro* analysis. The results demonstrated that high-molecular-weight polylactide experienced degradation during melt-spinning due to the high shear stress and elevated melt temperatures, while low-molecular-weight polylactide with low melt viscosity remained unaffected by melt processing. Additionally, the thermally generated lactide monomer presented interesting possibilities for controlling the hydrolytic degradation rate of PLA. Fambri et al. [156] employed a PL-*co*-D-LA copolymer (70/30) to produce biocompatible and compostable fibers through melt-spinning. The resulting filaments had a diameter of 120 μm and a maximum strength of 200 MPa. *In vitro* biodegradation assessments in phosphate-buffered saline (PBS) indicated that the mechanical properties remained satisfactory for up to 4 weeks, with a significant decrease in strength observed over time due to water sorption and a reduction in molar mass.

PHAs remain a fascinating option for producing biodegradable bio-based fibers. PHB and PHBV were introduced for fiber spinning by Liu et al. [157]. Qing et al. [158,159] conducted melt-spinning experiments with PHBH (containing 5.4 mol% hydroxyhexanoate) at various speeds ranging from 500 to 4000 m/min. They discovered that reducing the processing temperature (below the melting point of PHB, which is 170 $^{\circ}\text{C}$) and increasing the take-up speed led to improved crystallization, primarily due to the orientation of α -crystals and the formation of β -crystals. It is widely recognized that the presence of a crystalline structure, particularly the planar-zigzag conformation of PHAs, enhances the mechanical properties of the fibers [160].

Moreover, the modification of biodegradable polymers through co-polymerization or blending (considering miscibility-structure-property relationships for the best compatibilization) can be explored to facilitate melt-spinning or enhance the performance of the compound [161]. While composite and blend fibers will be discussed separately, biocopolymers have shown promising results thus far. Saito et al. [162,163] demonstrated that the mechanical properties of P(3HB-*co*-4HB) (PHBH) can be tailored, ranging from hard to soft, by incorporating varying molar fractions of the 4HB comonomer. In a related study, Omura et al. [164] produced marine biodegradable fibers with high strength and elasticity through melt-spinning of a PHBH containing 16% comonomer. The spinning process was conducted at a temperature lower than the polymer's melting point (approximately 160 $^{\circ}\text{C}$). *In situ* wide-angle X-ray diffraction (WAXD) and differential scanning calorimetry (DSC) measurements revealed the presence of persistence crystals in the fibers. These fibers exhibited complete degradation when exposed to seawater from Tokyo Bay or freshwater from Sanshiro Pond in less than one month. The researchers observed the formation of periodically stacked lamellar structures, with lamellae measuring around 200 nm and

comprising at least 30 lamellae, following the biodegradation of the amorphous region on the fiber surface. The results of their study are illustrated in Figure 5 below.

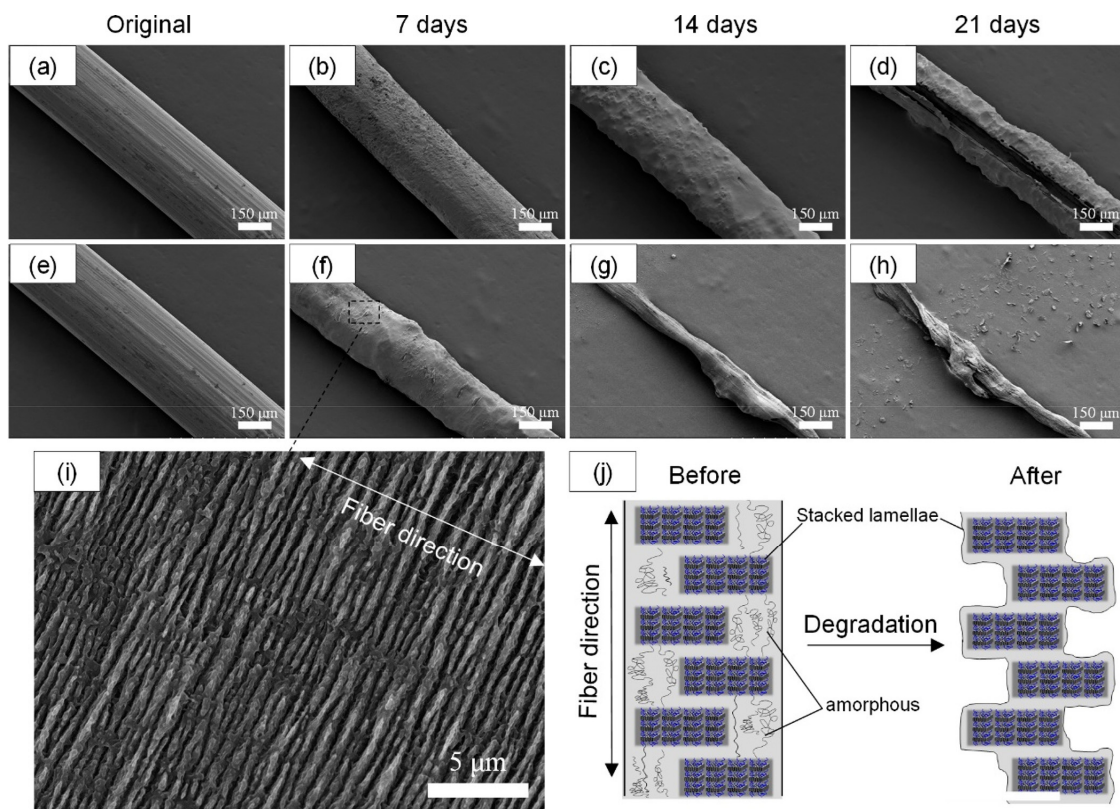


Figure 5. SEM images of PHBH (16% comonomer) fibers: (a,e) before biodegradation, after (b) 1, (c) 2, and (d) 3 weeks in Sanshiro Pond fresh water, and after (f) 1, (g) 2, and (h) 3 weeks in Tokyo Bay seawater; (i) stacked lamellae structure; and (j) expected mechanism illustrating the presence of oriented lamellae crystals [164]. Reprinted with permission.

Miyao et al. [165] utilized a Liquid Isothermal Bath during the melt-spinning process to enhance the mechanical properties of PHBH fibers containing 5.4 mol% comonomer. By incorporating a liquid bath with temperatures ranging from 30 to 100 °C at a depth of 20 cm and 1 m from the spinneret, they successfully increased the strength of the fibers from 100 MPa to 176 MPa. Similarly, Tanaka et al. [166] achieved high-strength fibers with a tensile strength exceeding 1 GPa and a modulus of 8 GPa using PHBV (8% HV content). Notably, they achieved these exceptional results without the use of nucleation agents or other additives. The fibers were directly quenched in ice water to obtain an amorphous state, followed by a 24 h immersion in ice water to induce small crystal nuclei during isothermal crystallization. The fibers were then subjected to drawing at room temperature and annealing subsequently. It is worth mentioning that this procedure is time-consuming and costly. Rebia et al. [167] adopted a similar approach by performing isothermal crystallization on melt-spun monofilament PHBH fibers for 24, 48, and 72 h. They employed dip-coating using a propolis-incorporated ethanol and acetone solution, followed by drawing above T_g . However, the monofilaments dip-coated for 24 and 72 h exhibited a reduction in tensile strength and an increase in elongation at break. The crystallinity of the dip-coated monofilaments decreased, leading to an increase in the thickness of the lamellar crystal after applying the dip-coating for 15 cycles. This method appears to result in more porous fibers, which contrasts with the objective of achieving good mechanical properties. Selli et al. [168] conducted monofilament melt-spinning of PHBH with the aim of understanding the relationship between structure and property in melt-spun fibers from three different copolymer grades. They sought to develop an unscalable melt-spinning method for producing fine

biodegradable PHBH filaments without the need for an ice water bath or offline drawing techniques. Their findings revealed that a synergistic interaction between a highly oriented non-crystalline mesophase and highly oriented α -crystals contributed to increased tensile strength. Aging the filaments over a period of 33 months resulted in increased tensile strength and decreased elongation at break due to an increase in crystallinity over time. They also noted that although higher ultimate tensile strength (UTS) can be achieved for PCL fibers, PCL is less biodegradable than PHBH and is more suitable for long-term degradation applications. Bansode et al. [124] synthesized PLGA through polymerization and performed melt-spinning to compare the resulting fibers with PCL fibers and electro-spun fibers for applications in tissue engineering and drug delivery. Further research on electro-spun PCL fibers is reported by Leonés et al. [169]. Gurarslan et al. [170] developed PCL coalesced fibers by forming stoichiometric inclusion complex crystals in a urea medium, followed by spinning and cold drawing. They demonstrated that the drawn coalesced PCL fibers exhibited the highest crystallinity, orientation, and a 65% higher modulus compared to the as-received PCL fibers, which can be attributed to the intrinsic alignment of the coalesced polymers. They also reported a linear correlation between birefringence (orientation) and tensile modulus.

Meanwhile, different bio-based and biodegradable polymers such as PLA, PHBH, and PEF (poly(ethylene 2,5-furan dicarboxylate)) are considered by Kikutani [171] for the replacement of PET fibers. They could reach an even take-up speed of 6000 m/min. PGA is also a high-crystalline polymer with a high biodegradation rate (due to hydrolysis). This makes it interesting for investigation by melt-spinning in homopolymer or modified copolymer schemes. Yang et al. [172] could make PGA yarns with 645 mN/tex tenacity via melt-spinning as-spun yarns at 30 m/min speed and drawing five times afterward. Hot water shrinkage measurement is used by them to assess internal stress. They asserted that reducing the winding speed during the spinning process resulted in decreased internal stress within the as-spun fibers, ultimately leading to an increased drawing ratio. Consequently, the drawn fibers exhibited notably superior mechanical properties. Meanwhile, they reported a lower orientation increment via increasing the windup rates (due to processing close to the melting point, high viscosity, and fast crystallization, preventing the molecular flow), which is in contrast with the processing of conventional synthetic fibers in the literature by Ziabicki or others [173,174]. Moreover, they found that by increasing the winding speed of as-spun yarns (from 30 to 400 m/min), the drawability decreased (from 5 to 2) and the final tenacity of the yarn dropped (from 645 to 233 mN/tex), while the water shrinkage (internal stresses) increased (from 3 to 40%). They obtained the highest tenacity via drawing at 45 °C and 10 m/min as optimal conditions. They stated the molecular entanglement as a barrier causing limited drawability. Therefore, Saigusa et al. [175] modified the spinning process by adding a heating chamber in the vicinity of the spinning head and lowering the take-up speed in the processing of PGA. This resulted in a low Deborah number and better melt structure control in the spin-line, and accordingly, they could obtain fibers with higher strength and toughness after in-line drawing. This was attributed to a reduction in entanglement density. They used a spinneret with 24 holes, and after extrusion at 245 °C, the yarn passed the heating chamber with a 120 cm length and 120 °C temperature and was collected on the first godet via a speed of 100–300 m/min, while the godet had almost the same speed and solid drawing happened between the second and last godet, and the winding speed reached up to 1500 m/min. The yarn spun at the modified spin line showed higher orientation (birefringence 0.018 versus 0.013), higher thermal shrinkage, higher tenacity (780 versus 650 mN/tex), and lower elongation at break. Saigusa et al., in another work [118], investigated the effect of carboxylic acid content and glycolic acid (generated during melt-spinning via glycolide due to the type and amount of tin catalyst used in the polymerization process) on the hydrolysis of PGA fibers. They also proved that hydrolytic degradation of the drawn fibers can be delayed by adding the thermal stabilizer. They used molecular weight and tensile properties as an indication of biodegradation after immersing in phosphate buffer solution. They also mentioned order

structure and pH as some other parameters altering hydrolytic biodegradation. It was also mentioned that hydrolysis starts from/via carboxylic end groups. Therefore, PLGA is showing a lower hydrolytic biodegradation rate (compared to PGA), which is due to capping carboxylic groups [176]. Malafeev et al. [177] produced absorbable sutures with 91 MPa strength via spinning of PLGA with 10% GA comonomer through a DSM microextruder within a 1 mm diameter die. Fu et al. [178] selected PGA to make a monofilament for Acupoint catgut-embedding therapy due to its good formability and biodegradability. They also applied 1–3% chitosan via dip-coating on PGA monofilaments. They resulted in higher swelling and mechanical properties and improved antibacterial efficacy and cytocompatibility for the coated fibers. However, the biodegradation rate is decreased due to the protective function of the chitosan coating. In another work [179], they made PGA monofilaments and coated them with chitosan while comparing the results with the counterpart PLA monofilament. They used a maximum 300 m/min take-up speed while applying a drawing ratio of 6. They resulted in filaments with about 250 μm diameter and could achieve 76.8 cN strength for PLA and 57.3 cN for PGA monofilament.

In a different work, Khare et al. [180] polymerized PLGA, highlighting modification possibilities via changing comonomer ratios. They produced PLGA microfibers through centrifugal melt-spinning. Guo et al. [181] studied the effect of the inherent viscosity of PGA along with melt-spinning parameters (including drawing ratio and drawing temperature) on tensile strength and biodegradation rate in phosphate buffer solution (PBS-pH 7.4) within two weeks. Their trials resulted in 923 mN/tex tenacity and 62% crystallinity for the sample spun from a higher IV polymer with a lower drawing temperature and a maximum drawing ratio of 6. Moreover, the degradation rate of PGA fiber was affected by various factors. PGA fiber produced with a higher drawing ratio exhibited slower degradation, while elevating the drawing temperature resulted in faster degradation. Additionally, PGA fiber made from polymers with a higher inherent viscosity (IV) experienced a slower degradation process. Miao et al. [182] investigated in vitro degradation of PGA and PLGA (with 8% LA) fibers with different heat setting temperatures. They found that PGA fibers are more susceptible to degradation than PLGA, and the biodegradation rate is reduced by increasing the heat setting temperature. They suggested a four-step biodegradation mechanism in their model. They also found that crystallinity is increased in the early stage of biodegradation of PGA, indicating that hydrolytic biodegradation starts in amorphous regions and is followed by further degradation in crystalline domains. Only a small amount of mass from the PGA and PLGA samples was lost during the initial degradation stages. However, the mechanical properties experienced a noticeable decrease due to the rapid degradation of the amorphous regions. Moreover, cleavage-induced crystallization occurred in the middle stage. Interestingly, the initial crystallinity of 70% is increased in the first step and decreased afterwards. The initial tenacity was about 600 mN/tex which was reduced gradually. However, the difference between these biodegradation steps is reduced by introducing LA units into PGA (a different mechanism for PLGA). Gruter [6] reported some recent studies about the biodegradation of PGA and PLGA (with different LA content) in his group, which resulted in faster hydrolysis and soil biodegradation than cellulose (the same trend as the high-Tg PISOX-HDO copolymer). He gave his opinion about the future of polyesters, with particular emphasis on making lactide from biomass and glycolic acid from CO_2 as the ultimate circular feedstock for making negative carbon footprint materials to approach the net zero emission goal. He also mentioned fantastic barrier properties, thermal stability, and non-enzymatic hydrolysis as highlighted factors for making marine-degradable products from PGA.

Younes et al. conducted several studies [183–189] on melt-spinning, characterization, and simulation of different properties of aliphatic-aromatic copolyester (AAC) fibers, focusing on PBAT. They used a laboratory melt-spinning plant to produce multifilament yarns (30 or 55 filaments). They employed a factorial experimental design and statistical analysis to simulate and model the effects of various processing parameters, including polymer grade or MFI, extrusion temperature, drawing temperature and ratio, and speeds, on vari-

ous fiber properties such as diameter, orientation, crystallinity, mechanical performance, and shrinkage. Li et al. [109] performed multifilament melt-spinning of PBST with a take-up speed of 2000 m/min. The spun fibers exhibited higher flexibility compared to PBT (polybutylene terephthalate) and had a melting point around 180 °C. This study also investigated the isothermal crystallization kinetics at low supercooling and found that the Avrami exponent (n value) for PBST fibers ranged from 2.9 to 3.3, indicating heterogeneous nucleation and three-dimensional spherulitic growth. The equilibrium melting temperature of PBST fibers was determined to be 206.5 °C using the Hoffman-Weeks method. The temperature at the maximum crystallization rate for PBST fibers was found to be approximately 90 °C. Kang et al. [190] conducted a study on a similar aliphatic-aromatic copolymer, PBAS/PBT (poly(butylene adipate-*co*-butylene succinate)/polybutylene terephthalate) block copolymer. They revealed that only the abundant component in the block copolymer could form crystals. When the molar ratio of aliphatic to aromatic units approached 1:1, neither the aliphatic nor aromatic units could crystallize effectively. Fuoco et al. [191] produced multifilament yarns from PLLA (poly(L-lactide)) and PLLA-*co*-PC (poly(L-lactide-*co*-propylene carbonate)) with varying comonomer content (5, 10, and 18 mol%) through high-speed melt-spinning with a fixed take-up speed of 1800 m/min. They investigated the relationship between the composition, polymer structure, processing parameters, and physical properties of the fibers. They found a linear correlation between the as-spun fiber properties and the linear density. Increasing the comonomer content in the polymer structure resulted in decreased crystallinity and tensile strength due to a reduced arrangement possibility. Additionally, increasing the linear density led to lower fiber orientation. However, increasing the drawing temperature could partially compensate for the decrease in crystallinity and tensile strength. The researchers achieved improved tensile properties and higher crystallinity by applying a second-stage hot drawing process, resulting in a degree of crystallinity increase from 0–52% to 25–66%. The obtained tensile strength ranged from 302 to 610 MPa, while Young's modulus reached values of 4.9–8.4 GPa. Notably, the first godet in their spinning line had a surprising speed of 1760 m/min, while the winding speed was 1800 m/min. This indicates that they applied more melt drawing during the spinning step, taking advantage of the initial melt strength, and further oriented the fibers in the solid state afterwards.

Baimark et al. [192] conducted a study on the synthesis and characterization of a block copolymer composed of L-lactide (LL) and ϵ -caprolactone (CL). The objective was to develop an absorbable surgical suture with a balance between mechanical properties and biodegradability. The block copolymer was processed through melt-spinning using a piston and cylinder apparatus to produce a monofilament. The small-scale piston apparatus allowed for the processing of samples as small as 10 g through a 1 mm diameter capillary. The resulting monofilament was quenched in a water bath and subsequently drawn and annealed. Annealing led to a minor reduction in strength, which was attributed to crystal transformation. The final fiber, with a diameter of 160 μ m, exhibited a tensile strength exceeding 500 MPa, approaching that of a commercial suture of similar size. The authors highlighted the importance of controlling the copolymer's chemical microstructure (composition, monomer sequencing) during the synthesis steps as well as the fiber's physical microstructure (matrix morphology, orientation) during the processing steps. These factors were identified as key elements in developing a new biodegradable fiber for surgical sutures. Another study by Murayama et al. [193] focused on the development of an absorbable suture using PHBH. In addition to conducting *in vitro* and *in vivo* degradability tests, the researchers performed a porcine abdominal wall suture test on melt-spun fibers. They proposed the developed filament as a safe alternative to existing monofilament sutures, as it effectively prevented unwanted knot loosening. Overall, both studies aimed to create biodegradable sutures with appropriate mechanical properties and degradation characteristics, highlighting the importance of material synthesis and processing techniques in achieving desired fiber properties for medical applications.

He et al. [194] conducted a study on the synthesis of a new aliphatic polyesteramide (PEA) copolymer using ϵ -caprolactone and 6-aminocaproic acid through a melt-polycondensation method. The aim was to achieve good thermal and mechanical properties in the fibers by incorporating amide groups and hydrogen bonds while maintaining biodegradability through the aliphatic polyester structure. The fibers were produced via melt-spinning, extruding the copolymer through a capillary rheometer with a diameter of 0.9 mm at a temperature of 105 °C. After extrusion, the fibers were drawn three times at 45 °C. The resulting fibers had a diameter of 125 μ m and exhibited over 2% moisture absorption, a strength of 125 MPa, and over 60% weight reduction after alkaline treatment. The weight reduction and property degradation were attributed to surface erosion in a concentrated alkaline solution. This erosion enhanced water absorption and decreased the strength of the fibers (hydrolysis), leading to increased biodegradability.

In another study by Shi et al. [82], fibers were produced from a random copolymer called (PB TSA). The characterization of the melt-spun fibers revealed a PBT-like diffraction pattern in wide-angle X-ray diffraction (WAXD). However, in ^{13}C spin-lattice relaxation time (T1C) measurements via NMR spectroscopy, two different components were observed for the aliphatic units, where the longer and shorter T1C components corresponded to the crystalline and amorphous domains, respectively. This indicated that the crystal structure of PB TSA fibers was formed through the mixed crystallization of its comonomers. Despite the random arrangement, the mixed crystallization behavior enabled the PB TSA fibers to develop a well-formed PBT-like crystal structure. Additionally, the introduction of soft segments (BA and BS) into the BT crystal lattice resulted in a lower melting temperature for PB TSA fibers (115 °C), which was over 100 °C lower than that of PBT fibers. The crystal structure of the PB TSA fiber was found to be predominantly formed by the BT unit, and it exhibited a highly oriented crystal structure. The PB TSA fiber demonstrated a rubber-like stress-strain curve, and its modulus and tensile strength were significantly lower compared to those of PBT fibers. Notably, the PB TSA fiber had a crystallite size of up to 7.8 nm. Alternating copolymers such as poly(butylene or tri-methylene terephthalate/succinate) (PB TS or PTMTS) and poly(butylene or tri-methylene terephthalate/adipate) (PB TA or PTMTA) exhibited a similar crystal structure to that of PBT. The crystalline structure of a polymer strongly influences its properties, including biodegradability, thermal properties, and mechanical properties. In the case of PBAT, solid-state ^{13}C NMR results indicated that only the BT units were included in the crystalline region, while the BA units were excluded.

Profiled (non-solid) fibers are always interesting in melt-spinning. This can also be found in reports on biodegradable man-made fibers. Naeimirad et al. [195] investigated the effect of polymer throughput (gear pump speed), drawing ratio, and winding speed on the mechanical properties and diameter of melt-spun PLA hollow fibers. Selli et al. [196] reported the production of hollow filaments from PCL in addition to solid fibers. El-Salmawy et al. [197] produced ProNectin F-coated biodegradable hollow fibers along with normal solid cross-sections from PLLA homopolymer and P(LA-co-CL) copolymer and studied the coating efficiency, physical properties, and cell adhesion. The coating efficiency was similar for both types of fibers; however, the ProNectin F-coated PLLA fibers showed approximately seven times higher cytocompatibility compared to the coated copolymer fibers. The molecular orientation in the hollow fibers was found to be much higher than that in the drawn solid fibers. Mechanical testing revealed an increase in tensile strength and a decrease in the thickness of the fiber wall with increased nitrogen flow rates and melt draw ratios.

Bauer et al. [198] employed optimized melt-spinning techniques to fabricate high-strength and highly oriented PCL monofilament and multifilament yarns with adjustable cross-sectional geometries, including solid and snowflake-shaped fibers. These fibers were designed for tendon and ligament tissue engineering applications. The researchers used a braiding technique to create the final structure. During a 24-week exposure to PBS at 37 °C, the snowflake-shaped fibers showed a slightly faster strength loss compared to the round fibers. However, the multifilament yarns did not exhibit accelerated strength

loss compared to the monofilament yarns, suggesting that the surface area alone did not contribute significantly to the degradation rate. Park et al. [199] produced profiled fibers with non-solid cross-sections by spinning PCL through circular, triangular, or cruciform capillaries. The aim was to obtain fibers with a high surface-area-to-volume ratio for the development of woven scaffolds for tissue engineering. The degradation of the shaped fibers was notably faster than that of circular fibers due to the enlarged surface area of the shaped fibers.

Regardless of recycling biodegradable plastics, Tavanaie et al. [200] mentioned composting and depolymerization as conventional end-lives for PLA. However, these methods can be costly. The researchers explored an alternative approach by performing melt recycling of PLA plastic waste to produce biodegradable PLA fibers through a melt-spinning process. The results showed that it is possible to spin PLA fibers from recycled waste with acceptable properties. The drying pre-treatment of the recycled PLA flakes, melt extrusion temperature, and drawing operations were found to have important effects on the mechanical and structural properties of the recycled PLA fibers.

3.2. Blend and Composite Fibers

Polymers can be modified through blending with other polymers or by compounding with additives, enabling improvements in processing, mechanical properties, specific functionality, and biodegradation behavior [31,201]. However, when blending polymers to enhance mechanical properties, it is important to consider the potential impact on biodegradation behavior. While blending PLA with PCL can lead to improved mechanical properties and biodegradability of PLA under home composting conditions [202], it may also result in a decrease in the biodegradation potential of PCL. Hence, the final properties of blend fibers depend on the nature of the blend components and their interfacial compatibility [31,201].

Furthermore, Furuhashi et al. [203] blended PLLA and PDLA and investigated the influence of drawing temperature on the crystallization of PLA blend fibers. So far, thanks to annealing and hot drawing, fibers mainly consisting of the stereocomplex crystal phase with a higher melting point have been achieved. Their findings revealed that PLA fibers drawn at 90 °C exhibited higher crystallinity and mechanical properties (520 MPa strength and 8.5 GPa modulus). However, higher drawing temperatures resulted in a decrease in the intensity of crystal reflections, indicating reduced crystal orientation. Padee et al. [204] employed a twin-screw extruder to blend PLA and poly(trimethylene terephthalate) PTT at various PTT contents (0–50 wt%) for fiber melt-spinning. The spinning of PLA/PTT blend fibers posed challenges due to the differing melting characteristics of PLA and PTT. However, successful spinning of PLA/PTT blend fibers was achieved at a 10 wt% PTT content with a barrel temperature of 250 °C, making them suitable for textile applications. Jompang et al. [205] and Panichsombat et al. [206] investigated the melt spinnability of PLA/PBS blends at different ratios (90:10, 80:20, 70:30, 60:40, and 50:50). The spinnability was found to depend directly on the miscibility of the blends. At a 90:10 PLA/PBS ratio, the blend exhibited miscibility and could be processed into fibers. However, spinning became difficult when the PBS content exceeded 10 wt% due to the immiscibility of the blend matrices. Park et al. [207] blended 5–15% PBAT in PBS to enhance the tensile strength and elongation of extruded monofilaments at a speed of approximately 80 m/min. Their results showed that the monofilaments achieved optimized physical properties when the PBAT content was 5%. Hassan et al. [208] conducted research on PLA fibers and observed an increasing trend in elongation at break due to the overall ductility of the material imparted by PBS (a highly ductile polymer). As expected, an increase in PBS loadings resulted in a decrease in tensile strength and modulus due to reduced crystallinity and the presence of highly ductile PBS. Similarly, Pisva et al. [209] utilized PBSA as a blend component (10–50%) with PLA to enhance toughness. The blends exhibited a sea-island morphology (see Figure 7d), with a finely dispersed PBSA phase in the PLA matrix at low PBSA content and dispersed as large droplets at high PBSA content. The rubbery behavior of PBSA improved the brittleness of PLA, while the tensile strength decreased

with increasing PBSA content. In a different study, Li et al. [210] prepared blends of polyoxymethylene (POM)/PLLA at ratios of 95/5, 90/10, and 80/20 through melt extrusion. The spinnability of the blends was confirmed through rheological characterization, successive self-nucleation, and annealing thermal fractionation analysis. Morphological observations revealed that the prepared fibers exhibited a smooth surface and uniform diameter distribution at the ultimate draw ratios. Although the presence of PLLA reduced the crystallinity of the POM domain in the fibers, the post-drawing process enhanced the crystalline orientation of lamellar folded-chain crystallites, resulting in a relatively high tensile strength of 791 MPa and partial hydration capability in both acid and alkali media for the blend fibers.

After the production of hollow fibers from PHB [211], a blend of PCL in PHB (70/30 wt%) was created through dissolution and precipitation from the solvent to enhance the mechanical properties, particularly the flexibility of the melt-spun hollow fibers (Figure 7g). It was demonstrated that the blend obtained from precipitated material exhibited good processability, while granulate material or powder mixtures were not suitable for spinning due to phase separation phenomena [211]. Additionally, Huang et al. [202] performed the blending of PCL with PLA using electron-induced reactive processing, followed by fiber production through piston spinning. The modified PLA/PCL blends exhibited improved melt strength and elastic behavior, attributed to the formation of long chain branches and enhanced chain entanglements. The PLA/PCL blends treated with 12.5 kGy demonstrated 2.4-fold higher impact toughness compared to neat PLA, indicating superior interfacial adhesion and chain interactions between the two phases. However, fibers spun from irradiated blends showed similar initial modulus but reduced tenacity compared to fibers spun from non-irradiated blends. Barral et al. [212] performed melt-spinning of monofilament (1 mm diameter) and multifilament yarn (80 filaments, 50–70 μm diameter) from PLA/PCL (including 10–40 wt% PCL) with different settings. Moreover, Vieira et al. [213,214] studied the viscoelastic properties of PLA/PCL monofilament (including 10% PCL) with a 400 μm diameter to understand the elastic-plastic deformation of the compound in creep and fatigue conditions. They found that a good approach for dimension stability validation of biodegradable parts for application in biomedical devices *In vitro* biodegradation of fibers was studied in Dulbecco's Modified Eagle Medium (DMEM) media at 50 °C for 35 days. The blend filament is also compared with PCL, PLA, and PGA. The results showed that the incorporation of PCL slowed down the hydrolytic degradation of PLA. Moreover, multifilaments showed slower MW reduction (compared to monofilaments). Furthermore, Visco et al. [215] used Ethyl Ester L-Lysine Tri-isocyanate (LTI) as a compatibilizer in PLA/PCL blend extrusion. They could produce 1.5 mm monofilaments and result in 0.3 mm diameter threads after drawing. They reported a 1% (phr) concentration of LTI as the best ratio for crosslinking and miscibility, while suggesting changing the ratio of PCL/PLA to modify the stiffness. They suggested this approach for making absorbable sutures due to their bioactivity and prohibition of bacterial growth along with hydrolytic degradation in simulated body fluid (SBF).

Blends of PHAs and PLAs are commonly used to optimize both polymers in various aspects. Chen et al. [216] conducted a study on the spinnability and fiber properties of a PHBH/PLA blend with a ratio of 35/65 [217]. The presence of the 4HB phase in the comonomer disrupted the stereoregularity in the 3HB phase, resulting in reduced overall crystallinity. However, their efforts led to fibers with exceptional mechanical properties, including high tensile strength (904 MPa), tensile modulus (28.42 GPa), and elongation at break (81%). They also reported good spinnability, with no apparent adhesion or fiber breakage during the spinning process. Li et al. [218] investigated the dependence of the orientation crystallinity factor (f_c) of PLA/PHBV blend fibers on the PHBV content. However, in the drawn fibers, the f_c of PLA showed less dependence on the PHBV content and take-up speed. Tavanaie et al. [97] evaluated the biodegradability of PP fibers modified with disposable recycled r-PLA plastic flakes. They incorporated 30% r-PLA in the fiber melt-spinning of PP and assessed the spun fibers via disintegration and biodegradation methods such as soil burial tests, CO₂ evolution analysis, weight loss, mechanical properties,

average molecular weight measurements, and analysis of surface morphology changes. While different testing methods yielded varying values for the biodegradation process, the results from CO₂ evolution analysis, weight loss, and variation of mechanical properties showed good agreement among different degradation methods. After incubation in soil for an extended period, the modified fibers exhibited a significant decrease in initial moduli (up to 72%) and tenacity (up to 53%). Furthermore, dye uptake of the PLA-modified PP fiber samples improved, and some showed excellent washing and light fastness properties [219]. However, there are concerns about the biodegradability of PP fibrillates at the end of their life cycle or the potential release of microplastics into the environment.

Using previous research [220] as a reference, Takasaki et al. [221] conducted melt-spinning of racemate polylactide (r-PLA, an equal blend of PLLA and PDLA) at high speeds of up to 7500 m/min to study the formation of stereocomplex crystals. Stereocomplex crystals have a higher melting temperature than homocrystals. The amount of stereocomplex crystals was higher under spinning conditions involving higher take-up velocity, a lower throughput rate, and a lower extrusion temperature. The high winding speeds applied higher tensile stress to the spinning line, leading to orientation-induced crystallization. Additionally, annealing improved the fibers' mechanical properties and thermal stability. These findings contradict the reported β to α retransformation observed elsewhere [166].

Composite fibers, in line with this concept, exhibit optimized and combined properties that arise from the incorporation of filler particles into a host polymer material [222,223]. When biodegradable plastics are filled with particles, it alters their rheological behavior, including melt strength and spin head pressure, as well as affecting crystallization, stretchability, ultimate diameters, and surface morphology. This approach is commonly used to introduce specific functionalities such as conductivity, color, or hydrophobicity to composite fibers. It is important to consider the size of the filler particles, which should typically be smaller than one-third of the final diameter of the fiber, and ensure their proper dispersion and distribution during the spinning and compounding processes. Incorporating fillers into the polymer matrix increases the resistance to flow, which can lead to fibers with larger diameters. The mechanical properties of biocomposite fibers heavily rely on the dispersion of fillers and their interaction with the polymer matrix, with interfacial adhesion playing a crucial role in controlling the transfer of stress between the polymer and the fillers during loading [31]. Additionally, the biodegradation of all added fillers (such as chain extenders, colors, reinforcing agents, modifiers, etc.) should be taken into account in the development of biodegradable fibers. Achieving good dispersion and interaction between the filler and the polymer matrix is essential for enhancing the resulting mechanical performance. The efficiency of dispersion, surface morphology, and size of the fiber blends depend on the composition and miscibility of the blend/compound, while processing parameters such as take-up speed and drawing ratio also significantly impact the final properties of the fibers. Gozdemir et al. [224] added low-cost soy fillers (residue and flour) to PLA to reduce material costs and increase the degradation rate. The presence of soy fillers accelerated the overall degradation of PLA/soy fibers by approximately 2-fold in a basic medium. This acceleration was attributed to the preferential dissolution of soy, leading to an increased surface area within the PLA matrix. However, due to the partial thermal degradation of both soy fillers at PLA melt temperature, they could only be melt-compounded into PLA up to a maximum of 5 wt%. Despite the reduction in melt drawability caused by the incorporation of solid soy fillers, it was still sufficient to produce fibers as thin as 25 to 50 μm using a nominal draw ratio of 100. In another study by Xue et al. [225], nano-hydroxyapatite was incorporated into PCL during melt-spinning to enhance the mechanical and medical performance of the fibers for bone tissue engineering applications.

Chen et al. [226] focused on producing thermochromic functional biodegradable fibers using PLLA and microcapsules through scalable melt-spinning. They achieved a yarn of 36 filaments with a hot drawing ratio of 3.6 and a take-up speed of 800 m/min. The PLA fibers exhibited excellent tenacity ranging from 370 to 470 mN/tex and demonstrated

reversible and stable thermochromic behavior over a temperature range of 31 °C. The performance of the fibers was attributed to the mesophase content and the nucleating effect of the microcapsules, which promoted the formation of microcrystals between the lamellae. However, the presence of a high concentration of microcapsules within the PLA fibers led to their agglomeration, hindering the formation of the mesophase and resulting in a decrease in fiber tenacity.

In addition to low thermal stability, PHAs also have low crystallization behavior, which is crucial in melt-spinning. To improve the crystallization behavior of PHAs for melt-spinning, researchers have explored various approaches such as polymer structure modification, nucleating additives, and processing adjustments. Hufenus et al. [227,228] modified the drawing setup for fiber-spinning of PHB by incorporating an intermediate godet in the draw-off direction. They used boron nitride (BN) as a nucleating agent and tri-n-butyl citrate (TBC) as a plasticizer. This approach led to improved melt strength, allowing the fibers to withstand the subsequent drawing procedure. The resulting crystalline structure exhibited a highly ordered amorphous phase trapped between the aligned lamellae of the crystalline α -phase. These fibers showed long-term stability, with a maximum tensile strength of 215 MPa at a 20% tensile strain. The researchers also found that TBC plasticizer inhibited secondary crystallization, which otherwise leads to brittleness and poor mechanical performance, as well as the conglutination of as-spun fibers. This approach resulted in PHB fibers with highly oriented crystalline morphology and acceptable mechanical properties. Hinuber et al. [211] investigated the melt-spinning of hollow PHB fibers using different nucleating agents such as boron nitride (BN), hydroxyapatite (HAP), and thymine (THY). However, when using a conventional extrusion spin line, the nucleation effect was not observed, and the fibers became sticky and unprocessable. Conventional nucleating agents such as boron nitride or talc cannot be used in medical applications due to their blood incompatibility. Vogel and coworkers [217] employed reactive extrusion with dicumyl peroxide (DCP) to enhance the crystallization behavior of PHB. The addition of DCP at concentrations of 0.2, 0.3, and 0.5 wt.% improved the crystallization behavior, allowing for higher draw ratios up to 7.5. The resulting fibers exhibited increased tensile modulus, tensile stress at break, and elongation at break compared to neat PHB. In a similar vein, Xiang et al. [229] used DCP and tungsten disulfide (WS₂) as initiators and heterogeneous nucleating agents in the reactive melt processing of PHBV. The composite fibers demonstrated high mechanical performance, a higher nucleation temperature, and a rapid crystallization rate due to the synergistic effect of heterogeneous nucleation, long chain branched structure, and draw-induced crystallization. The incorporation of WS₂ resulted in higher tensile strength (189 MPa) compared to neat PHBV fibers (34.01 MPa). In an unpublished internal work, Orotic Acid (OTA) was found to induce faster crystallization compared to other nucleating agents added to PHB powders [230].

In addition to nucleating agent-modified PHAs, Zhang et al. [88] employed tetramethylenedicarboxylic dibenzoylhydrazide (TMC-306) as a nucleating agent for PLLA. TMC-306 could be dissolved completely in the PLLA melt and, upon cooling, reorganize into fine fibrils. The presence of these nucleating agent fibrils acted as templates, inducing the growth of kebab-like PLLA lamellae perpendicular to their long axis. This resulted in PLLA fibers with superior mechanical strength (a significant increase of 78% in tensile strength) and enhanced heat resistance (a decline of 1069% in boiling water shrinkage). In a similar approach, Siebert et al. [231] utilized N,N'-bis(2-hydroxyethyl)-terephthalamide (BHET) as a nucleating agent by incorporating 1–2% in PLA. The objective was to compare its nucleating effect with talc, which served as a reference material, for industrial-scale melt-spinning. The fibers were spun at different take-up velocities (800, 1400, and 2000 m/min) and subjected to drawing at various ratios (1.1–4.0) until reaching a final winding speed of 3600 m/min. This study revealed that the fiber draw ratio and take-up velocity were the most influential factors impacting tenacity and elongation. However, the addition of BHET as a nucleating agent resulted in a reduction in the mechanical performance of the fibers. Consequently, BHET was not considered an efficient nucleating agent in this

context. Gu et al. [232] developed biodegradable fibers with good mechanical properties through the melt-spinning and hot drawing of in situ PBST/NP (NP = titanium tetraiso-propoxide and silica nanoparticles) nanocomposites. The nanoparticles (NPs) served as nucleating agents, enhancing the crystallization rate. The evolution of the fibers during uniaxial stretching was investigated in real-time using synchrotron radiation small-angle X-ray scattering, coupled with a thermomechanical setup, to analyze the effects of drawing temperatures and NPs on the lamellar structure. It was observed that the presence of NPs and high drawing temperatures facilitated the formation and perfection of new lamellae.

In their study, Aouat et al. [233] conducted the melt-spinning process to produce PLA fibers, as well as PLA/cellulose nanowhiskers (CNWs) and PLA/microcrystalline cellulose (MCC) composites loaded at 1 and 3 wt.%. They utilized PLA-grafted maleic anhydride (PLA-g-MA) as a compatibilizer and polyethylene glycol (PEG) as a plasticizer. The findings indicated that the incorporation of MCC into the PLA matrix, regardless of the loading rate, was not favorable for multifilament fiber spinning compared to CNWs. This was due to the limited drawability and inadequate dispersion of MCC within the PLA matrix. In contrast, Zhang et al. [234] employed twin-screw reactive extrusion followed by melt-spinning to perform in situ graft co-polymerization of L-lactide onto cellulose. This modification led to the formation of PLA long-chain branches, which hindered the thermal and photodegradation of regenerated cellulose and impeded cellulose crystallization. The resulting cellulose-graft-poly lactide blend fiber exhibited a smooth surface and ductile cross-section, attributed to the disruption of the hydrogen bond network of cellulose and the improved thermoplastic properties conferred by the PLA branches. In comparison to other commercially available cellulose fibers, the in situ graft copolymerization of cellulose with PLLA yielded cellulose-based fibers with superior mechanical properties.

In a different approach, Tran et al. [235] obtained PLA nanofibrils with an average diameter of 60 nm by processing PLA/polyvinyl alcohol (PVA) blends at a weight ratio of 30/70, followed by the removal of the PVA matrix. Different blend ratios were tested using a twin-screw microextruder before melt-spinning through a spinneret and subsequent continuous drawing to obtain PLA fibrils in a PVA matrix. The filament yarns were then woven into three-dimensional textile structures. Similarly, Zhang et al. [236] melt-spun PLLA/low density polyethylene (LDPE) blend fibers (24 filaments, 400 m/min take-up) using a similar approach, resulting in immiscibility and the formation of fibrillated PLA nanofibers with a minimum diameter of 92 nm after drawing and removal of the LDPE component. The fibers exhibited 60% crystallinity and high orientation. However, the removal of LDPE presented a significant challenge. In another work by Huang et al. [237], PLA/PGA blend fibers were produced to extract PGA nanofibers via dissolving PLA matrix in Chloroform. The same approach has been used by You et al. [238] on electro-spun PGA/PLA nanofibers. The melt-spinning process was conducted using a PGA/PLA ratio of 92/8 through a spinneret containing 24 holes (260 μm diameter) via a 1000–2500 m/min take-up speed. Their findings suggested that the PGA phase begins as minuscule granules within the molten PLA, transforms into nanoscale granules during the extrusion of filaments, and ultimately undergoes deformation into nanofibers in the resulting as-spun and drawn fibers. So far, nanofibers with a diameter of 93 nm have been achieved. They highlighted the miscibility of PLA and PGA. Meanwhile, Magazzini et al. [239] indicated the costly production of PGA and tried to blend it with PLA and PCL. They observed PGA domains with size-dependence to the polymer ratio. PGA content was even at 30%, while it accelerated the hydrolysis rate, particularly in the case of PLA. They indicated them as promising combinations. However, due to the rheological behavior and melt point difference, the processing of PGA/PCL might be challenging, especially for making a fiber. Liu et al. [240] used bifunctional isocyanate (HDI) along with multifunctional epoxy oligomer (ADR) as hybrid chain extenders for blending PLA/PGA through the reactive extrusion process. In addition, Deshpande et al. [241] blended PGA/PLA with different ratios and compared it with PLA/PCL. The blend of PLA/PCL is also used in electrospinning to make nanofibers [242]. Moreover, Akhir et al. [243] used polyethylene glycol (PEG)

in the 5–30 wt% range to blend with PLA and make finer fibers. This is attributed to the plasticization effect of PEG. Further studies on the blending of PLA, e.g., with PGA, PCL, PHB, PBAT, and other copolymers are reviewed elsewhere [244,245]. In a different work by Gupta et al. [246], poly(ϵ -caprolactone-*co*-lactide) PLCL is blended in 10–50 wt% with PCL. The compound is converted to a monofilament and drawn afterwards to make a filament 130 μ m in diameter. Although the pure PCL filament showed 60% crystallinity and 500 MPa strength, adding amorphous PLCL caused a reduction in both of these characteristics. The morphological results showed a rougher surface at higher PLCL content and also limited miscibility between PCL and PLCL. Furthermore, Li et al. [247] used hyper-branched polyesters (HBP) for the modification of PBAT, enabling the production of hydrophilic microfibers through centrifugal melt-spinning.

3.3. Bicomponent Filament Yarns and Staple Fibers

In addition to blending or compounding, two or more different polymers can make a single fiber with a distinguished boundary between them, known as a multicomponent with the desired configuration(s). Bicomponent fibers are a common example of multicomponent fibers comprising two co-extruded polymers forming a single fiber with one or more interfaces. The aim of this approach is to use/modify the properties of two polymers or to use the functionality of additives for specific purposes. Some more details can be found elsewhere [142,248,249]. Figure 6 shows typical examples of different cross-sections, which include the core/sheath (C/S) (concentric or eccentric), side-by-side (S/S), islands-in-the-sea (I/S), and segmented-pie configuration [54,248,250,251].

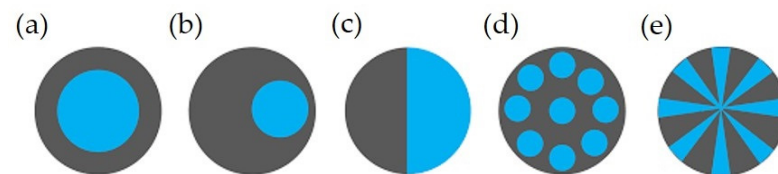


Figure 6. Different cross sections of bicomponent fibers: (a) core/sheath (concentric), (b) core/sheath (eccentric), (c), side-by-side, (d) islands-in-the-sea, and (e) Segmented pie [31]. Reprinted with permission.

The Advanced Fibers group at Empa (Switzerland) has performed several studies on the melt-spinning of bicomponent fibers from bio-based and biodegradable polymers, particularly PHAs. They reported that PHB and PHBV exhibit the crystallization rates required for extrusion processes [252]. They produced mono- and bicomponent filaments from PHBV (Enmat Y1000) and PLLA (Natureworks 6200D). According to their findings, PHB with a molecular weight of approximately 500,000 Da could not be drawn into fibers, mainly due to its low crystallization rate. This resulted in the formation of large spherulitic structures, leading to brittle fibers with poor mechanical properties. The presence of HV (hydroxyvalerate) in the PHBV copolymer could be controlled during biosynthesis and resulted in a reduction in crystallinity. However, it was not possible to produce pure PHBV fibers due to winding issues caused by the stickiness of the fiber. Similarly, Hufenus et al. [253] demonstrated the influence of the configuration of PLA and PHBV in bicomponent fibers on their processability. They found that fibers could be successfully produced when PHBV was used as the core and PLA as the sheath, whereas the opposite configuration resulted in processing difficulties. In their study, they achieved fibers with a maximum tensile modulus of 7.1 GPa using a core composition of 46 wt% PHBV and a sheath composition of 54% PLA. Additionally, they conducted *in vitro* biocompatibility tests as part of their investigation [228].

In their study, Shi et al. [126] conducted ultra-high-speed bicomponent spinning of PBT as the sheath and biodegradable PBAT as the core. They discovered that PBAT fibers exhibited a well-developed and highly oriented crystal structure similar to that of PBT, despite the inherent randomness and the 1:1 composition of PBAT. This phenomenon was

attributed to the unique mixed crystallization behavior of the butylene adipate and butylene terephthalate units present in PBAT. The bicomponent spinning process enhanced the processability of both polymer components in PBT/PBAT fibers due to the mutual interaction between the two polymer melts along the spin line. This improvement in processability was observed compared to the spinning of corresponding single-component fibers. Moreover, the structure development of the PBT component in PBT/PBAT fibers was significantly enhanced, resulting in improved thermal and mechanical properties. On the other hand, the structure development of the PBAT component was largely suppressed, leading to a nearly non-oriented structure in both the crystalline and amorphous phases. However, the sheath of the PBT/PBAT filament remained tacky even during winding, which posed challenges for filament take-up. This tackiness issue was attributed to the elastic nature and slow crystallization kinetics of PBAT, particularly when processed together with PBT. In the study by Prahsarn et al. [254], a bicomponent melt-spinning process was successfully employed to produce fibers from a blend of PLA and PBS in a high ratio of 50:50. The resulting bicomponent fibers exhibited a segmented-pie configuration and did not split, indicating good compatibility between PLA and PBS. Similarly, Yang et al. [255] utilized bicomponent melt-spinning to produce side-by-side fibers from PLLA and low-melting point PLDA (LM-PLA) with the aim of creating biodegradable 3D self-crimped yarns. They used a spinneret with 24 holes of 300 μm diameter, and the spun yarns were drawn and collected at a take-up speed of 2000 m/min. The resulting filaments had a diameter of 400 μm , and the strength and elongation at break were measured to be 3.01 cN/dtex and 15.1%, respectively. The effects of dry and wet heat treatment on the structure and properties of the filaments were also studied. It was observed that the crystallization ability of LM-PLA was weaker than that of PLA under the same conditions, which played a key role in the formation of the three-dimensional crimped structure of the fibers during heat treatment. Meanwhile, PVA is a water-soluble polymer that is sometimes mistakenly considered biodegradable in certain reports. In the study by Song et al. [256], the solubility of PVA was utilized to produce PA6/PVA islands-in-the-sea fibers and environmentally friendly ultra-fine PA6 fibers (2–5 μm) through a water-splitting process. The effects of sea/island mass ratios and different spinning speeds on the properties of PVA/PA6 islands-in-the-sea partially-oriented yarn (POY) were investigated. This technique can be used to produce microfilaments and ultra-fine fibers from bio-based or biodegradable polymers by combining them with PVA after plasticizer-assisted thermoplastic modification.

Some selected images of the discussed works are illustrated in Figure 7, while all the reported research is summarized in Table 2.

Table 2. Summary of recent studies on melt-spinning of biodegradable fibers, including materials, processing, physical performance, biodegradation, and application.

Author(s)	Polymer(s)	Processing	Performance(s)	Application	Ref.
Monocomponent fibers					
Mezghani et al. (1997)	PLLA	High-speed melt-spinning (up to 5000 m/min)	Best results at 3000 m/min, 43% crystallinity, 385 MPa, 6 GPa	Development for textiles	[89]
Schmack et al. (1998)	PLA	Yarn melt-spinning (12 F ² , 300 µm, DR ³ 6, 6000 m/min)	UTS ⁴ 430 MPa, UTM ⁵ 6 GPa, 20% crystallinity	Textiles	[150]
Yuan et al. (2000)	PLLA	Monofilament spinning (1 mm, 1 m/min), drawing	MW reduction, Ø 110 µm, 63% crystallinity, UTS 600 MPa	Textiles	[153]
Nazhat et al. (2001)	PLLA	Monofilament spinning through 1 mm die, DR of 4.8	Fibers with 260–300 µm diameter	Composite for bone tissue	[259]
Schmack et al. (2003)	PLA (1–8% D, 2–7 PDI)	Yarn melt-spinning (12 F, 300 µm, DR 6, 5000 m/min)	Better fibers at lower D content and PDI, higher speed, and DR	Textiles	[151]
Takasaki et al. (2003)	PLA (1.5, 8.1, 16.4% D)	Monofilament spinning (500 µm, 5000–10,000 m/min)	Better at low D%, high speed and DR (45% crystallinity, 570 MPa)	Textiles	[152]
Nishimura et al. (2004)	PLLA	12 Filaments spinning and 2-stage drawing in water	18 times drawing, 70% crystallinity, UTS 810 MPa	Technical	[154]
EL-Salmawy et al. (2004)	PLLA, P(LA-co-CL)	ProNectin F-coated hollow monofilament spinning	Higher adhesion PLLA fibers, better orientation hollow fibers	Nerve tissue regeneration	[197]
Baimark et al. (2005)	P(LL-co-CL)	2-step synthesis, piston-spinning 1 mm, water bath	Drawn filament, 160 µm, 530 MPa, 168 °C MP,	Absorbable surgical suture	[192]
Fambri et al. (2006)	PLDLA	Melt-spinning at below 100 m/min speed	Filaments 120 µm in diameter and UTS 200 MPa	Tissue engineering	[156]
Park et al. (2007)	PLA	Spinning at high speeds and batch heat treatment	Speed and heat, 69% crystallinity, 6 g/den, lower biodegradation	N/A	[144]
Kim et al. (2008)	PLLA	One-step melt-spinning process	Well-developed α-crystallites at high take-up speeds (3500 m/min)	Textile	[260]
Paakinaho et al. (2009)	PLDLA	Multifilament (8 and 12 F) spinning and hot drawing	High MW, faster thermal degradation, hydrolysis effect of lactide	Tissue repair	[155]
Tavanaie et al. (2014)	r-PLA	Monofilament spinning (1 mm, 70 m/min), cold draw	Strength: 491 MPa, orientation: 0.96, durability	Textiles and clothing	[200]
Naeimirad et al. (2018)	PLA	Hollow multifilament yarn	Liquid-filled, higher hollowness by increasing throughput	Agriculture and drug delivery	[195]
Ali et al. (2019)	PLA	POY and FDY spun filament yarns	Lower diameter and higher crystallinity @ 600 m/min	Textile and technical	[147]
Fuoco et al. (2019)	PLA, PLA-co-TCM	Melt-spinning (1800 m/min) and after drawing	17 µm filaments (125 den), 60% crystallinity, 302–610 MPa	Clothing textiles	[191]
Fu et al. (2019)	PLA	Spinning (300 m/min, DR 6) and chitosan dip-coating	Ø 253 µm, Strength 78.6 cN, EAB 57%	Acupoint catgut embedding	[179]
Chirag et al. (2021)	PLA	69 filaments melt-spinning with different parameters	62–1000 dtex, 25–340 mN/tex, 14–62% crystallinity	Textiles	[148]
Gordeyev et al. (2000)	PHB	High-drawn melt-spun yarns	DR of 2, and hot drawing and annealing resulted in 330 MPa	Research only	[261]
Yamane et al. (2001)	Non-pure PHB	Melt-spinning	Impurities for nucleating, fast crystallization, 300 micron fibers	Load bearing in medicine	[262]
Schmack et al. (2000)	PHB	Spinning with DR of 6.9 and speed up to 3500 m/min	Low crystal size with high rate, Strength of 27 cN/tex	Development	[263]
Iwata et al. (2004)	UHMW-PHB	Spinning, ice quenching, drawing, and annealing	Fiber diameter 40 µm, strength 1.3 GPa, modulus of 18.1 GPa	High-performance	[264]
Antipov et al. (2006)	PHB and copolymers	Optimized melt-spinning	Min thermal degradation, UTS 330 MPa, UTM 7.7 GPa	R&D	[265]
Tanaka et al. (2006)	PHBV	Spinning, ice quenching, drawing, and annealing	Suitable copolymer and spinning: UTS 1 GPa, UTM 8 GPa	High performance	[166]
Qing et al. (2015)	PHBH	Spinning at different temperatures, 500 µm spinneret	Better crystallization (α-crystal orientation) at high speeds	Technical	[158]
Krins et al. (2021)	PHA	Melt-spinning of different biodegradable filaments	Marine degradable	Maritime	[143,266]
Perret et al. (2019, 2020)	P3HB	Melt-spinning, stress-annealing	Low stress: viscoelastic (α crystal to mesophase transformation) high stress: high strength (UTS 184 MPa)	Shock-absorbing ductile textiles	[267–271]

Table 2. Cont.

Author(s)	Polymer(s)	Processing	Performance(s)	Application	Ref.
Rebia et al. (2020)	PHBH	Monofilament-spinning, isothermal crystallization, and drawing	Dip-coated biodegradable fibers	Drug delivery and the dyeing approach	[167]
Miyao et al. (2020)	PHBH	Liquid isothermal bath, mono (1 mm) melt-spinning	Better crystallization, 1000 m/min speed, UTS 170 MPa	Technical and textile	[165]
Omura et al. (2021)	PHBH	Gram scale spinner, 1 hole 1 mm, 1.8 m/min, DR 5	Elastic, marine biodegradable, UTS 200 MPa, 200% elongation	Agricultural, fishery, or medical	[164]
Selli et al. (2022)	PHBH	Monofilament spinning (500 μ m, L/D 4, 140–160 °C)	\varnothing 130 μ m, UTS 291 MPa, orientation 0.98, 35% crystallinity	Textile and medical	[168]
Murayama et al. (2023)	PHBH	Monofilament spinning, knot making	250 μ m knots, UTS 167 MPa, biodegradable (in vitro and in vivo)	Absorbable and safe suture	[193]
Mochizuki et al. (1997)	PCL	Melt-spinning	Effect of draw ratio on the mechanical properties of PCL filament	Biomedical	[113,114]
Charuchinda et al. (2003)	PCL	Small-scale monofilament melt-spinning	Effect of processing parameters on fiber properties like diameter	Biomedical and others	[115]
Park et al. (2013)	PCL	Profiled fibers via piston spinner	Faster degradation in NaOH solution due to high SSA	Tissue engineering	[199]
Krishnanand et al. (2013)	PCL	Intrinsic birefringence	UTM 3.473 GPa for crystalline and 0.071 GPa for amorphous	Amorphous orientation	[272]
Pal et al. (2013)	PCL	Reactive monofilament extrusion (BCY crosslinking)	Fiber diameter 66 μ m, UTS 2500 MPa, lower degradation	Tissue engineering	[257]
Gurarslan et al. (2014)	PCL-coalesced	Treatment in urea, monofilament spinning, drawing	Higher modulus and crystallinity due to intrinsic alignment	Tissue engineering	[170]
Selli et al. (2020)	PCL	Monofilament spinning, modified drawing	600 m/min, mesophase, 55% crystallinity, 59 μ m, 315 mN/tex	Technical and mechanical	[273]
Selli et al. (2019)	PCL	Melt-spinning with different cross sections	Hollow fibers and solid fibers with smooth surface	Technical and medical	[196]
Bauer et al. (2022)	PCL	Cross-section modified mono and multifilament	DR 9.25, 65% crystallinity, 690 mN/tex, Hermans orientation 0.9	Tendon and Ligament	[198]
Yang et al. (2007)	PGA	Melt-spinning (255 °C, 30 m/min)	Less internal stress, DR 5, UTS 654 mN/tex	Medical sutures	[215]
Guo et al. (2011)	PGA	Melt-spinning (240 °C, 20 m/min), DR (2–6 @40–50 °C)	Different degradation rates via IV, DR, and Drawing temperature	Biomedical	[181]
Fu et al. (2018)	PGA	Monofilament spinning and chitosan dip-coating	Higher mechanical, swelling, antibacterial, lower biodegradation	Acupoint catgut embedding	[178]
Fu et al. (2019)	PGA	Spinning (300 m/min, DR 6) and chitosan dip-coating	\varnothing 245 μ m, Strength 57.3 cN, EAB 18%	Acupoint catgut embedding	[179]
Saigusa et al. (2020)	PGA	Optimized melt-spinning (24F, 250 μ m, 245 °C)	Guide roller at 300 m/min, take-up at 1500 m/min, UTS 780 mN/tex	Biomedical	[118,175]
Miao et al. (2021)	PGA, PLGA (8% LA)	Extrusion (250 °C, DR 4.5 @ 60 °C, set @100–140 °C)	Faster degradation of PGA in PBS starting from amorphous	Biomedical	[182]
Shi et al. (2005)	PBAT (44% BT)	High speed melt-spinning (5000 m/min)	PBT-like crystal structure and good mechanical properties	Tough products	[82]
Yunes et al. (2011)	PBAT	Factorial DOE, spinning (30/55 F, 0.4 mm, 36 m/min)	Simulation (temperature, MFI, speed, orientation, crys%, etc.)	Biodegradable textiles	[184–189]
Mantia et al. (2017)	PBAT (Bioflex, Mater-Bi)	Extrusion via capillary, cold and hot after drawing	Orientation, high modulus, strength, and thermomechanical resistance	High performance mission	[274,275]
He et al. (2004)	PEA	Copolymerization, monofilament spinning, drawing	125 μ m, UTS 125 MPa, Alkaline reduction	N/A	[194]
Shi et al. (2006)	PBTSA	4 filaments yarn, 2000 m/min	Elastic yarn	Testing new copolymer	[126]
Li et al. (2010)	PBST	36F melt-spinning (1 mm), isothermal crystallization	UTS 360 MPa, 35% crystallinity, Tm 180 °C	Sustainable textiles	[109]
Bansode et al. (N/A)	PLGA	Melt-spinning and electro-spinning	Fine fibers (21–27 μ m), biocompatible, and degradable	Tissue engineering, drug delivery	[124,180]
Malafeev et al. (2017)	PLGA (90/10)	Microextruder spinning (\varnothing 1 mm, 20 m/min)	UTS 91 MPa	Bio-resorbable suture	[177]
Schick et al. (2023)	PBS TPS, and PBAT	Melt-spinning via FET-100, 48F, max 1000 m/min	DPF 4, 100 mN/tex < PP (500 mN/tex), 70% crystallinity	Lower mechanical performance	[87]
Kim et al. (2023)	PBSA	Provided by National Institute of Fisheries Science	80% biodegradation and physiochemical reduction via composting	Fish nets	[130]

Table 2. Cont.

Author(s)	Polymer(s)	Processing	Performance(s)	Application	Ref.
Blends and composite fibers					
Takasaki et al. (2003)	r-PLA (PLLA + PDLA)	Monofilament spinning (0.5 mm, 7500 m/min)	Ø 40 µm, 40% crystallinity, including stereocomplex, UTS 500 MPa	Technical	[221]
Furuhashi et al. (2006)	PLLA/PDLA	Melt-spinning, drawing, and annealing	Draw @90 °C, stereocomplex crystals, UTS 520 MPa, UTM 8.5 GPa	Textiles	[203]
P-Art et al. (2011)	PLA/PHBV (90/10)	Blend biofiber multifilament spinning	Effect of draw speed on tenacity and linear density	Socks knitting	[71]
M-Garcia et al. (2016)	PLA/(CNC)-g-PLLA	Composite fiber spinning along with grafting	Smooth surface, alignment of the CNC and PLA molecular chains	Specific high properties	[276]
Jompang et al. (2013)	PLA/PBS	Multifilament blend yarns	Miscibility at 10% of PBS	Modified textile yarns	[205]
Padee et al. (2013)	PLA/PTT	Blend fiber spinning via different ratios	Successful spinning at 10% PTT, Crystallinity improvement	Textile fibers	[204]
Persson et al. (2013)	PLA/HAP	Composite fibers	Rough surface	Biomedical	[277]
John et al. (2013)	PLA/CNW	Compounding (10 wt%) and melt-spinning (1–3 wt%)	Rough fibers, 90–95 µm, concentration of CNW, crystallinity	Biomedicine	[278]
Zhang et al. (2014)	PLLA-g-Cellulose	Reactive co-extrusion, direct spinning 500 m/min	Smooth surface, ductile cross-section, better properties 41 mN/tex	Textile	[234]
Tavanaie et al. (2014)	r-PLA/PP (0–50%)	Monofilament spinning (1 mm, 70 m/min), cold draw	Tenacity 430 mN/tex, 42% crystallinity, dyability	Textiles and clothing	[97,219]
Zhang et al. (2014)	PLLA/TMC-306 NA	Compounding (0.1–0.5 wt%) and spinning (18 F, 0.4 mm, 150 m/min), hot drawing (DR 2.5)	Optimum at 0.3 wt%, 57% crystallinity, UTS 600 MPa,	High performance textile fibers	[88]
Rizvi et al. (2014)	PLA/MWCNT	Composite fibers	Rough and irregular surface	Smart textiles	[279]
Hoai et al. (2014)	PLA/PVA	Blending, spinning (<100 m/min), water dissolving	Nanofibrils 60 nm in diameter, filament Ø 164 µm (243 DPF)	Scaffolds for tissue engineering	[235]
Zhang et al. (2014)	PLA/LDPE	Blend spinning (24 F, 0.3 mm, 400 m/min) and DR 2	Immiscible, Extraction, 92 nm PLA fiber, 60% crystallinity	Filtration	[236]
Li et al. (2015)	PLA/PHBV	Blend melt-spinning and hot drawing	Higher heat-resistance, softness, and tenacity	Textile	[218]
Pisva-Art et al. (2016)	PLA/PBSA	Blending, fiber spinning, drawing 4 times, annealing	Modify brittleness of PLA, UTS 300 MPa	Textile	[209]
Hassan et al. (2017)	PLA/PBS	Blend fiber spinning	Effect of PBS ratio (ductility)	Healthcare products	[208]
Huang et al. (2018)	PLA (92%)/PGA (8%)	Blend spinning (24F, 260 µm, DR 1.4, 2500 m/min)	93 nm diameter nanofibers	Tissue Engineering	[237]
Aouat et al. (2018)	PLA/MA/CNW, MCC	Composite fiber spinning	Poor dispersion for MCC (Vs. CNW), fillers alter the diameter	Biomedical, technical	[233]
Panichsombat et al. (2019)	PLA/PBS	Blend fibers	Miscibility via PBS below 10%	Textile fibers	[206]
Gilmore et al. (2019)	PLA/PLA-co-PCL	Blend modified process	Grooved fibers with wicking performance	Wicking	[280]
Visco et al. (2019)	PLA/LTI/PCL	Reactive extrusion (160 °C, air quench, after drawing)	Thread filament 300 µm diameter, UTS 45 MPa, EAB 450%	Absorbable antibacterial sutures	[215]
Li et al. (2019)	PLLA/POM	Blending, melt-spinning (72 F, 300 µm), Drawing	Modification, higher crystallinity via drawing, 791 MPa, hydration	Technical	[210]
Chen et al. (2020)	PLA/PHBH	65/35 the best ratio for crystallization	UTS 904 MPa, UTM 28.42 GPa, EAB 81%	Balanced performance	[216]
Güzdemir et al. (2020)	PLA/Soy	Composite biofiber, 3 spinning holes-500 µm	Larger and non-uniform diameter, 56 MPa	Disposable nonwoven fabrics	[224]
Akhir et al. (2021)	PLA/PEG	Fine melt-spun fibers	Diameter reduction by PEG concentration (18 µm)	Ductility, and surface roughness	[243]
Barral et al. (2021)	PLA/PCL (10 to 40%)	Mono (1 mm), and multifilament (80 F, 50–70 µm)	Adding PCL reduced hydrolytic degradation of PLA in DMEM	Bioresorbable implants	[212]
Chen et al. (2022)	PLLA/microcapsules	Compounding, powder mixing, melt-spinning	Mesophase content, 470 mN/tex, Thermochromic effect	Smart textiles	[226]
Siebert et al. (2022)	PLA/BHET	48 F, 250 µm, spinning through FET-100, 3000 m/min	Slow nucleating effect, 50% crystallinity, 270 mN/tex	Textile and technical	[231]
Huang et al. (2022)	PLA/PCL	EIReP, piston spinning (0.3 mm, 2000 m/min)	Better melt strength and elastic behavior, lower crystallinity	Testing the compound	[202]

Table 2. Cont.

Author(s)	Polymer(s)	Processing	Performance(s)	Application	Ref.
Vogel et al. (2007)	P3HB/DCP	Melt-spinning and drawing by max ratio of 7	Nucleating effect, about 200 MPa UTS	Textile	[217]
Hinüber et al. (2011)	PHB/PCL	Blend hollow fibers	Phase separation in spinning due to Tm difference	Biomedical	[211]
Hinuber et al. (2011)	P3HB/NA	Nucleating-assisted hollow fiber piston-spinning	Regular surface and an inner diameter of between 50 and 500 μm	Nerve repair with artificial tubes	[211,258]
Kabe et al. (2012)	PHB/UHMW-PHB	Blend film casting, nucleation via 5–10% UHMW	Faster crystallization, β -form crystals, slower degradation	Biodegradable alternatives	[281]
Hufenus et al. (2015)	P3HB/NA	Nucleating, intermediate draw-off spinning	Induced oriented crystallization, stability, and 215 MPa strength	Textile yarns	[227]
Xiang et al. (2019)	PHBV/DCP/WS2	Monofilament spinning (0.5 mm, 550 m/min)	UTS 189 MPa, heterogeneous nucleation, branching, 73% crys	Textiles	[229]
Gupta et al. (2012)	PCL/PLCL (10–50%)	Monofilament extrusion and drawing	UTS 500 MPa, 60% crystallinity. Reduction by PLCL content.	Biomedical	[246]
Xue et al. (2019)	PCL/HAP	Composite fibers	Enhanced mechanical performance	Bone scaffold	[225]
Park et al. (2010)	PBS/PBAT	Blend monofilament melt-spinning (80 m/min)	Tensile strength reduction in more than 5% PBAT content	Technical	[207]
Zhou et al. (2016)	PBS/MFC	Composite yarns	Effect of drawing and take-up speed on dispersion of filler	Extensive	[282]
Gu et al. (2019)	PBST/NP	In situ polymerization and spinning	150 dtex yarn, UTS 240 MPa, 42.3% crystallinity, orientation 0.54	High-performance	[232]
Li et al. (2021)	PBAT/HBP	Centrifugal melt-spinning	Hydrophilic microfibers	Medical	[247]
Multicomponent fibers					
Shi et al. (2006)	PBAT/PBT	Bico (core/sheath)	Structure development of PBT (via PBAT)	Thermo-bonds	[126]
M. Zinn et al. (2010)	PHBV/PLA	Bico (PHBV only in core possible)	No toxicity	Medical tendon repair	[252]
Hufenus et al. (2012)	PHBV/PLA	Bico melt-spinning (PHBV core and PLA sheath)	UTS 410 MPa for PLA, 340 MPa for bico	Medical	[228,253]
Prahsarn et al. (2016)	PLA/PBS	Hollow segmented-pie bicomponent fibers	Good compatibility, 132 mN/tex, EAB 101%, 25 μm diameter	Biomedical, technical	[254]
Yang et al. (2020)	PLA/LM-PLA	Side-by-Side bicomponent melt-spinning (24 F)	3D structure after self-crimping, 400 μm , 300 mN/tex,	Alternative of PET/PTT	[255]

² Filaments. ³ Drawing Ratio. ⁴ Ultimate Tensile Strength. ⁵ Ultimate Tensile Modulus.

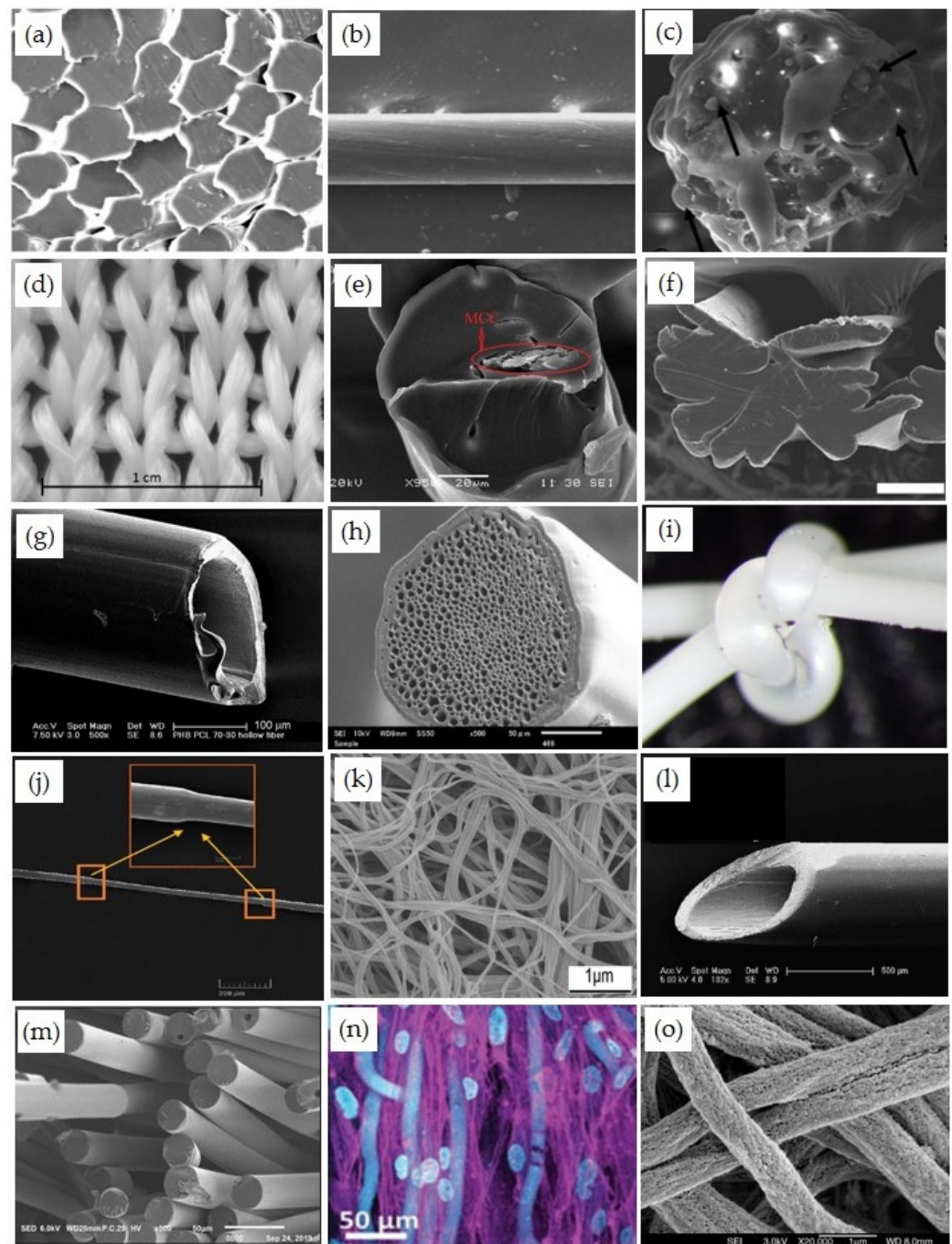


Figure 7. Some photos from melt-spun biodegradable polymer fibers: (a) PBS fibers with 30 micron diameter [117], (b) BC- treated PCL fiber [257], (c) PLA fibers containing 5% soy [224], (d) 3D woven structure from PLA fibers derived from PLA/PVA blend [235], (e) PLA/PLA-g-MA/MCC composite fiber [233], (f) PCL monofilament with Snowflake cross-section [198], (g) Hollow fiber of PHB/PCL 70/30 [211], (h) PHBH monofilaments one-step-drawing after 24 isothermal crystallization [167], (i) Surgical knot on PHBH monofilament [193], (j) Irregularity (necking point) on drawn r-PLA filament [200], (k) Extracted PLLA nanofibers from PLLA/LDPE [236], (l) Hollow PHB fibers [258], (m) PLA/PEG fibers [243], (n) F-actin (magenta) and cell nuclei on PGA fibers [123], and (o) porous ultrafine PGA fibers by dissolving PLA in spun blend fiber [238]. All the figures were reprinted with permission from the publishers.

4. Discussion

The extensive work that has been performed so far, which is summarized in this literature review, shows the complexity of making biodegradable fibers via melt-spinning biodegradable plastics. Furthermore, the complexity of environmental parameters and biodegradation steps can be considered in application (if the fiber is spun with the desired performance). This is due to interconnection (illustrated in Figure 8) between different aspects of the polymer itself, processing parameters, mechanical properties of the fibers, the target application requirements, biodegradation, and the effect of the end-of-life environment. Meanwhile, there are different barriers, such as thermal instability of biodegradable polymers, low crystallization rate, low T_g and melting point, and low intensity for biodegradation in some environments, particularly the oceans, that are the final destination of most of the microplastics. Therefore, a detailed understanding of all the aspects and the subsequent discussion about the relations between the parameters are essential [283].

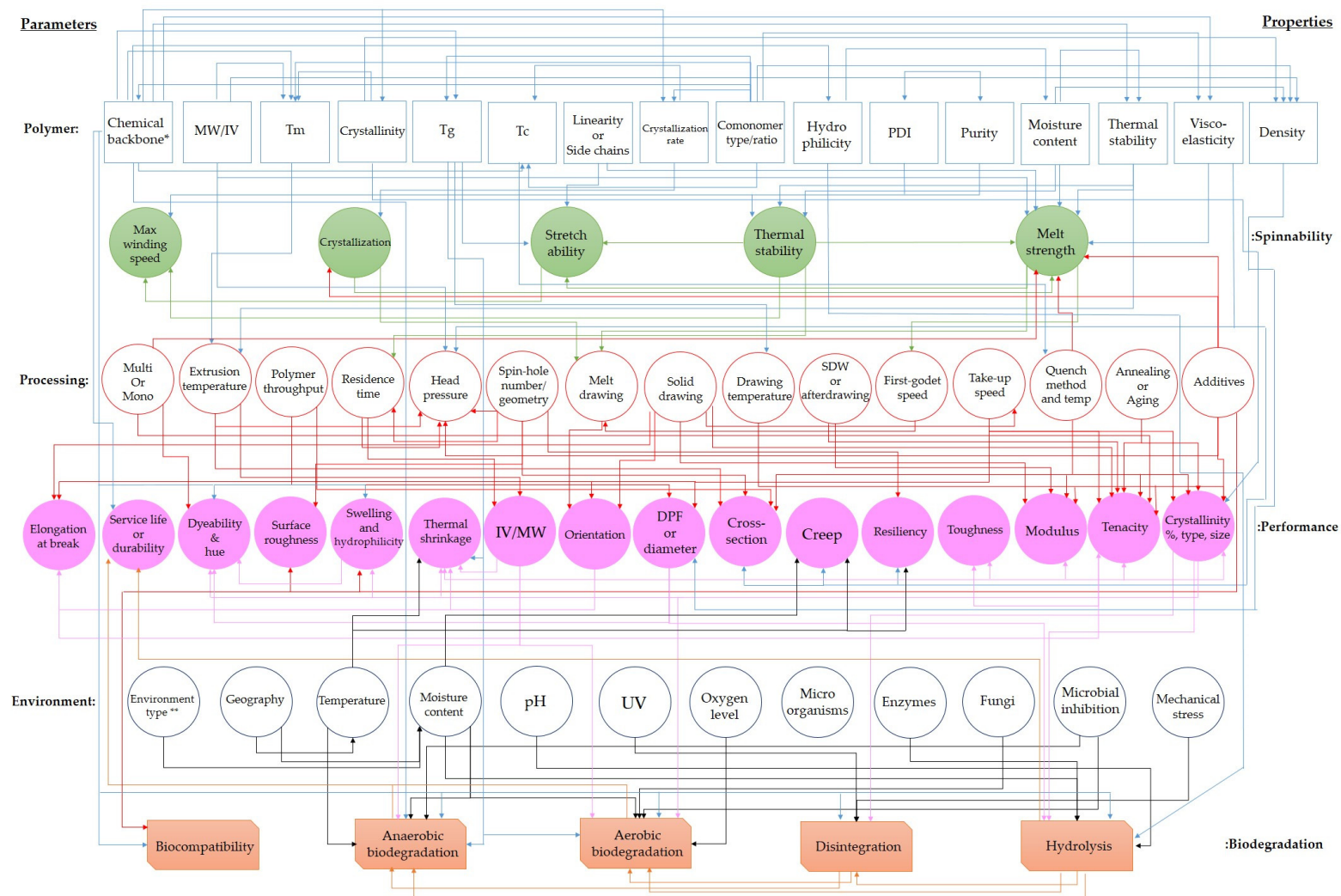


Figure 8. Schematic illustration of the complex correlation between effective parameters (with polymer or compound origin, processing parameters, and environmental conditions) and the processability, performance, and biodegradation of melt-spun biodegradable fibers. * Functional groups, aromatic/aliphatic segments, branches, copolymer type (block, random), etc. ** Compositing (industrial or home), soil, fresh water, marine, in vitro (PBS), in vivo, etc.

4.1. Processing

For good process control and sufficient fiber properties, Hufenus et al. [54] suggested five crucial properties a polymer should have:

1. Thermal stability: The polymer should have sufficient thermal stability to withstand the extrusion temperature and shear strain during processing without significant degradation or cross-linking.
2. Low polydispersity index: The polymer should have a relatively low polydispersity index to ensure consistent melt flow rheology. A polydispersity index below three is often desired for a stable melt-spinning process.
3. Appropriate molecular weight: The polymer should have an appropriate molecular weight that provides enough melt strength to prevent filament breakage during processing. It should not be too viscous to impair processability.
4. Uniformity and purity: The polymer should be uniform and free from impurities to prevent clogging of the processing equipment and fluctuations in the processing conditions.
5. Linear structure: Linear polymers (versus branched) are preferred for melt-spinning because their molecular chains can easily unfold and align along the strain direction, facilitating orientation and crystallization and improving fiber properties.

For instance, PHAs have garnered interest in addressing the processing challenges associated with thermal degradation and low crystallization behavior, thereby enabling the production of desirable filament yarns at desired speeds. Researchers such as Gordeyev et al. [261] and Schmack et al. [263] have explored the influence of temperature and drawing speed on the crystallization behavior of PHB. Some research groups have even patented biodegradable aliphatic polyester fibers [284,285]. Iwata et al. [264] have also successfully produced high-strength PHB fibers (1 GPa) through sophisticated quenching, drawing, and annealing techniques. This complex procedure may be challenging for industrial implementation. Their investigations, utilizing wide-angle X-ray diffraction (WAXD) and various microscopy techniques, revealed the core-sheath structure of the fibers, with the sheath consisting of α -form crystals and the core consisting of both α - and β -form crystals. The quenching process resulted in faster cooling of the fiber sheath, leading to higher crystallinity in the core region. Subsequently, Kabe et al. [281] prepared blend films by solvent-casting of PHB and UHMW-PHB (ultra-high molecular weight poly(3-hydroxybutyrate)) at different ratios (95/5 and 90/10) and subjected them to cold-drawing. Their results showed that the maximum radial growth rate of spherulites and the corresponding temperature were identical for films of different compositions.

However, the blend films exhibited a shorter half-time of crystallization compared to PHB alone, attributed to UHMW-PHB acting as a nucleating agent. Through 12 rounds of stretching, the resulting films demonstrated a tensile strength of 242 MPa. X-ray diffraction analysis indicated that the cold-drawn films with high tensile strength contained both helix (α -form) and planar zigzag (β -form) conformations, suggesting a correlation between film strength and the amount of β -form structure. The researchers also proposed a mechanism for the crystallization process.

Indeed, the use of nucleating agents is a well-known technique to promote crystallization in polymers. Nucleating agents introduce inhomogeneities into the polymer melt, serving as sites for nucleation and leading to an increase in the number of nuclei and the crystallization rate while simultaneously reducing the spherulite size [286]. Typically, the size of nucleation agents is around 3 μm , and boron nitride has been identified as one of the most effective nucleating agents for PHB [287]. In addition to nucleating agents, the processability of copolyesters can be significantly improved by incorporating a stiff chain segment through the copolymerization of aliphatic polyesters with an aromatic liquid crystal element [95]. This incorporation of a rigid component enhances the polymer's ability to align and crystallize, leading to improved melt-processing properties. These strategies, such as nucleating agents and copolymerization, contribute to the optimization

of polymer processing by promoting crystallization and improving the processability of the materials.

As a summary, melt-spinning, particularly of biodegradable plastics, is a sensitive polymer processing method (shown in Figure 8), for which all the relevant parameters (such as MW, moisture content, melt viscosity, thermal degradation, melt strength, crystallization behavior, T_g , etc.) need to be considered for successful trials toward the proposed yarn/fiber desired for the target application. However, some approaches are mentioned for overcoming the challenges, such as using the most suitable biodegradable thermoplastic polymer or the right (high) MW, controlling the processing temperatures, using an isothermal bath to alter the quenching rate, adding nucleating agents to alter crystallization, blending with complementary polymers or additives, adjusting the speeds or drawing the filaments in molten, cold, or hot states, and many other possibilities that need to be tested. Furthermore, the fiber diameter tends to decrease with increasing winding speed and spinning temperature. As the spinning temperature increases, the melt viscosity decreases and the extent of fiber stretching increases; hence, the diameter decreases. Furthermore, the higher processing temperature may cause lower head pressure (due to viscosity decrement), thermal degradation of biodegradable plastics, and dripping or spinning instabilities, while at a higher temperature, it takes longer for heat to dissipate when the fiber cools. In contrast, a lower processing temperature will result in higher melt viscosity, pressure build-up in the spin beam (due to the elastic behavior and incomplete melting), and faster crystallization due to the nucleating action of persistent crystals [143].

4.2. Crystallinity and Orientation

The properties of melt-spun biodegradable fibers, such as thermal properties, mechanical performance, and biodegradation rate, are strongly influenced by the degree of crystallinity and molecular orientation within the fiber structure. While crystallinity affects the mechanical properties of polymers, molecular orientation is considered a secondary factor in controlling the overall mechanical properties of fibers [31]. However, both crystallinity and orientation are influenced by various factors, including the polymer's molecular structure, crystallization rate, and nucleating additives, as well as processing parameters such as temperatures, drawing techniques, drawing ratios, take-up speed, quenching rate, and annealing [31,82]. By carefully tailoring these processing parameters, crystallinity and crystal orientation can be enhanced, leading to improved fiber properties [265,273].

It is important to note that while crystallinity and crystal orientation contribute to the mechanical properties of fibers, there is evidence suggesting that crystals may persist during biodegradation. For example, studies have shown that increasing spinning speed and heat treatment can result in higher crystallinity and tenacity in melt-spun PLA fibers but lower biodegradation rates [144]. Similarly, highly oriented non-crystalline mesophases have been observed in drawn PCL filaments, indicating the influence of crystallinity, crystal size, and crystal perfection on the mechanical properties [273]. Additionally, optimizing the polymer structure and its processing parameters can minimize thermal degradation effects, as observed in as-spun PHB fibers with higher crystallinity displaying hard elasticity [265]. Copolymers with high comonomer content, on the other hand, exhibit lower crystallinity [164,265]. The presence of stiff benzene rings in PBAT fibers contributes to their high molecular orientation and crystallization behavior, leading to high intrinsic birefringence and molecular rigidity [82]. Furthermore, well-developed crystallites and crystallite orientations have been achieved in PLLA fibers at higher uptake speeds, highlighting the importance of molecular orientation in crystallization and mechanical properties [260].

Zhou et al. [282] observed the formation of a shish-kebab structure in PBS/MFC (Microfibrillated cellulose) fibers at high take-up speeds, which was attributed to interfacial crystallization. They investigated the effect of hydroxyl apatite (HAP) filler loading and drawing ratio on the fiber properties and found that the crystallinity of the as-spun fibers increased with HAP concentration. However, for drawn fibers, the crystallinity showed a remarkable improvement but decreased with increasing HAP content [277].

Melt-spinning of virgin PHAs, particularly PHB, poses several challenges, including rapid thermal degradation, low melt elasticity, and control of the crystalline structure. PHB has a low crystallization rate due to its low nucleation density and brittleness, as well as variations in molecular weight and polymer quality [70,288]. To address these challenges, researchers have explored various approaches. One approach is the use of plasticizers or copolymers that lower the melting temperature, thereby increasing the processing window and preventing thermal degradation [289]. Additionally, researchers have investigated different parameters, such as temperature and drawing conditions, to control crystallization during melt-spinning. Various additives and electron beam techniques have also been explored [70]. These strategies aim to enhance the processability and improve the crystalline structure of PHA fibers.

Modifying the physical properties of PHA fibers can also be achieved by controlling the type of crystals that form within the fibers. Applying mechanical stresses to the fibers while maintaining a specific temperature can induce changes in crystal structure, specifically between spherulite- α and fibril- β forms [290]. Research by Isaka et al. [166] has shown that the second drawing of PHA fibers increases crystal orientation and promotes the conversion of amorphous phases to β -form crystals, resulting in improved tensile properties (Figure 9). On the other hand, annealing and relaxation processes lead to a reduction in β -form crystals and a conversion to α -form crystals, resulting in lower tensile properties. The emphasis is placed on increased chain orientation rather than solely focusing on reducing thermal degradation. These findings align with the research conducted by Yang et al. [93], which investigated the β -to- α phase transition in PHBV films through in situ WAXD, SAXS, and DSC analyses. The mesophase content within the fibers is another important factor influencing fiber structure and final properties, as observed in both PCL and PHB fibers [168,268,291].

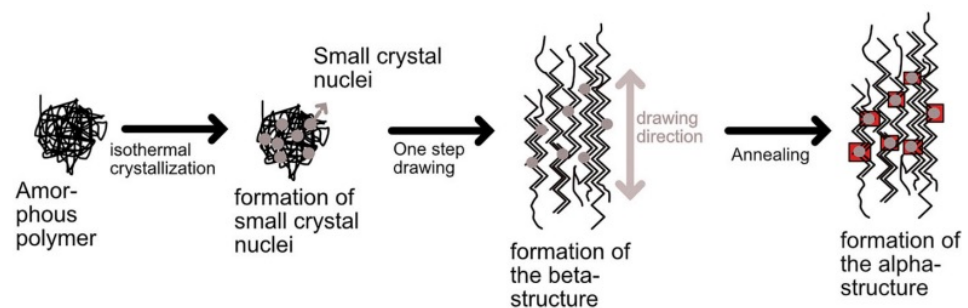


Figure 9. Schematic illustration from the conversion of α -crystals (represented by red boxes) and β -crystals (represented by zigzag lines) during quenching, drawing, and annealing steps [166]. Reprinted with permission.

As a summary, crystallization and orientation are crucial for achieving desirable mechanical properties in the melt-spinning of biodegradable plastics. However, some polymers, such as PHAs, have limitations (thermal degradation and low crystallization rate) that show up via sticking to the godet or other challenges in the spinning process. Adding nucleating agents can solve the problem; however, only to some extent. To the best of our knowledge, no multifilament yarn has been made from pure PHA so far. With the concept, some copolymerization designs may help crystallize or even have an inverse effect. Moreover, processing parameters, e.g., drawing temperature, drawing ratio, quench rate and annealing, and take-up speed, can affect crystallinity. The most preferable crystal types in fibers are in β -form, while spherulites can cause brittleness of the fibers. Orientation-induced crystallization and mesophase contents can affect crystallinity in fiber processing positively. A narrow crystal size distribution, crystal perfection, and orientation of crystals, as well as mesophase content, are all important factors that influence the mechanical properties of polymer fibers [273].

4.3. Physical-Mechanical Characteristics

The processability of polymer materials and the properties of fibers are influenced by various factors. Intrinsic properties of the polymer, such as viscosity and melt strength, have an impact on melt processability. Additionally, the crystallization behavior of the polymer can affect both the spinnability of the fibers and their final performance. The processing of biodegradable polymers poses challenges due to their poor melt strength and low thermal stability. To overcome these challenges and improve processability and performance, techniques such as blending biodegradable plastics (e.g., PLA/PHA) or incorporating comonomers during synthesis (e.g., PHBV) are commonly employed. Achieving good miscibility between the polymer components and controlling the crystallization rate are important considerations. It is worth noting that thermal degradation can occur during processing, leading to a reduction in molecular weight, particularly in the pre-compounding stage [31,266]. The physical and mechanical characteristics of fibers, such as cross-section, diameter or fineness, strength, elongation, stiffness, and crystallinity, are influenced by both the inherent properties of the polymer and the processing parameters employed during fiber formation (details can be seen in Figure 8).

Mantia et al. [275] emphasized the challenges in obtaining biodegradable polymer fibers with suitable mechanical properties for specific applications. They highlighted the importance of crystallinity and orientation control as key factors in tailoring the mechanical properties of the fibers. To investigate this further, they conducted a systematic study on the influence of cold stretching on the mechanical and thermomechanical properties of fibers made from different biodegradable polymer systems. Additionally, they examined the effect of hot drawing on the mechanical properties of the same fibers, which were melt-spun from Mater-Bi and Bioflex (commercial PBAT) [274]. The results revealed that orientation significantly affected the mechanical properties, and factors such as relaxation time, crystallization temperatures, and cooling rates had contrasting effects on the mechanical behavior of the fibers. Furthermore, mechanical properties were found to be influenced not only by the relative amounts of α - and β -form crystals but also by molecular orientation and total crystalline content [263]. These findings demonstrate that by controlling the processing conditions and altering the fiber structure, it is possible to achieve high tensile strength in biodegradable fibers [166]. The molecular weight of a polymer typically influences the tensile strength of melt-spun fibers. However, Taneka et al. [292] reported that the molecular orientation achieved through drawing has a greater impact on the mechanical properties than the molecular weight itself. In another study by Pal et al. [257], using bilactone, bis-(ϵ -caprolactone-4-yl) (BCY) in melt-spinning of PCL resulted in crosslinking of the polymer, compensating for the molecular weight reduction that occurs under melt-spinning conditions. This approach led to monofilament fibers with a tenacity as high as 2500 MPa. The inclusion of BCY through covalent attachment to PCL chains provided additional stability to the macromolecular architecture, and the polymer chain orientation remained relatively unaffected during fiber formation. This compensation for molecular weight reduction is particularly significant for PCL, which is highly sensitive to melt-spinning conditions. In another report by the same group, Aminlashgari et al. [293] mentioned in situ crosslinking of PCL by BCY to compensate for molecular weight reduction during melt-spinning. They also performed electrospray ionization-mass spectrometry to understand the effect of BCY loading and crosslinking on the final biodegradation rate. Antipov et al. [265] observed reversible recovery of spun PHA sample dimensions upon loading and unloading, indicating a behavior characteristic of hard-elastic fibers. They also observed the reversible formation of a strain-induced columnar mesophase with a pseudohexagonal arrangement of conformationally disordered chains, along with the orthorhombic crystalline and amorphous phases of the initial material. This strain-induced reversible formation of the mesophase in both PHA homopolymers and copolymers was classified as a mechano-thermotropic phenomenon. In a separate study, Persson et al. [277] observed a remarkable increase in elongation-at-break from 11% to 186% by varying the drawing temperature.

As a summary, in addition to the biodegradable plastics' intrinsic characteristics, e.g., chemical backbone, copolymer structure and type, blend composition, molecular weight, crystallinity and re-crystallization behavior, and so on, melt-spinning parameters such as spinning temperature, take-up speed and draw ratio, and draw temperature have a significant role in determining the final structure and properties of the fibers, including fiber diameter, mechanical properties, molecular orientation and crystallinity, and composting or biodegradation rate in different environments [31,195].

4.4. Biodegradation

Biodegradability is a significant advantage of melt-spun fibers, particularly in situations where the end-life or recycling options are uncertain [53]. The ability to undergo true and fast biodegradation without the release of toxic chemicals can be beneficial in settings where other forms of recycling may not be available. However, further research is needed to fully understand the impact of microplastics as intermediates in the biodegradation process [1]. The rate and time of biodegradation depend on various factors, such as physico-chemical and microbial aspects, material properties, processing history, and environmental conditions [70]. Factors including polymer crystallinity, surface morphology, side-chain length, shape, moisture, temperature, UV exposure, nutrition levels, mechanical stress, types of available bacteria, pH, and oxygen levels can influence the biodegradation process within its different steps [36].

Researchers have made efforts to enhance the strength and properties of biodegradable plastics without compromising their biodegradability. It is crucial to find a balance between improving mechanical properties and maintaining biodegradability, which requires further investigation [294]. In some studies, the focus has been on processing and mechanical evaluations, while the biodegradation aspect has been referred to material certificates, other studies, applications, or future works [192]. Chen et al. [95] conducted a review on aromatic/aliphatic copolyesters based on aliphatic and aromatic diacids, diols, and ester monomers, aiming to combine excellent mechanical properties with biodegradability. Kabe et al. [281] demonstrated enzymatic degradation of cold-drawn blend films using PHA depolymerase, suggesting that the rate of enzymatic degradation can be controlled by the addition of ultra-high molecular weight PHB (UHMW-PHB). Kim et al. [130] conducted an industrial composting test on PBEAS fishnets, resulting in 82% mineralization after 45 days in aerobic conditions with a weight loss of 78.4%. They also reported a significant reduction in the molecular weight and mechanical properties of these fishnets. XRD and DSC analysis showed no significant changes in crystallinity and crystal properties even after decomposition, indicating simultaneous biodegradation in the crystalline and amorphous regions (this is in conflict with some other aforementioned reports about PGA fibers). This approach was suggested as a replacement for Nylon 6,6 fishnets to address pollution in the seas and oceans. The incorporation of fertilizers can be beneficial for soil fertility upon degradation of the material. For example, PLA-based geotextiles have shown improvements in soil fertility as the polymer degrades in soil [31]. However, this bio-based polymer does not include any elements such as phosphate or sulfur for this purpose. Gonsalves et al. [295] investigated the hydrolytic degradation in buffer solution and the biodegradation by fungi of two types of non-alternating PEAs. They found that the random PEAs were readily degradable under the attack of the fungus *Cr. laurentii*. Biodegradation of this copolymer occurred through surface erosion catalyzed by enzymes, while abiotic hydrolysis occurred both on the surface and in the bulk of the copolymer [194].

As a summary, some studies reported exactly the amount of CO₂ evolution as the right evidence of biodegradation. However, there are also studies that investigate the oxygen demand. Moreover, weight loss, MW, crystallinity, and mechanical property reduction are considered; however, they are mostly looking at disintegration (the first phase of biodegradation). That means, as long as the polymer is not converted to biomasses (CO₂, water, and methane), there can be no claim on biodegradation. This became more critical when disintegrated polymer parts or oligomers became more hazardous when they could

not be utilized by the aforementioned organisms. Another issue for consideration is that biodegradation needs to happen in the desired condition and after the life of the product. Meanwhile, different material parameters, e.g., polymer structure, crystallinity, surface-to-volume ratio (SSA), hydrophilicity, and so on, are effective in biodegradation, while end-life environmental conditions (either composting, soil, fresh water, or marine) such as temperature, moisture content, oxygen level, light and UV, pH, available microorganisms and fungi, and many others can influence the biodegradation pathways and rate.

5. Applications

According to a report published by European Bioplastics [4], about 13% of all bio-based and biodegradable plastics produced are used for fiber production (almost close to the number of 14.9% mentioned in Figure 1 for the portion of the textile market from plastic production). This equates to around 300,000 tons per year, of which PLA alone accounts for a considerable portion. Biodegradable polymers other than those mentioned previously are often considered to have limited importance in textile applications due to factors such as high cost or poor textile properties [117]. While biodegradable polymers have the potential to replace conventional fibers in certain applications, they still face limitations such as low melt strength, thermal degradation, limited processing temperature range, moisture absorption and hydrolysis sensitivity, high cost, processability challenges, and low mechanical properties, which hinder their widespread use [296]. However, efforts have been made to address these drawbacks through various strategies, including the development of biphasic structures such as copolymers, blends, or composites through compounding. These approaches, including copolymerization during synthesis, as mentioned in previous sections, significantly contribute to property modifications, particularly in terms of biodegradation rate and mechanical properties, while also helping to lower the cost of the final product. Compounding and structural modifications of polymers with chain extenders have proven beneficial in enhancing melt strength. Additionally, reducing the melt-spinning temperature can increase the melt viscosity and strength of the material. Blending with another bio-based or biodegradable polymer can also help to improve melt strength. It is important to ensure that the material is adequately dried to remove any excess moisture absorbed before processing. This drying process is necessary during melt compounding as well as spinning [31].

Biodegradable polymers have applications in short-lived scenarios where end-of-life biodegradation is not a concern [31]. Various biodegradable polymers can be suitable for different application lifetimes. For example, Prambauer et al. [131] evaluated the potential use of biodegradable polymers such as PBS, PHBV, and PBAT in short-life geotextile applications. Melt-spun biodegradable fibers can also find applications in other short-term uses, such as agricultural woven or non-woven bags for nut picking and horticulture twines [297].

In the medical sector, biodegradable fibers are extensively used for absorbable surgical sutures. PGA, PLGA, and PHAs are among the biodegradable polymer materials commonly employed in these sutures. Chang et al. [69] provided a comprehensive review of medical fibers, including the clinical applications of biodegradable plastic fibers. They noted that PGA and PLGA sutures are resorbable within 60 days, while silk sutures are permanent. Furthermore, biodegradable polymer fibers have been explored for tissue engineering and biomolecule delivery systems. Miranda et al. [298] conducted a review highlighting various spun fibers from biodegradable plastics for these applications. Gilmore et al. [280] produced woven fabric using grooved wicking fibers made of PLA and PLA-co-CL for medical purposes. Fan et al. [299] investigated the 3D orientation of microvascular structures using biodegradable plastic fibers. Additionally, PLLA fibers have been used for reinforcing hydroxyapatite in bone tissue engineering, as reported by Nazhat et al. [259]. They performed dynamic mechanical analysis to simulate the physiological loading of the composite. PHA materials/products, including melt-spun fibers, have shown potential for pharmaceutical and therapeutic applications [300]. Andriano et al. [301] indicated

the fast biodegradation rate of PGA and the slow biodegradation of PLLA as limitations for some biomedical applications, such as tissue engineering. Therefore, they developed modified PLDLA copolymers (with 5–15% D content) for making melt-spun and drawn (3–9 times) yarns for this purpose. Aromatic and aliphatic copolyesters are emerging as a new class of biodegradable materials that can replace certain conventional plastics in biomedical and environmentally friendly fields [95]. Melt-spun biodegradable fibers find applications in melt-binding fibers, hygiene articles, and other products that require less robust physical properties [87]. As already mentioned, geotextiles are another area where melt-spun biodegradable fibers can be used [131]. Meanwhile, companies such as Senbis Polymer Innovation have developed various bio-based polymer fibrous products for technical applications in agriculture, gardening, fishing, and more. Some examples, e.g., biodegradable trimmerline (GreenLine), biodegradable artificial grass (GreenBlade), horticulture twine (GreenTwine), marine degradable mussel socks, and dolly rope, are shown in Figure 10 [297,302].

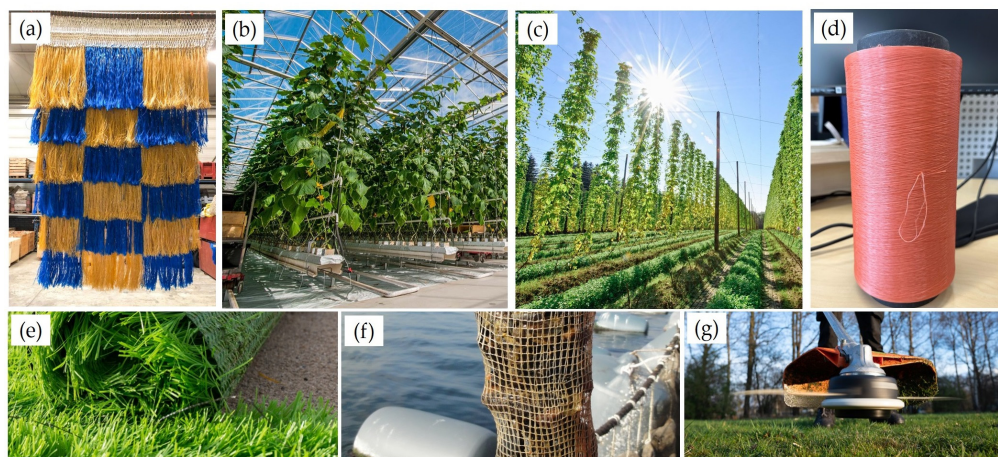


Figure 10. Some melt-spun biodegradable developments: (a) marine degradable fishing net protection (Dolly rope), (b) compostable horticulture twine (GreenTwine); (c) compostable hope rope; (d) biodegradable textile yarn; (e) biodegradable artificial grass (GreenBlade); (f) marine degradable mussel socks; and (g) biodegradable trimmerline (GreenLine) [297]. Reprinted with permission.

PGA has been applied for biomedical applications, e.g., surgical sutures, due to its excellent biodegradability [118]. So far, many commercial products such as Dexon[®], Maxon[™], Polysorb[™], and Vicryl[®] are known on the market [237]. More information about the biomedical applications of PGA can be found elsewhere [123].

Last but not least, textiles, including apparel products, remain the main market for the application of spun biodegradable fibers, particularly as an alternative to polyester fibers, which will pave the way for the green transition. Meanwhile, other functionalities, e.g., flame-retardancy, soft finishing, sustainable dyeing, etc., on biodegradable fibers can be considered for better textile performances.

6. Conclusions

Recent advances in the melt-spinning of biodegradable fibers are presented. Although biodegradable polymers face certain barriers (e.g., thermal degradation, low crystallization rates, and limited melt strength) when it comes to melt-spinning, researchers have demonstrated the ability to achieve significant results by modifying either the co-polymer structure/compound or the spinning process. These advancements include achieving even take-up speeds exceeding 7000 m/min, tensile strength of 1 GPa, modulus of 10 GPa, and 70% crystallinity. Most studies focus on establishing correlations between polymer structure, melt-spinning parameters, and the biodegradation assessment environment, as these factors profoundly affect processing, fiber performance, and biodegradation rates. These

interconnections are illustrated schematically. Biodegradable fibers represent a promising solution for textiles and other fibrous products with unclear end-lives, especially in addressing the issue of MP pollution in oceans. Furthermore, copolymers have yielded more promising results compared to homopolymers or blends. This is due to the avoidance of polymer incompatibilities and the preservation of mechanical strength and recyclability/degradability, which tend to become more complex as the number of different materials within a product increases. Additionally, copolymers offer greater flexibility in tailoring performance attributes. However, the selection of the most suitable material should be based on the intended application and the required performance criteria. Moreover, the compilation of studies provides a comprehensive overview of the polymers used in this context, as well as other process details and outcomes, which can serve as a foundation for future research endeavors aimed at bridging existing gaps and facilitating the development of biodegradable fibers for various sectors.

7. Outlook

There is a main issue to be pointed out for melt-spun biodegradable fibers, which is that processability, mechanical properties, and biodegradation rate are often conflicting objectives. In other words, generating materials with the desired mechanical performance and spinnability while at the same time having a high biodegradation rate is a difficult task. That means having a good processable polymer that results in a high-performance fiber [303] and leads to a marine degradable product [45,304] is a mission with many barriers [305]. For instance, high MW and crystallization behavior are necessary for thermal stability and feasible spinning, and high mechanical properties and crystalline structures are in conflict with biodegradability. Moreover, aromatic groups are needed in the polymer backbone for better fracture toughness, while they can lower the biodegradation rate. Furthermore, biodegradability may limit the lifetime or durability of the final product. Likewise, degradable fibers are only desirable in some applications. However, optimization is always possible, and there is hope for going toward a polymer fiber that is desirable for the target application, durable for the long term, and biodegradable in the end-life environment in accordance with sustainability goals. To achieve this, it is of utmost importance to know the properties of polymers, especially those properties that interfere with the processability or durability of the products that are manufactured with them, in order to create new ways to improve them, taking into account the processes by which their degradation mechanisms are carried out. So far, these suggestions can be mentioned as an outlook:

- Using bio-based materials in parallel with biodegradation is more preferable, while shifting to Carbon Capture Utilization (CCU) is considered.
- Adjusting the final performance of biodegradable fibers based on the final application demands a balanced, smart strategy.
- Finding the best biodegradable alternative for polyester fibers for textiles and fashion brands that is competitive in different aspects of physical properties, comfort, and price while also being more sustainable.
- The influence of further textile-processing methods such as crimping or texturizing, twisting, waving, or knitting, and finishing and dyeing (especially chemicals) on the final textiles/clothes (from performance and biodegradation aspects) can be interesting and should be more intensively investigated.
- Drawbacks such as low melting points and low glass transition temperatures, poor degradation resistance to high temperatures and poor hydrolytic resistance to strong alkaline conditions, high elongation requirements, and relatively poor storage stability should be taken into account when finding an appropriate solution in production and processing methods.
- Field tests in actual application situations such as comfort, wearing, washing, and fastness of biodegradable textiles should be studied.

- Decreasing the price of bio-based and biodegradable polymer fibrous products by increasing production volume can also pave the way for marketing and expansion of their applications.

Exploration of new synthetic routes is required to lower the price of biodegradable materials with desirable physical properties. The design of new bio-polyesters [306–308] or copolymers [108,309–311] and the incorporation of appropriate comonomers or functional groups have to be conducted to expand the properties, elucidate the relationships between the structures and properties, and optimize the spinnability of biodegradable polymers. Finally, it is worth mentioning that some of these objectives are under consideration within the running “PolyBioDeg” project [283,312] and also other proposed projects [28] by Senbis Polymer Innovations for paving the way in the roadmap [313] for the development of biodegradable polymers and fiber applications.

Author Contributions: Conceptualization, M.N. and B.K.; writing—original draft preparation, M.N.; writing—review and editing, M.N., B.K. and G.-J.M.G.; visualization, final edits, and remarks B.K. and G.-J.M.G. All authors have read and agreed to the published version of the manuscript.

Funding: This research was funded by the European Union’s Horizon research and innovation program under the Marie Skłodowska-Curie Actions Postdoctoral Fellowship (MSCA-PF) with the grant agreement number 101110810 (PolyBioDeg).

Institutional Review Board Statement: Not applicable.

Informed Consent Statement: Not applicable.

Data Availability Statement: The data presented in this study are available on request from the corresponding author(s).

Acknowledgments: The authors would like to acknowledge the European Commission for the financial support provided through the Marie Skłodowska-Curie Actions Postdoctoral Fellowship (MSCA-PF) under the European Commission Horizon program for the PolyBioDeg project with grant agreement number 101110810. Also, the authors would like to thank Gerard Nijhoving and Jeroen van der Vlist for their valuable support during the project.

Conflicts of Interest: The authors declare no conflict of interest.

References

1. Rosenboom, J.-G.; Langer, R.; Traverso, G. Bioplastics for a circular economy. *Nat. Rev. Mater.* **2022**, *7*, 117–137. [CrossRef]
2. Andrady, A.L.; Neal, M.A. Applications and societal benefits of plastics. *Philos. Trans. R. Soc. B Biol. Sci.* **2009**, *364*, 1977–1984. [CrossRef] [PubMed]
3. Plastics Europe. *Plastics—The Facts 2019*; Plastics Europe: Brussels, Belgium, 2019.
4. Available online: https://docs.european-bioplastics.org/publications/market_data/2022/Report_Bioplastics_Market_Data_2022_short_version.pdf (accessed on 15 August 2023).
5. Geyer, R.; Jambeck, J.R.; Law, K.L. Production, use, and fate of all plastics ever made. *Sci. Adv.* **2017**, *3*, e1700782. [CrossRef] [PubMed]
6. Gruter, G.-J.M. Using carbon above the ground as feedstock to produce our future polymers. *Curr. Opin. Green Sustain. Chem.* **2022**, *40*, 100743. [CrossRef]
7. Narancic, T.; Cerrone, F.; Beagan, N.; O’Connor, K.E. Recent advances in bioplastics: Application and biodegradation. *Polymers* **2020**, *12*, 920. [CrossRef]
8. Defruyt, S. Towards a new plastics economy. *Field Actions Sci. Rep. J. Field Actions* **2019**, 78–81.
9. Jambeck, J.R.; Geyer, R.; Wilcox, C.; Siegler, T.R.; Perryman, M.; Andrady, A.; Narayan, R.; Law, K.L. Plastic waste inputs from land into the ocean. *Science* **2015**, *347*, 768–771. [CrossRef]
10. Narancic, T.; O’Connor, K.E. Microbial biotechnology addressing the plastic waste disaster. *Microb. Biotechnol.* **2017**, *10*, 1232. [CrossRef]
11. Laborda, E.; Del-Busto, F.; Bartolomé, C.; Fernández, V. Analysing the Social Acceptance of Bio-Based Products Made from Recycled Absorbent Hygiene Products in Europe. *Sustainability* **2023**, *15*, 3008. [CrossRef]
12. Bucci, K.; Tulio, M.; Rochman, C. What is known and unknown about the effects of plastic pollution: A meta-analysis and systematic review. *Ecol. Appl.* **2020**, *30*, e02044. [CrossRef]
13. Hong, M.; Chen, E.Y.-X. Chemically recyclable polymers: A circular economy approach to sustainability. *Green Chem.* **2017**, *19*, 3692–3706. [CrossRef]

14. Alberti, C.; Enthaler, S. Depolymerization of End-of-Life Poly (lactide) to Lactide via Zinc-Catalysis. *ChemistrySelect* **2020**, *5*, 14759–14763. [CrossRef]
15. Wei, R.; Breite, D.; Song, C.; Gräning, D.; Ploss, T.; Hille, P.; Schwerdtfeger, R.; Matysik, J.; Schulze, A.; Zimmermann, W. Biocatalytic degradation efficiency of postconsumer polyethylene terephthalate packaging determined by their polymer microstructures. *Adv. Sci.* **2019**, *6*, 1900491. [CrossRef] [PubMed]
16. Roohi; Zaheer, M.R.; Kuddus, M. PHB (poly- β -hydroxybutyrate) and its enzymatic degradation. *Polym. Adv. Technol.* **2018**, *29*, 30–40. [CrossRef]
17. European Commission. The Waste Incineration Directive. 2000. Available online: <http://ec.europa.eu/environment/archives/air/stationary/wid/legislation.htm> (accessed on 15 August 2023).
18. European Commission. *A European Strategy for Plastics in A Circular Economy*; European Commission: Brussels, Belgium, 2018.
19. Miri, S.; Saini, R.; Davoodi, S.M.; Pulicharla, R.; Brar, S.K.; Magdouli, S. Biodegradation of microplastics: Better late than never. *Chemosphere* **2022**, *286*, 131670. [CrossRef] [PubMed]
20. United Nations. *Strengthening Actions for Nature to Achieve the Sustainable Development Goals*; United Nations: New York, NY, USA, 2022.
21. Tian, L.; van Putten, R.J.; Gruter, G.J.M. Plastic pollution. The role of (bio) degradable plastics and other solutions. In *Biodegradable Polymers in the Circular Plastics Economy*; Wiley-VCH: Weinheim, Germany, 2022; pp. 59–81.
22. Iheanacho, S.; Ogbu, M.; Bhuyan, M.S.; Ogunji, J. Microplastic pollution: An emerging contaminant in aquaculture. *Aquac. Fish.* **2023**, *8*, 603–616. [CrossRef]
23. Amato-Lourenço, L.F.; Carvalho-Oliveira, R.; Júnior, G.R.; dos Santos Galvão, L.; Ando, R.A.; Mauad, T. Presence of airborne microplastics in human lung tissue. *J. Hazard. Mater.* **2021**, *416*, 126124. [CrossRef]
24. Leslie, H.A.; Van Velzen, M.J.; Brandsma, S.H.; Vethaak, A.D.; Garcia-Vallejo, J.J.; Lamoree, M.H. Discovery and quantification of plastic particle pollution in human blood. *Environ. Int.* **2022**, *163*, 107199. [CrossRef]
25. Center for International Environmental Law (CIEL). Plastic & Climate. The Hidden Costs of a Plastic Planet. 2020. Available online: <https://www.ciel.org/plasticandclimate/> (accessed on 15 August 2023).
26. Kershaw, P. *Marine Plastic Debris and Microplastics—Global Lessons and Research to Inspire Action and Guide Policy Change*; United Nations Environment Programme: New York, NY, USA, 2016.
27. World Economic Forum (WEF). *Top 10 Emerging Technologies 4–15 (WEF, 2019)*; World Economic Forum: Cologny, Switzerland, 2023.
28. A Biodegradable Fibre as Polyester Replacement for Textiles, Maritime Forum. 2022. Available online: <https://maritime-forum.ec.europa.eu/en/node/7480> (accessed on 15 August 2023).
29. Hannover, I. *Biopolymers—Facts and Statistics*; Institute for Bioplastics and Biocomposites—Hochschule Hannover: Hannover, Germany, 2021.
30. Arikan, E.B.; Ozsoy, H.D. A review: Investigation of bioplastics. *J. Civ. Eng. Arch.* **2015**, *9*, 188–192.
31. Motloung, M.P.; Mofokeng, T.G.; Mokhena, T.C.; Ray, S.S. Recent advances on melt-spun fibers from biodegradable polymers and their composites. *Int. Polym. Process.* **2022**, *37*, 523–540. [CrossRef]
32. Spierling, S.; Knüpfer, E.; Behnsen, H.; Mudersbach, M.; Krieg, H.; Springer, S.; Albrecht, S.; Herrmann, C.; Endres, H.-J. Bio-based plastics-A review of environmental, social and economic impact assessments. *J. Clean. Prod.* **2018**, *185*, 476–491. [CrossRef]
33. Nofal, R.M. Biodegradable Textiles, Recycling, and Sustainability Achievement. In *Handbook of Biodegradable Materials*; Springer: Berlin/Heidelberg, Germany, 2023; pp. 1449–1485.
34. Chen, X.; Memon, H.A.; Wang, Y.; Marriam, I.; Tebyetekerwa, M. Circular Economy and sustainability of the clothing and textile Industry. *Mater. Circ. Econ.* **2021**, *3*, 12. [CrossRef]
35. Sharma, V.; Sehgal, R.; Gupta, R. Polyhydroxyalkanoate (PHA): Properties and modifications. *Polymer* **2021**, *212*, 123161. [CrossRef]
36. Acharjee, S.A.; Bharali, P.; Gogoi, B.; Sorhie, V.; Walling, B. Alemtoshi PHA-based bioplastic: A potential alternative to address microplastic pollution. *Water Air Soil Pollut.* **2023**, *234*, 21. [CrossRef]
37. Cai, Y.; Yang, T.; Mitrano, D.M.; Heuberger, M.; Hufenus, R.; Nowack, B. Systematic study of microplastic fiber release from 12 different polyester textiles during washing. *Environ. Sci. Technol.* **2020**, *54*, 4847–4855. [CrossRef]
38. Cai, Y.; Lin, J.; Gimeno, S.; Begnaud, F.; Nowack, B. Country-Specific Environmental Risks of Fragrance Encapsulates Used in Laundry Care Products. *Environ. Toxicol. Chem.* **2022**, *41*, 905–916. [CrossRef]
39. Cai, Y.; Mitrano, D.M.; Hufenus, R.; Nowack, B. Formation of fiber fragments during abrasion of polyester textiles. *Environ. Sci. Technol.* **2021**, *55*, 8001–8009. [CrossRef]
40. Patti, A.; Acierno, D. Towards the sustainability of the plastic industry through biopolymers: Properties and potential applications to the textiles World. *Polymers* **2022**, *14*, 692. [CrossRef]
41. De Haan, W.P.; Quintana, R.; Vilas, C.; Cózar, A.; Canals, M.; Uviedo, O.; Sanchez-Vidal, A. The dark side of artificial greening: Plastic turfs as widespread pollutants of aquatic environments. *Environ. Pollut.* **2023**, *334*, 122094. [CrossRef]
42. Armstrong, M. Where the Ocean’s Microplastics Come From, 2022. Available online: <https://www.statista.com/chart/17957/where-the-oceans-microplastics-come-from/> (accessed on 15 August 2023).
43. Stanvay, D. Plastic entering oceans could nearly triple by 2040 if left unchecked—Research. *Reuters*, 8 March 2023.
44. Michael, C. Plastic in the depths: How pollution took over our oceans. *The Guardian*, 25 July 2022.

45. Manshoven, S.; Smeets, A.; Malarciuc, C.; Tenhunen-Lunkka, A.; Mortensen, L.F. *Microplastic Pollution from Textile Consumption in Europe*; VTT: Espoo, Finland, 2022.
46. *Microplastics from Textiles: Towards a Circular Economy for Textiles in Europe*; European Environment Agency: Copenhagen, Denmark, 2022.
47. Cesa, F.S.; Turra, A.; Baruque-Ramos, J. Synthetic fibers as microplastics in the marine environment: A review from textile perspective with a focus on domestic washings. *Sci. Total Environ.* **2017**, *598*, 1116–1129. [[CrossRef](#)]
48. Habib, R.Z.; Thiemann, T. Microplastic in the marine environment of the Red Sea—A short review. *Egypt. J. Aquat. Res.* **2022**, *48*, 383–388. [[CrossRef](#)]
49. MacArthur, E. *Beyond Plastic Waste*; American Association for the Advancement of Science: Washington, DC, USA, 2017; Volume 358, p. 843.
50. Babaahmadi, V.; Amid, H.; Naeimirad, M.; Ramakrishna, S. Biodegradable and multifunctional surgical face masks: A brief review on demands during COVID-19 pandemic, recent developments, and future perspectives. *Sci. Total Environ.* **2021**, *798*, 149233. [[CrossRef](#)] [[PubMed](#)]
51. Wiedemann, S.G.; Nguyen, Q.V.; Clarke, S.J. Using LCA and Circularity Indicators to Measure the Sustainability of Textiles—Examples of Renewable and Non-Renewable Fibres. *Sustainability* **2022**, *14*, 16683. [[CrossRef](#)]
52. Dusselier, M.; Lange, J.-P. *Biodegradable Polymers in the Circular Plastics Economy*. John Wiley & Sons: Hoboken, NJ, USA, 2022.
53. Science Advice for Policy by European Academies. *Biodegradability of Plastics in the Open Environment*; Evidence Review Report No. 8; SAPEA: Brussels, Belgium, 2020; pp. 52–57.
54. Hufenus, R.; Yan, Y.; Dauner, M.; Kikutani, T. Melt-spun fibers for textile applications. *Materials* **2020**, *13*, 4298. [[CrossRef](#)] [[PubMed](#)]
55. Bao, H.; Hong, Y.; Yan, T.; Xie, X.; Zeng, X. A systematic review of biodegradable materials in the textile and apparel industry. *J. Text. Inst.* **2023**, 1–20. [[CrossRef](#)]
56. Flury, M.; Narayan, R. Biodegradable plastic as an integral part of the solution to plastic waste pollution of the environment. *Curr. Opin. Green Sustain. Chem.* **2021**, *30*, 100490. [[CrossRef](#)]
57. Narayanan, M.; Kandasamy, S.; Kumarasamy, S.; Gnanavel, K.; Ranganathan, M.; Kandasamy, G. Screening of polyhydroxybutyrate producing indigenous bacteria from polluted lake soil. *Heliyon* **2020**, *6*, e05381. [[CrossRef](#)]
58. Narancic, T.; Verstichel, S.; Reddy Chaganti, S.; Morales-Gamez, L.; Kenny, S.T.; De Wilde, B.; Babu Padamati, R.; O'Connor, K.E. Biodegradable plastic blends create new possibilities for end-of-life management of plastics but they are not a panacea for plastic pollution. *Environ. Sci. Technol.* **2018**, *52*, 10441–10452. [[CrossRef](#)]
59. Nakajima, H.; Dijkstra, P.; Loos, K. The recent developments in biobased polymers toward general and engineering applications: Polymers that are upgraded from biodegradable polymers, analogous to petroleum-derived polymers, and newly developed. *Polymers* **2017**, *9*, 523. [[CrossRef](#)]
60. Mecking, S. Nature or petrochemistry?—Biologically degradable materials. *Angew. Chem. Int. Ed.* **2004**, *43*, 1078–1085. [[CrossRef](#)]
61. Rai, P.; Mehrotra, S.; Priya, S.; Gnansounou, E.; Sharma, S.K. Recent advances in the sustainable design and applications of biodegradable polymers. *Bioresour. Technol.* **2021**, *325*, 124739. [[CrossRef](#)] [[PubMed](#)]
62. Leja, K.; Lewandowicz, G. Polymer biodegradation and biodegradable polymers—A review. *Pol. J. Environ. Stud.* **2010**, *19*, 255–266.
63. Polman, E.M.; Gruter, G.-J.M.; Parsons, J.R.; Tietema, A. Comparison of the aerobic biodegradation of biopolymers and the corresponding bioplastics: A review. *Sci. Total Environ.* **2021**, *753*, 141953. [[CrossRef](#)] [[PubMed](#)]
64. Nanda, S.; Patra, B.R.; Patel, R.; Bakos, J.; Dalai, A.K. Innovations in applications and prospects of bioplastics and biopolymers: A review. *Environ. Chem. Lett.* **2022**, *20*, 379–395. [[CrossRef](#)]
65. Emadian, S.M.; Onay, T.T.; Demirel, B. Biodegradation of bioplastics in natural environments. *Waste Manag.* **2017**, *59*, 526–536. [[CrossRef](#)]
66. Chen, S.; Wu, Z.; Chu, C.; Ni, Y.; Neisiany, R.E.; You, Z. Biodegradable elastomers and gels for elastic electronics. *Adv. Sci.* **2022**, *9*, 2105146. [[CrossRef](#)]
67. Vinod, A.; Sanjay, M.; Suchart, S.; Jyotishkumar, P. Renewable and sustainable biobased materials: An assessment on biofibers, biofilms, biopolymers and biocomposites. *J. Clean. Prod.* **2020**, *258*, 120978. [[CrossRef](#)]
68. Ganesh, S.; Lakshmanan Saraswathy, J.; Raghunathan, V.; Sivalingam, C. Extraction and characterization chemical treated and untreated lycium ferocissimum fiber for epoxy composites. *J. Nat. Fibers* **2022**, *19*, 6509–6520. [[CrossRef](#)]
69. Chang, C.; Ginn, B.; Livingston, N.K.; Yao, Z.; Slavin, B.; King, M.W.; Chung, S.; Mao, H.-Q. *Medical fibers and biotextiles*. In *Biomaterials Science*; Academic Press: Cambridge, MA, USA, 2020; pp. 575–600.
70. Kopf, S.; Åkesson, D.; Skrifvars, M. Textile Fiber Production of Biopolymers—A Review of Spinning Techniques for Polyhydroxyalkanoates in Biomedical Applications. *Polym. Rev.* **2023**, *63*, 200–245. [[CrossRef](#)]
71. Pivsa-Art, S.; Srisawat, N.; Narongchai, O.; Pivasupree, S.; Pivsa-Art, W. Preparation of knitting socks from poly (lactic acid) and poly [(R)-3-hydroxybutyrate-co-(R)-3-hydroxyvalerate](PHBV) blends for textile industrials. *Energy Procedia* **2011**, *9*, 589–597. [[CrossRef](#)]
72. Alaswad, S.O.; Mahmoud, A.S.; Arunachalam, P. Recent Advances in Biodegradable Polymers and Their Biological Applications: A Brief Review. *Polymers* **2022**, *14*, 4924. [[CrossRef](#)] [[PubMed](#)]

73. Nair, N.; Sekhar, V.; Nampoothiri, K.; Pandey, A. Biodegradation of biopolymers. In *Current Developments in Biotechnology and Bioengineering*; Elsevier: Amsterdam, The Netherlands, 2017; pp. 739–755.
74. Narayan, R.; Balakrishnan, S.; Kubik, D.A.; Gencer, M.A. Biodegradable Polymer Masterbatch, and a Composition Derived Therefrom Having Improved Physical Properties. U.S. Patent US8008373B2, 30 August 2011.
75. Yang, Y.; Zhang, M.; Ju, Z.; Tam, P.Y.; Hua, T.; Younas, M.W.; Kamrul, H.; Hu, H. Poly (lactic acid) fibers, yarns and fabrics: Manufacturing, properties and applications. *Text. Res. J.* **2021**, *91*, 1641–1669. [[CrossRef](#)]
76. Van den Oever, M.; Molenveld, K.; van der Zee, M.; Bos, H. *Bio-Based and Biodegradable Plastics: Facts and Figures: Focus on Food Packaging in the Netherlands*; Wageningen Food & Biobased Research: Wageningen, The Netherlands, 2017.
77. Van der Zee, M. 1. Methods for evaluating the biodegradability of environmentally degradable polymers. In *Handbook of Biodegradable Polymers*; De Gruyter: Berlin, Germany, 2020; pp. 1–22.
78. Van der Zee, M.; Stoutjesdijk, J.; Van der Heijden, P.; De Wit, D. Structure-biodegradation relationships of polymeric materials. 1. Effect of degree of oxidation on biodegradability of carbohydrate polymers. *J. Environ. Polym. Degrad.* **1995**, *3*, 235–242.
79. Mochizuki, M.; Hirami, M. Biodegradable fibers made from truly-biodegradable thermoplastics. In *Polymers and Other Advanced Materials: Emerging Technologies and Business Opportunities*; Springer: Berlin/Heidelberg, Germany, 1995; pp. 589–596.
80. Tavanaie, M.A. Engineered biodegradable melt-spun fibers. In *Engineered Polymeric Fibrous Materials*; Elsevier: Amsterdam, The Netherlands, 2021; pp. 191–232.
81. Available online: https://docs.european-bioplastics.org/publications/EUBP_Facts_and_figures.pdf (accessed on 20 August 2023).
82. Shi, X.; Ito, H.; Kikutani, T. Characterization on mixed-crystal structure and properties of poly (butylene adipate-co-terephthalate) biodegradable fibers. *Polymer* **2005**, *46*, 11442–11450. [[CrossRef](#)]
83. Espinosa, M.J.C.; Blanco, A.C.; Schmidgall, T.; Atanasoff-Kardjalieff, A.K.; Kappelmeyer, U.; Tischler, D.; Pieper, D.H.; Heipieper, H.J.; Eberlein, C. Toward biorecycling: Isolation of a soil bacterium that grows on a polyurethane oligomer and monomer. *Front. Microbiol.* **2020**, *11*, 404. [[CrossRef](#)]
84. Terzopoulou, Z.; Tsanaktis, V.; Bikiaris, D.N.; Exarhopoulos, S.; Papageorgiou, D.G.; Papageorgiou, G.Z. Biobased poly (ethylene furanoate-co-ethylene succinate) copolyesters: Solid state structure, melting point depression and biodegradability. *RSC Adv.* **2016**, *6*, 84003–84015. [[CrossRef](#)]
85. Olabisi, O.; Adewale, K. *Handbook of Thermoplastics*; CRC Press: Boca Raton, FL, USA, 2016; Volume 41.
86. Gruter, G.J.M.; Lange, J.P. Tutorial on Polymers—Manufacture, Properties, and Applications. In *Biodegradable Polymers in the Circular Plastics Economy*; Wiley-VCH: Weinheim, Germany, 2022; pp. 83–111.
87. Schick, S.; Groten, R.; Seide, G.H. Performance Spectrum of Home-Compostable Biopolymer Fibers Compared to a Petrochemical Alternative. *Polymers* **2023**, *15*, 1372. [[CrossRef](#)]
88. Zhang, H.; Bai, H.; Liu, Z.; Zhang, Q.; Fu, Q. Toward high-performance poly (L-lactide) fibers via tailoring crystallization with the aid of fibrillar nucleating agent. *ACS Sustain. Chem. Eng.* **2016**, *4*, 3939–3947. [[CrossRef](#)]
89. Mezghani, K.; Spruiell, J. High speed melt spinning of poly (L-lactic acid) filaments. *J. Polym. Sci. Part B Polym. Phys.* **1998**, *36*, 1005–1012. [[CrossRef](#)]
90. Roungpaisan, N.; Takasaki, M.; Takarada, W.; Kikutani, T. Mechanism of fiber structure development in melt spinning of PLA. In *Poly (Lactic Acid) Synthesis, Structures, Properties, Processing, Applications, and End of Life*; John Wiley & Sons: Hoboken, NJ, USA, 2022; pp. 425–438.
91. Teijin News Release, 7 December 20223. Available online: https://www.teijin.com/news/2022/12/07/20221207_01.pdf (accessed on 15 August 2023).
92. Fattahi, F.S.; Khoddami, A.; Izadian, H. Review on production, properties, and applications of poly (lactic acid) fibers. *J. Text. Sci. Technol.* **2015**, *5*, 11–17.
93. Yang, J.; Liu, X.; Zhao, J.; Pu, X.; Shen, Z.; Xu, W.; Liu, Y. The Structural Evolution of β -to- α Phase Transition in the Annealing Process of Poly (3-hydroxybutyrate-co-3-hydroxyvalerate). *Polymers* **2023**, *15*, 1921. [[CrossRef](#)] [[PubMed](#)]
94. Xu, J.; Guo, B.H. Poly (butylene succinate) and its copolymers: Research, development and industrialization. *Biotechnol. J.* **2010**, *5*, 1149–1163. [[CrossRef](#)]
95. Chen, Y.; Tan, L.; Chen, L.; Yang, Y.; Wang, X. Study on biodegradable aromatic/aliphatic copolyesters. *Braz. J. Chem. Eng.* **2008**, *25*, 321–335. [[CrossRef](#)]
96. Guimarães, T.C.; Araújo, E.S.; Hernández-Macedo, M.L.; López, J.A. Polyhydroxyalkanoates: Biosynthesis from alternative carbon sources and analytic methods: A short review. *J. Polym. Environ.* **2022**, *30*, 2669–2684. [[CrossRef](#)]
97. Tavanaie, M.A.; Gevari, A. Biodegradability study of polypropylene fibers blended with disposable recycled poly (lactic acid) plastic flakes. *Turk. J. Chem.* **2019**, *43*, 424–434. [[CrossRef](#)]
98. Robledo-Ortíz, J.R.; González-López, M.E.; Martín del Campo, A.S.; Pérez-Fonseca, A.A. Lignocellulosic materials as reinforcement of polyhydroxybutyrate and its copolymer with hydroxyvalerate: A review. *J. Polym. Environ.* **2021**, *29*, 1350–1364. [[CrossRef](#)]
99. Dilkes-Hoffman, L.S.; Lant, P.A.; Laycock, B.; Pratt, S. The rate of biodegradation of PHA bioplastics in the marine environment: A meta-study. *Mar. Pollut. Bull.* **2019**, *142*, 15–24. [[CrossRef](#)]
100. Van der Walle, G.A.M.; De Koning, G.J.M.; Weusthuis, R.A.; Eggink, G. Properties, modifications and applications of biopolyesters. *Biopolyesters* **2001**, *71*, 263–291.
101. Koller, M.; Mukherjee, A. A new wave of industrialization of PHA biopolyesters. *Bioengineering* **2022**, *9*, 74. [[CrossRef](#)]

102. Bond, E.B.; Autran, J.-P.M.; Mackey, L.N.; Noda, I.; O'donnell, H.J. Fibers comprising starch and biodegradable polymers. U.S. Patent US6946506B2, 20 September 2005.
103. Kaseem, M.; Hamad, K.; Deri, F. Thermoplastic starch blends: A review of recent works. *Polym. Sci. Ser. A* **2012**, *54*, 165–176. [[CrossRef](#)]
104. Martinez Villadiego, K.; Arias Tapia, M.J.; Useche, J.; Escobar Macías, D. Thermoplastic starch (TPS)/polylactic acid (PLA) blending methodologies: A review. *J. Polym. Environ.* **2022**, *30*, 75–91. [[CrossRef](#)]
105. Zhang, Y.; Rempel, C.; Liu, Q. Thermoplastic starch processing and characteristics—A review. *Crit. Rev. Food Sci. Nutr.* **2014**, *54*, 1353–1370. [[CrossRef](#)] [[PubMed](#)]
106. Heisig, C.; Diedenhoven, J.; Jensen, C.; Gehrke, H.; Turek, T. Selective hydrogenation of biomass-derived succinic acid: Reaction network and kinetics. *Chem. Eng. Technol.* **2020**, *43*, 484–492. [[CrossRef](#)]
107. Varghese, S.A.; Pulikkalparambil, H.; Rangappa, S.M.; Siengchin, S.; Parameswaranpillai, J. Novel biodegradable polymer films based on poly (3-hydroxybutyrate-co-3-hydroxyvalerate) and Ceiba pentandra natural fibers for packaging applications. *Food Packag. Shelf Life* **2020**, *25*, 100538. [[CrossRef](#)]
108. Wang, Y.; Davey, C.J.; Van der Maas, K.; Van Putten, R.-J.; Tietema, A.; Parsons, J.R.; Gruter, G.-J.M. Biodegradability of novel high Tg poly (isosorbide-co-1, 6-hexanediol) oxalate polyester in soil and marine environments. *Sci. Total Environ.* **2022**, *815*, 152781. [[CrossRef](#)]
109. Li, F.; Luo, S.; Yu, J. Mechanical, thermal properties and isothermal crystallization kinetics of biodegradable poly (butylene succinate-co-terephthalate)(PBST) fibers. *J. Polym. Res.* **2010**, *17*, 279–287. [[CrossRef](#)]
110. Rafiqah, S.A.; Khalina, A.; Harmaen, A.S.; Tawakkal, I.A.; Zaman, K.; Asim, M.; Nurrazi, M.; Lee, C.H. A review on properties and application of bio-based poly (butylene succinate). *Polymers* **2021**, *13*, 1436. [[CrossRef](#)]
111. Azimi, B.; Nourpanah, P.; Rabiee, M.; Arbab, S. Poly (ϵ -caprolactone) fiber: An overview. *J. Eng. Fibers Fabr.* **2014**, *9*, 155892501400900309. [[CrossRef](#)]
112. Meng, Q.; Hu, J. Study on poly (ϵ -caprolactone)-based shape memory copolymer fiber prepared by bulk polymerization and melt spinning. *Polym. Adv. Technol.* **2008**, *19*, 131–136. [[CrossRef](#)]
113. Hayashi, T.; Nakayama, K.; Mochizuki, M.; Masuda, T. Studies on biodegradable poly (hexano-6-lactone) fibers. Part 3. Enzymatic degradation in vitro (IUPAC Technical Report). *Pure Appl. Chem.* **2002**, *74*, 869–880. [[CrossRef](#)]
114. Mochizuki, M.; Hayashi, T.; Nakayama, K.; Masuda, T. Studies on biodegradable poly (hexano-6-lactone) fibers. Part 2: Environmental degradation. *Pure Appl. Chem.* **1999**, *71*, 2177–2188. [[CrossRef](#)]
115. Charuchinda, A.; Molloy, R.; Siripitayananon, J.; Molloy, N.; Sriyai, M. Factors influencing the small-scale melt spinning of poly (ϵ -caprolactone) monofilament fibres. *Polym. Int.* **2003**, *52*, 1175–1181. [[CrossRef](#)]
116. Douglas, P.; Andrews, G.; Jones, D.; Walker, G. Analysis of in vitro drug dissolution from PCL melt extrusion. *Chem. Eng. J.* **2010**, *164*, 359–370. [[CrossRef](#)]
117. Veit, D. *Fibers: History, Production, Properties, Market*; Springer Nature: Berlin/Heidelberg, Germany, 2023.
118. Saigusa, K.; Saijo, H.; Yamazaki, M.; Takarada, W.; Kikutani, T. Influence of carboxylic acid content and polymerization catalyst on hydrolytic degradation behavior of Poly (glycolic acid) fibers. *Polym. Degrad. Stab.* **2020**, *172*, 109054. [[CrossRef](#)]
119. Murcia Valderrama, M.A.; van Putten, R.-J.; Gruter, G.-J.M. PLGA barrier materials from CO₂. The influence of lactide co-monomer on glycolic acid polyesters. *ACS Appl. Polym. Mater.* **2020**, *2*, 2706–2718. [[CrossRef](#)]
120. Wang, Y.; Murcia Valderrama, M.A.; van Putten, R.-J.; Davey, C.J.; Tietema, A.; Parsons, J.R.; Wang, B.; Gruter, G.-J.M. Biodegradation and non-enzymatic hydrolysis of poly (lactic-co-glycolic acid)(PLGA12/88 and PLGA6/94). *Polymers* **2021**, *14*, 15. [[CrossRef](#)]
121. Ginde, R.M.; Gupta, R.K. In vitro chemical degradation of poly (glycolic acid) pellets and fibers. *J. Appl. Polym. Sci.* **1987**, *33*, 2411–2429. [[CrossRef](#)]
122. Samantaray, P.K.; Little, A.; Haddleton, D.M.; McNally, T.; Tan, B.; Sun, Z.; Huang, W.; Ji, Y.; Wan, C. Poly (glycolic acid)(PGA): A versatile building block expanding high performance and sustainable bioplastic applications. *Green Chem.* **2020**, *22*, 4055–4081. [[CrossRef](#)]
123. Budak, K.; Sogut, O.; Aydemir Sezer, U. A review on synthesis and biomedical applications of polyglycolic acid. *J. Polym. Res.* **2020**, *27*, 208. [[CrossRef](#)]
124. Bansode, S.H.; Khare, P.V.; Mahanwar, P.A. Synthesis of PLGA and Its Fabrication for the Tissue Engineering by Electro and Melt Spinning.
125. Xu, W. In A study on the synthesis, modification and current market status of PBAT. *E3S Web Conf.* **2023**, *385*, 04007. [[CrossRef](#)]
126. Shi, X.; Ito, H.; Kikutani, T. Structure development and properties of high-speed melt spun poly (butylene terephthalate)/poly (butylene adipate-co-terephthalate) bicomponent fibers. *Polymer* **2006**, *47*, 611–616. [[CrossRef](#)]
127. Zhang, W.; Wang, Q.; Wang, G.; Liu, S. Synthesis and characterization of bio-based poly (ethylene 2, 5-furandicarboxylate)-b-poly (butylene adipate-co-terephthalate) copolymers. *J. Appl. Polym. Sci.* **2022**, *139*, e52803. [[CrossRef](#)]
128. Zhou, W.; Wang, X.; Yang, B.; Xu, Y.; Zhang, W.; Zhang, Y.; Ji, J. Synthesis, physical properties and enzymatic degradation of bio-based poly (butylene adipate-co-butylene furandicarboxylate) copolyesters. *Polym. Degrad. Stab.* **2013**, *98*, 2177–2183. [[CrossRef](#)]
129. Baidurah, S. Methods of analyses for biodegradable polymers: A review. *Polymers* **2022**, *14*, 4928. [[CrossRef](#)] [[PubMed](#)]

130. Kim, J.; Park, S.; Bang, J.; Jin, H.J.; Kwak, H.W. Biodegradation in Composting Conditions of PBEAS Monofilaments for the Sustainable End-Use of Fishing Nets. *Glob. Chall.* **2023**, *7*, 2300020. [CrossRef]
131. Prambauer, M.; Wendeler, C.; Weitzenböck, J.; Burgstaller, C. Biodegradable geotextiles—An overview of existing and potential materials. *Geotext. Geomembr.* **2019**, *47*, 48–59. [CrossRef]
132. Austin, H.P.; Allen, M.D.; Donohoe, B.S.; Rorrer, N.A.; Kearns, F.L.; Silveira, R.L.; Pollard, B.C.; Dominick, G.; Duman, R.; El Omari, K. Characterization and engineering of a plastic-degrading aromatic polyesterase. *Proc. Natl. Acad. Sci. USA* **2018**, *115*, E4350–E4357. [CrossRef]
133. Mohee, R.; Unmar, G. Determining biodegradability of plastic materials under controlled and natural composting environments. *Waste Manag.* **2007**, *27*, 1486–1493. [CrossRef]
134. Viera, J.S.; Marques, M.R.; Nazareth, M.C.; Jimenez, P.C.; Sanz-Lázaro, C.; Castro, Í.B. Are biodegradable plastics an environmental rip off? *J. Hazard. Mater.* **2021**, *416*, 125957. [CrossRef]
135. EN 13432; Packaging—Requirements for Packaging Recoverable through Composting and Biodegradation—Test Scheme and Evaluation Criteria for the Final Acceptance of Packaging. Institute for Standardization of Serbia: Belgrade, Serbia, 2000.
136. ASTM D6400; Standard Specification for Labeling of Plastics Designed to be Aerobically Composted in Municipal or Industrial Facilities. ATSM International: West Conshohocken, PA, USA, 2021.
137. Available online: <https://www.tuv-at.be/green-marks/certifications/ok-biodegradable/> (accessed on 20 August 2023).
138. Haider, T.P.; Völker, C.; Kramm, J.; Landfester, K.; Wurm, F.R. Plastics of the future? The impact of biodegradable polymers on the environment and on society. *Angew. Chem. Int. Ed.* **2019**, *58*, 50–62. [CrossRef]
139. Available online: <https://nova-institute.eu/press/> (accessed on 20 August 2023).
140. SkyQuest Technology. *Biodegradable Plastics Market Size, Share & Trends Analysis, by Type (PLA, Starch Blends, PHA, Biodegradable Polyesters), End Use Industry (Packaging, Consumer Goods, Textile, Agriculture & Horticulture), Region and Forecast Period 2022–2030*; SkyQuest Technology: Westford, MA, USA, 2022.
141. Khatami, K.; Perez-Zabaleta, M.; Owusu-Agyeman, I.; Cetecioglu, Z. Waste to bioplastics: How close are we to sustainable polyhydroxyalkanoates production? *Waste Manag.* **2021**, *119*, 374–388. [CrossRef] [PubMed]
142. Naeimirad, M.; Zadhoush, A.; Kotek, R.; Esmaeely Neisiany, R.; Nouri Khorasani, S.; Ramakrishna, S. Recent advances in core/shell bicomponent fibers and nanofibers: A review. *J. Appl. Polym. Sci.* **2018**, *135*, 46265. [CrossRef]
143. Krins, B. Biodegradable yarns—Overview of the state-of-the-art. In Proceedings of the Dornbirn Global Fiber Congress, Dornbirn, Austria, 15–17 September 2021.
144. Park, C.H.; Hong, E.Y.; Kang, Y.K. Effects of spinning speed and heat treatment on the mechanical properties and biodegradability of poly (lactic acid) fibers. *J. Appl. Polym. Sci.* **2007**, *103*, 3099–3104. [CrossRef]
145. Warnock, M.; Davis, K.; Wolf, D.; Gbur, E. Soil Burial Effects on Biodegradation and Properties of Three Cellulosic Fabrics. *AATCC Rev.* **2011**, *11*, 53–57.
146. Situ Biosciences. *AATCC 30—Antifungal Test—Textiles*; Situ Biosciences: Wheeling, IL, USA, 2020.
147. Ali, A.; El-Dessouky, H. An insight on the process–property relationships of melt spun polylactic acid fibers. *Text. Res. J.* **2019**, *89*, 4959–4966. [CrossRef]
148. Gajjar, C.R.; Stallrich, J.W.; Pasquinnelli, M.A.; King, M.W. Process–Property Relationships for Melt-Spun Poly (lactic acid) Yarn. *ACS Omega* **2021**, *6*, 15920–15928. [CrossRef]
149. Ebrahimi, H. Poly (Lactic Acid) Structure-Process-Property Relationships. Ph.D. Thesis, North Carolina State University, Raleigh, NC, USA, 2021.
150. Schmack, G.; Tändler, B.; Vogel, R.; Beyreuther, R.; Jacobsen, S.; Fritz, H.G. Biodegradable fibers of poly (L-lactide) produced by high-speed melt spinning and spin drawing. *J. Appl. Polym. Sci.* **1999**, *73*, 2785–2797. [CrossRef]
151. Schmack, G.; Tändler, B.; Optiz, G.; Vogel, R.; Komber, H.; Häußler, L.; Voigt, D.; Weinmann, S.; Heinemann, M.; Fritz, H.G. High-speed melt spinning of various grades of polylactides. *J. Appl. Polym. Sci.* **2004**, *91*, 800–806. [CrossRef]
152. Takasaki, M.; Ito, H.; Kikutani, T. Structure development of polylactides with various D-lactide contents in the high-speed melt spinning process. *J. Macromol. Sci. Part B* **2003**, *42*, 57–73. [CrossRef]
153. Yuan, X.; Mak, A.F.; Kwok, K.W.; Yung, B.K.; Yao, K. Characterization of poly (L-lactic acid) fibers produced by melt spinning. *J. Appl. Polym. Sci.* **2001**, *81*, 251–260. [CrossRef]
154. Nishimura, Y.; Takasu, A.; Inai, Y.; Hirabayashi, T. Melt spinning of poly (L-lactic acid) and its biodegradability. *J. Appl. Polym. Sci.* **2005**, *97*, 2118–2124. [CrossRef]
155. Paakinaho, K.; Ellä, V.; Syrjälä, S.; Kellomäki, M. Melt spinning of poly (l/d) lactide 96/4: Effects of molecular weight and melt processing on hydrolytic degradation. *Polym. Degrad. Stab.* **2009**, *94*, 438–442. [CrossRef]
156. Fambri, L.; Bragagna, S.; Migliaresi, C. *Biodegradable Fibers of Poly-L, DL-Lactide 70/30 Produced by Melt Spinning*; Macromolecular symposia, 2006; Wiley Online Library: Hoboken, NJ, USA, 2006; pp. 20–25.
157. Liu, Q.; Zhang, H.; Deng, B.; Zhao, X. Poly (3-hydroxybutyrate) and Poly (3-hydroxybutyrate-co-3-hydroxyvalerate): Structure, Property, and Fiber. *Int. J. Polym. Sci.* **2014**, *2014*, 374368. [CrossRef]
158. Qin, Q.; Takarada, W.; Kikutani, T. Fiber structure formation in melt spinning of bio-based aliphatic co-polyesters. *AIP Conf. Proc.* **2015**, *1664*, 080004.
159. Qin, Q.; Takarada, W.; Kikutani, T. Fiber structure development of PHBH through stress-induced crystallization in high-speed melt spinning process. *J. Fiber Sci. Technol.* **2017**, *73*, 49–60. [CrossRef]

160. Iwata, T.; Tanaka, T. Manufacturing of PHA as Fibers. In *Plastics from Bacteria: Natural Functions and Applications*; Springer: Berlin/Heidelberg, Germany, 2010; pp. 257–282.
161. Imre, B.; Pukánszky, B. Compatibilization in bio-based and biodegradable polymer blends. *Eur. Polym. J.* **2013**, *49*, 1215–1233. [[CrossRef](#)]
162. Saito, Y.; Doi, Y. Microbial synthesis and properties of poly (3-hydroxybutyrate-co-4-hydroxybutyrate) in *Comamonas acidovorans*. *Int. J. Biol. Macromol.* **1994**, *16*, 99–104. [[CrossRef](#)]
163. Saito, Y.; Nakamura, S.; Hiramitsu, M.; Doi, Y. Microbial synthesis and properties of poly (3-hydroxybutyrate-co-4-hydroxybutyrate). *Polym. Int.* **1996**, *39*, 169–174. [[CrossRef](#)]
164. Omura, T.; Komiyama, K.; Maehara, A.; Kabe, T.; Iwata, T. Elastic marine biodegradable fibers produced from poly [(R)-3-hydroxybutylate-co-4-hydroxybutylate] and evaluation of their biodegradability. *ACS Appl. Polym. Mater.* **2021**, *3*, 6479–6487. [[CrossRef](#)]
165. Miyao, Y.; Takarada, W.; Kikutani, T. In Improvement of mechanical properties of biodegradable PHBH fibers through high-speed melt spinning process equipped with a liquid isothermal bath. *AIP Conf. Proc.* **2020**, *2289*, 020038.
166. Tanaka, T.; Fujita, M.; Takeuchi, A.; Suzuki, Y.; Uesugi, K.; Ito, K.; Fujisawa, T.; Doi, Y.; Iwata, T. Formation of highly ordered structure in poly [(R)-3-hydroxybutyrate-co-(R)-3-hydroxyvalerate] high-strength fibers. *Macromolecules* **2006**, *39*, 2940–2946. [[CrossRef](#)]
167. Rebia, R.A.; Shizukuishi, K.; Tanaka, T. Characteristic changes in PHBH isothermal crystallization monofilaments by the effect of heat treatment and dip-coating in various solvents. *Eur. Polym. J.* **2020**, *134*, 109808. [[CrossRef](#)]
168. Selli, F.; Hufenus, R.; Gooneie, A.; Erdoğan, U.H.; Perret, E. Structure–property relationship in melt-spun poly (hydroxybutyrate-co-3-hexanoate) monofilaments. *Polymers* **2022**, *14*, 200. [[CrossRef](#)]
169. Leonés, A.; Mujica-Garcia, A.; Arrieta, M.P.; Salaris, V.; Lopez, D.; Kenny, J.M.; Peponi, L. Organic and inorganic PCL-based electrospun fibers. *Polymers* **2020**, *12*, 1325. [[CrossRef](#)]
170. Gurarlan, A.; Caydamli, Y.; Shen, J.; Tse, S.; Yetukuri, M.; Tonelli, A.E. Coalesced poly (ϵ -caprolactone) fibers are stronger. *Biomacromolecules* **2015**, *16*, 890–893. [[CrossRef](#)]
171. Kikutani, T. Fiber Formation through Melt Spinning of Bio-polymers. In Proceedings of the International Conference on Technology and Social Science, Kiryu, Japan, 2–4 December 2020.
172. Yang, Q.; Shen, X.; Tan, Z. Investigations of the preparation technology for polyglycolic acid fiber with perfect mechanical performance. *J. Appl. Polym. Sci.* **2007**, *105*, 3444–3447. [[CrossRef](#)]
173. Ziabicki, A. *Fundamentals of Fibre Formation: The Science of Fibre Spinning and Drawing*; John Wiley & Sons: Hoboken, NJ, USA, 1976.
174. Fourné, F. *Synthetic Fibers: Machines and Equipment, Manufacture, Properties: Handbook for Plant Engineering, Machine Design, and Operation*; Hanser Publication: Cincinnati, OH, USA, 1999.
175. Saigusa, K.; Takarada, W.; Kikutani, T. Improvement of the mechanical properties of poly (glycolic acid) fibers through control of molecular entanglements in the melt spinning process. *J. Macromol. Sci. Part B* **2020**, *59*, 399–414. [[CrossRef](#)]
176. Tracy, M.; Ward, K.; Firouzabadian, L.; Wang, Y.; Dong, N.; Qian, R.; Zhang, Y. Factors affecting the degradation rate of poly (lactide-co-glycolide) microspheres in vivo and in vitro. *Biomaterials* **1999**, *20*, 1057–1062. [[CrossRef](#)]
177. Malafeev, K.; Moskalyuk, O.; Yudin, V.; Sedush, N.; Chvalun, S.; Elokhoyskii, V.Y.; Popova, E.; Ivan'kova, E. Synthesis and properties of fibers prepared from lactic acid–glycolic acid copolymer. *Polym. Sci. Ser. A* **2017**, *59*, 53–57. [[CrossRef](#)]
178. Fu, S.; Lu, Y.; Zhang, P. Development and characteristics of novel polyglycolic acid (PGA) monofilaments for acupoint catgut-embedding therapy applications. *Text. Res. J.* **2019**, *89*, 845–854. [[CrossRef](#)]
179. Fu, S.; Yang, D.; Zhang, P. Development and characterizations of polylactic acid (PLA) and polyglycolide acid (PGA) monofilaments for acupoint catgut embedding therapy applications. *J. Text. Inst.* **2019**, *110*, 1580–1587. [[CrossRef](#)]
180. Khare, P.V.; Bansode, S.H.; Mahanwar, P. Synthesis of Poly (Lactic-co-glycolic) acid and its micro fabrication by Centrifugal force melt spinning Technique. *Int. J. Adv. Eng. Manag. IJAEM* **2022**, *4*, 587–600.
181. Guo, Z.; Chen, S.H.; Zhang, P.H. The Effect of Melt-Spinning Technology on the Degradation of Poly (Glycolic Acid) Fiber In Vitro. *Adv. Mater. Res.* **2011**, *152*, 1240–1243. [[CrossRef](#)]
182. Miao, Y.; Cui, H.; Dong, Z.; Ouyang, Y.; Li, Y.; Huang, Q.; Wang, Z. Structural Evolution of Polyglycolide and Poly (glycolide-co-lactide) Fibers during In Vitro Degradation with Different Heat-Setting Temperatures. *ACS Omega* **2021**, *6*, 29254–29266. [[CrossRef](#)] [[PubMed](#)]
183. Younes, B. A statistical investigation of the influence of the multi-stage hot-drawing process on the mechanical properties of biodegradable linear aliphatic-aromatic co-polyester fibers. *Adv. Mater. Sci. Appl.* **2014**, *3*, 186–202. [[CrossRef](#)]
184. Younes, B.; Fotheringham, A. Factorial optimization of the effects of extrusion temperature profile and polymer grade on as-spun aliphatic–aromatic copolyester fibers. II. Crystallographic order. *J. Appl. Polym. Sci.* **2011**, *119*, 1896–1904. [[CrossRef](#)]
185. Younes, B.; Fotheringham, A. Factorial optimization of the effects of melt-spinning conditions on biodegradable as-spun aliphatic–aromatic copolyester fibers. III. Diameter, tensile properties, and thermal shrinkage. *J. Appl. Polym. Sci.* **2011**, *122*, 1434–1449. [[CrossRef](#)]
186. Younes, B.; Fotheringham, A.; El-Dessouky, H.M. Birefringent approach for assessing the influence of the extrusion temperature profile on the overall orientation of as-spun aliphatic-aromatic co-polyester fibers. *Polym. Eng. Sci.* **2009**, *49*, 2492–2500. [[CrossRef](#)]

187. Younes, B.; Fotheringham, A.; El-Dessouky, H.M. Factorial optimization of the effects of extrusion temperature profile and polymer grade on as-spun aliphatic–aromatic copolyester fibers. I. Birefringence and overall orientation. *J. Appl. Polym. Sci.* **2010**, *118*, 1270–1277. [[CrossRef](#)]
188. Younes, B.; Fotheringham, A.; El-Dessouky, H.M.; Haddad, G. Factorial optimization of the effects of melt-spinning conditions on as-spun aliphatic-aromatic copolyester fibers I. Spin draw ratio, overall orientation and drawability. *Int. J. Polym. Mater.* **2011**, *60*, 316–339. [[CrossRef](#)]
189. Younes, B.; Fotheringham, A.; Mather, R. Factorial Optimisation of the Effects of Melt Spinning Conditions on Biodegradable As-spun Aliphatic-Aromatic Co-Polyester Fibres: II. Die Head Pressure, Crystallographic Order and Thermo-graphic Measurement. *Int. Polym. Process.* **2011**, *26*, 150–163. [[CrossRef](#)]
190. Jung Kang, H.; Soon Park, S. Characterization and biodegradability of poly (butylene adipate-co-succinate)/poly (butylene terephthalate) copolyester. *J. Appl. Polym. Sci.* **1999**, *72*, 593–608. [[CrossRef](#)]
191. Fuoco, T.; Mathisen, T.; Finne-Wistrand, A. Poly (l-lactide) and poly (l-lactide-co-trimethylene carbonate) melt-spun fibers: Structure–processing–properties relationship. *Biomacromolecules* **2019**, *20*, 1346–1361. [[CrossRef](#)] [[PubMed](#)]
192. Baimark, Y.; Molloy, R.; Molloy, N.; Siripitayananon, J.; Punyodom, W.; Sriyai, M. Synthesis, characterization and melt spinning of a block copolymer of L-lactide and ϵ -caprolactone for potential use as an absorbable monofilament surgical suture. *J. Mater. Sci. Mater. Med.* **2005**, *16*, 699–707. [[CrossRef](#)] [[PubMed](#)]
193. Murayama, A.; Yoneda, H.; Maehara, A.; Shiomi, N.; Hirata, H. A highly elastic absorbable monofilament suture fabricated from poly (3-hydroxybutyrate-co-4-hydroxybutyrate). *Sci. Rep.* **2023**, *13*, 3275. [[CrossRef](#)]
194. He, Y.; Qian, Z.; Zhang, H.; Liu, X. Alkaline degradation behavior of polyestamide fibers: Surface erosion. *Colloid Polym. Sci.* **2004**, *282*, 972–978. [[CrossRef](#)]
195. Naeimirad, M.; Zadhoush, A.; Esmaeely Neisiany, R.; Salimian, S.; Kotek, R. Melt-spun PLA liquid-filled fibers: Physical, morphological, and thermal properties. *J. Text. Inst.* **2019**, *110*, 89–99. [[CrossRef](#)]
196. Selli, F.; Erdugan, Ü.H. Production and characterization of melt-spun (ϵ -caprolactone) fibers having different cross sections. In Proceedings of the TexTeh9—Advanced Textiles for a Better World Conference, Bucharest, Romania, 24–25 October 2019; p. 42.
197. El-Salmawy, A.; Kitagawa, T.; Ko, I.K.; Murakami, A.; Kimura, Y.; Yamaoka, T.; Iwata, H. Preparation and properties of ProNectin F-coated biodegradable hollow fibers. *J. Artif. Organs* **2005**, *8*, 245–251. [[CrossRef](#)]
198. Bauer, B.; Emonts, C.; Bonten, L.; Annan, R.; Merkord, F.; Vad, T.; Idrissi, A.; Gries, T.; Blaeser, A. Melt-Spun, Cross-Section Modified Polycaprolactone Fibers for Use in Tendon and Ligament Tissue Engineering. *Fibers* **2022**, *10*, 23. [[CrossRef](#)]
199. Park, S.; Lee, B.-K.; Na, M.; Kim, D. Melt-spun shaped fibers with enhanced surface effects: Fiber fabrication, characterization and application to woven scaffolds. *Acta Biomater.* **2013**, *9*, 7719–7726. [[CrossRef](#)]
200. Tavanaie, M.A. Melt recycling of poly (lactic acid) plastic wastes to produce biodegradable fibers. *Polym.-Plast. Technol. Eng.* **2014**, *53*, 742–751. [[CrossRef](#)]
201. Niaounakis, M. *Biopolymers: Processing and Products*; William Andrew: Norwich, NY, USA, 2014.
202. Huang, Y.; Brünig, H.; Müller, M.T.; Wießner, S. Melt spinning of PLA/PCL blends modified with electron induced reactive processing. *J. Appl. Polym. Sci.* **2022**, *139*, 51902. [[CrossRef](#)]
203. Furuhashi, Y.; Kimura, Y.; Yoshie, N.; Yamane, H. Higher-order structures and mechanical properties of stereocomplex-type poly (lactic acid) melt spun fibers. *Polymer* **2006**, *47*, 5965–5972. [[CrossRef](#)]
204. Padee, S.; Thumsorn, S.; On, J.W.; Surin, P.; Apawet, C.; Chaichalermwong, T.; Kaabuuathong, N.; Narongchai, O.; Srisawat, N. Preparation of poly (lactic acid) and poly (trimethylene terephthalate) blend fibers for textile application. *Energy Procedia* **2013**, *34*, 534–541. [[CrossRef](#)]
205. Jompong, L.; Thumsorn, S.; On, J.W.; Surin, P.; Apawet, C.; Chaichalermwong, T.; Kaabuuathong, N.; Narongchai, O.; Srisawat, N. Poly (lactic acid) and poly (butylene succinate) blend fibers prepared by melt spinning technique. *Energy Procedia* **2013**, *34*, 493–499. [[CrossRef](#)]
206. Panichsombat, K.; Panbangpong, W.; Poompiew, N.; Potiyaraj, P. Biodegradable fibers from poly (lactic acid)/poly (butylene succinate) blends. *IOP Conf. Ser. Mater. Sci. Eng.* **2019**, *600*, 012004. [[CrossRef](#)]
207. Park, S.-W.; Kim, S.-H.; Choi, H.-S.; Cho, H.-H. Preparation and physical properties of biodegradable polybutylene succinate/polybutylene adipate-co-terephthalate blend monofilament by melt spinning. *J. Korean Soc. Fish. Ocean Technol.* **2010**, *46*, 257–264. [[CrossRef](#)]
208. Hassan, E.A.; Elarabi, S.E.; Wei, Y.; Yu, M. Biodegradable poly (lactic acid)/poly (butylene succinate) fibers with high elongation for health care products. *Text. Res. J.* **2018**, *88*, 1735–1744. [[CrossRef](#)]
209. Pivsa-Art, W.; Pivsa-Art, S.; Fujii, K.; Nomura, K.; Ishimoto, K.; Aso, Y.; Yamane, H.; Ohara, H. Compression molding and melt-spinning of the blends of poly (lactic acid) and poly (butylene succinate-co-adipate). *J. Appl. Polym. Sci.* **2015**, *132*, 41856. [[CrossRef](#)]
210. Li, J.; Wang, Y.; Wang, X.; Wu, D. Crystalline characteristics, mechanical properties, thermal degradation kinetics and hydration behavior of biodegradable fibers melt-spun from polyoxymethylene/poly (l-lactic acid) blends. *Polymers* **2019**, *11*, 1753. [[CrossRef](#)]
211. Hinüber, C.; Häussler, L.; Vogel, R.; Brünig, H.; Heinrich, G.; Werner, C. Hollow fibers made from a poly (3-hydroxybutyrate)/poly- ϵ -caprolactone blend. *Express Polym. Lett.* **2011**, *5*, 643–652. [[CrossRef](#)]
212. Barral, V.; Dropsit, S.; Cayla, A.; Campagne, C.; Devaux, É. Study of the influence of pcl on the in vitro degradation of extruded pla monofilaments and melt-spun filaments. *Polymers* **2021**, *13*, 171. [[CrossRef](#)] [[PubMed](#)]

213. Vieira, A.; Medeiros, R.; Guedes, R.M.; Marques, A.; Tita, V. Visco-elastic-plastic properties of suture fibers made of PLA-PCL. *Mater. Sci. Forum* **2013**, *730*, 56–61. [[CrossRef](#)]
214. Vieira, A.; Vieira, J.; Guedes, R.; Marques, A. Degradation and viscoelastic properties of PLA-PCL, PGA-PCL, PDO and PGA fibres. *Mater. Sci. Forum* **2010**, *636*, 825–832. [[CrossRef](#)]
215. Visco, A.; Sclaro, C.; Giamporcaro, A.; De Caro, S.; Tranquillo, E.; Catauro, M. Threads made with blended biopolymers: Mechanical, physical and biological features. *Polymers* **2019**, *11*, 901. [[CrossRef](#)]
216. Chen, Z.; Zhao, Z.; Hong, J.; Pan, Z. Novel bioresource-based poly (3-Hydroxybutyrate-co-4-Hydroxybutyrate)/poly (Lactic Acid) blend fibers with high strength and toughness via melt-spinning. *J. Appl. Polym. Sci.* **2020**, *137*, 48956. [[CrossRef](#)]
217. Vogel, R.; Tändler, B.; Voigt, D.; Jehnichen, D.; Häußler, L.; Peitzsch, L.; Brüning, H. Melt spinning of bacterial aliphatic polyester using reactive extrusion for improvement of crystallization. *Macromol. Biosci.* **2007**, *7*, 820–828. [[CrossRef](#)]
218. Li, L.; Huang, W.; Wang, B.; Wei, W.; Gu, Q.; Chen, P. Properties and structure of polylactide/poly (3-hydroxybutyrate-co-3-hydroxyvalerate)(PLA/PHBV) blend fibers. *Polymer* **2015**, *68*, 183–194. [[CrossRef](#)]
219. Tavanaie, M.; Mahmudi, A. Green engineered polypropylene biodegradable fibers through blending with recycled poly (lactic acid) plastic wastes. *Polym. Plast. Technol. Eng.* **2014**, *53*, 1506–1517. [[CrossRef](#)]
220. Okihara, T.; Tsuji, M.; Kawaguchi, A.; Katayama, K.-I.; Tsuji, H.; Hyon, S.-H.; Ikada, Y. Crystal structure of stereocomplex of poly (L-lactide) and poly (D-lactide). *J. Macromol. Sci. Part B Phys.* **1991**, *30*, 119–140. [[CrossRef](#)]
221. Takasaki, M.; Ito, H.; Kikutani, T. Development of stereocomplex crystal of polylactide in high-speed melt spinning and subsequent drawing and annealing processes. *J. Macromol. Sci. Part B* **2003**, *42*, 403–420. [[CrossRef](#)]
222. Mazrouei-Sebdani, Z.; Naeimirad, M.; Peterek, S.; Begum, H.; Galmarini, S.; Pursche, F.; Baskin, E.; Zhao, S.; Gries, T.; Malfait, W.J. Multiple assembly strategies for silica aerogel-fiber combinations—A review. *Mater. Des.* **2022**, *223*, 111228. [[CrossRef](#)]
223. Reyhani, R.; Zadhoush, A.; Tabrizi, N.S.; Nazockdast, H.; Naeimirad, M. Synthesis and characterization of powdered CNT-doped carbon aerogels. *J. Non-Cryst. Solids* **2021**, *571*, 121058. [[CrossRef](#)]
224. Güzdemir, Ö.; Bermudez, V.; Kanhere, S.; Ogale, A.A. Melt-spun poly (lactic acid) fibers modified with soy fillers: Toward environment-friendly disposable nonwovens. *Polym. Eng. Sci.* **2020**, *60*, 1158–1168. [[CrossRef](#)]
225. Xue, W.; Chen, P.; Wang, F.; Wang, L. Melt spinning of nano-hydroxyapatite and polycaprolactone composite fibers for bone scaffold application. *J. Mater. Sci.* **2019**, *54*, 8602–8612. [[CrossRef](#)]
226. Chen, X.-X.; Yu, J.-C.; Chen, K.; Ji, P.; Chen, X.-L.; Pan, Z.-J. Facile and large-scale fabrication of biodegradable thermochromic fibers based on poly (lactic acid). *Chin. J. Polym. Sci.* **2022**, *40*, 1242–1251. [[CrossRef](#)]
227. Hufenus, R.; Reifler, F.A.; Fernández-Ronco, M.P.; Heuberger, M. Molecular orientation in melt-spun poly (3-hydroxybutyrate) fibers: Effect of additives, drawing and stress-annealing. *Eur. Polym. J.* **2015**, *71*, 12–26. [[CrossRef](#)]
228. Hufenus, R.; Reifler, F.A.; Haenggi, U.J. Biodegradable Fibers from Renewable Resources—Melt-spinning of Poly (3-hydroxybutyrate).
229. Xiang, H.; Chen, Z.; Zheng, N.; Zhang, X.; Zhu, L.; Zhou, Z.; Zhu, M. Melt-spun microbial poly (3-hydroxybutyrate-co-3-hydroxyvalerate) fibers with enhanced toughness: Synergistic effect of heterogeneous nucleation, long-chain branching and drawing process. *Int. J. Biol. Macromol.* **2019**, *122*, 1136–1143. [[CrossRef](#)]
230. Broekman, S. Crystallization of PHAs for melt-spinning (Internship report). In 2023.
231. Siebert, S.; Berghaus, J.; Seide, G. Nucleating agents to enhance poly (l-lactide) fiber crystallization during industrial-scale melt spinning. *Polymers* **2022**, *14*, 1395. [[CrossRef](#)]
232. Gu, J.; Wei, X.; Hou, X.; Wei, Z. Biodegradable Poly (butylene succinate-co-terephthalate) Fibers Incorporated with Nanoparticles under High Drawing Temperatures for Enhanced Mechanical Properties. *Macromol. Mater. Eng.* **2019**, *304*, 1900168. [[CrossRef](#)]
233. Aouat, T.; Kaci, M.; Devaux, E.; Campagne, C.; Cayla, A.; Dumazert, L.; Lopez-Cuesta, J.M. Morphological, mechanical, and thermal characterization of poly (lactic acid)/cellulose multifilament fibers prepared by melt spinning. *Adv. Polym. Technol.* **2018**, *37*, 1193–1205. [[CrossRef](#)]
234. Zhang, Y.; Li, X.; Yang, Y.; Lan, A.; He, X.; Yu, M. In situ graft copolymerization of L-lactide onto cellulose and the direct melt spinning. *RSC Adv.* **2014**, *4*, 34584–34590. [[CrossRef](#)]
235. An Tran, N.H.; Brüning, H.; Hinüber, C.; Heinrich, G. Melt spinning of biodegradable nanofibrillary structures from poly (lactic acid) and poly (vinyl alcohol) blends. *Macromol. Mater. Eng.* **2014**, *299*, 219–227. [[CrossRef](#)]
236. Zhang, X.; Jin, G.; Ma, W.; Meng, L.; Yin, H.; Zhu, Z.; Dong, Z.; Wang, R. Fabrication and properties of poly (l-lactide) nanofibers via blend sea-island melt spinning. *J. Appl. Polym. Sci.* **2015**, *132*, 41228. [[CrossRef](#)]
237. Huang, W.; Huang, X.; Wang, P.; Chen, P. Poly (glycolic acid) Nanofibers via Sea-Island Melt-Spinning. *Macromol. Mater. Eng.* **2018**, *303*, 1800425. [[CrossRef](#)]
238. You, Y.; Youk, J.H.; Lee, S.W.; Min, B.-M.; Lee, S.J.; Park, W.H. Preparation of porous ultrafine PGA fibers via selective dissolution of electrospun PGA/PLA blend fibers. *Mater. Lett.* **2006**, *60*, 757–760. [[CrossRef](#)]
239. Magazzini, L.; Grilli, S.; Fenni, S.E.; Donetti, A.; Cavallo, D.; Monticelli, O. The Blending of Poly (glycolic acid) with Polycaprolactone and Poly (l-lactide): Promising Combinations. *Polymers* **2021**, *13*, 2780. [[CrossRef](#)]
240. Liu, D.; Xie, Q.; Liu, Z.; Chen, J.; Zou, X.; Jing, B. Improvement of melt viscosity and compatibility of polyglycolic acid (PGA)/polylactic acid (PLA) blend via reactive blending with bifunctional and multifunctional hybrid chain extender. *J. Appl. Polym. Sci.* **2023**, *140*, e54501. [[CrossRef](#)]
241. Deshpande, S.; Bhati, P.; Ghosh, A.; Bhatnagar, N. Effect of PGA/PCL on the structure–property relation of PLA during tube extrusion. In Proceedings of the 10th World Biomaterials Congress, Montreal, QC, Canada, 17–22 May 2016; pp. 17–22.

242. Sharma, D.; Satapathy, B.K. Performance evaluation of electrospun nanofibrous mats of polylactic acid (PLA)/poly (ϵ -caprolactone)(PCL) blends. *Mater. Today Proc.* **2019**, *19*, 188–195. [[CrossRef](#)]
243. Akhbar, N.A.M.; Othman, M.; Buys, Y.F.; Shaffiar, N.; Jimat, D.N.; Shaharuddin, S.I.S. Characterisation and production of poly (lactic acid)/poly (ethylene glycol) microfiber via melt drawn spinning process. *IJUM Eng. J.* **2021**, *22*, 201–212. [[CrossRef](#)]
244. Vayshbeyn, L.I.; Mastalygina, E.E.; Olkhov, A.A.; Podzorova, M.V. Poly (lactic acid)-Based Blends: A Comprehensive Review. *Appl. Sci.* **2023**, *13*, 5148. [[CrossRef](#)]
245. Krishnan, S.; Pandey, P.; Mohanty, S.; Nayak, S.K. Toughening of polylactic acid: An overview of research progress. *Polym. Plast. Technol. Eng.* **2016**, *55*, 1623–1652. [[CrossRef](#)]
246. Gupta, B.; Geeta; Ray, A.R. Preparation of poly (ϵ -caprolactone)/poly (ϵ -caprolactone-co-lactide)(PCL/PLCL) blend filament by melt spinning. *J. Appl. Polym. Sci.* **2012**, *123*, 1944–1950. [[CrossRef](#)]
247. Li, X.; Liu, J.; Lu, Y.; Hou, T.; Zhou, J.; Zhang, X.; Zhou, L.; Sun, M.; Xue, J.; Yang, B. Melting centrifugally spun ultrafine poly butylene adipate-co-terephthalate (PBAT) fiber and hydrophilic modification. *RSC Adv.* **2021**, *11*, 27019–27026. [[CrossRef](#)]
248. Hufenus, R.; Yan, Y.; Dauner, M.; Yao, D.; Kikutani, T. Bicomponent fibers. In *Handbook of Fibrous Materials*; Wiley: Hoboken, NJ, USA, 2020; pp. 281–313.
249. Elahi, M.F.; Lu, W.; Guoping, G.; Khan, F. Core-shell fibers for biomedical applications—A review. *J. Bioeng. Biomed. Sci.* **2013**, *3*, 1–14. [[CrossRef](#)]
250. Hufenus, R. Novel synthetic fibers by multicomponent melt-spinning. In Proceedings of the XII International İzmir Textile and Apparel Symposium, Izmir, Turkey, 28–30 October 2010; pp. 299–307.
251. Hufenus, R. *Fiber Development by Multicomponent Melt-Spinning*; Research Gate: Berlin, Germany, 2011.
252. Zinn, M.; Dilettoso, S.; Lischer, S.; Maniura, K.; Milz, S.; Weisse, B.; Hufenus, R. Melt-Spun Fibers From Polyhydroxyalkanoate And Polylactate For Fiber Implant Applications. *Eur. Cells Mater.* **2010**, *20*, 12.
253. Hufenus, R.; Reifler, F.A.; Maniura-Weber, K.; Spierings, A.; Zinn, M. Biodegradable bicomponent fibers from renewable sources: Melt-spinning of poly (lactic acid) and poly [(3-hydroxybutyrate)-co-(3-hydroxyvalerate)]. *Macromol. Mater. Eng.* **2012**, *297*, 75–84. [[CrossRef](#)]
254. Praharn, C.; Klinsukhon, W.; Padee, S.; Suwannamek, N.; Roungpaisan, N.; Srisawat, N. Hollow segmented-pie PLA/PBS and PLA/PP bicomponent fibers: An investigation on fiber properties and splittability. *J. Mater. Sci.* **2016**, *51*, 10910–10916. [[CrossRef](#)]
255. Yang, B.; Wang, R.; Dong, Z.; Wu, J.; Kuang, M.; Jin, G.; Ma, H.; Wang, Y.; Zhang, Q.; Zhang, X. Three-dimensional crimped biodegradable poly (lactic acid) fibers prepared via melt spinning and controlled structural reorganization. *RSC Adv.* **2020**, *10*, 42890–42896. [[CrossRef](#)]
256. Song, B.; Cao, Y.; Wang, L.; Shen, Y.; Qian, X. Properties and Structure of Thermoplastic Polyvinyl Alcohol/Polyamide Sea-Island Fibers. *Polymers* **2023**, *15*, 2071. [[CrossRef](#)]
257. Pal, J.; Kankariya, N.; Sanwaria, S.; Nandan, B.; Srivastava, R.K. Control on molecular weight reduction of poly (ϵ -caprolactone) during melt spinning—A way to produce high strength biodegradable fibers. *Mater. Sci. Eng. C* **2013**, *33*, 4213–4220. [[CrossRef](#)] [[PubMed](#)]
258. Hinüber, C.; Häussler, L.; Vogel, R.; Brüning, H.; Werner, C. Hollow poly (3-hydroxybutyrate) fibers produced by melt spinning. *Macromol. Mater. Eng.* **2010**, *295*, 585–594. [[CrossRef](#)]
259. Nazhat, S.; Kellomäki, M.; Törmälä, P.; Tanner, K.; Bonfield, W. Dynamic mechanical characterization of biodegradable composites of hydroxyapatite and polylactides. *J. Biomed. Mater. Res.* **2001**, *58*, 335–343. [[CrossRef](#)] [[PubMed](#)]
260. Kim, M.S.; Kim, J.C.; Kim, Y.H. Effects of take-up speed on the structure and properties of melt-spun poly (L-lactic acid) fibers. *Polym. Adv. Technol.* **2008**, *19*, 748–755. [[CrossRef](#)]
261. Gordeyev, S.; Nekrasov, Y.P. Processing and mechanical properties of oriented poly (β -hydroxybutyrate) fibers. *J. Mater. Sci. Lett.* **1999**, *18*, 1691–1692. [[CrossRef](#)]
262. Yamane, H.; Terao, K.; Hiki, S.; Kimura, Y. Mechanical properties and higher order structure of bacterial homo poly (3-hydroxybutyrate) melt spun fibers. *Polymer* **2001**, *42*, 3241–3248. [[CrossRef](#)]
263. Schmack, G.; Jehnichen, D.; Vogel, R.; Tändler, B. Biodegradable fibers of poly (3-hydroxybutyrate) produced by high-speed melt spinning and spin drawing. *J. Polym. Sci. Part B Polym. Phys.* **2000**, *38*, 2841–2850. [[CrossRef](#)]
264. Iwata, T.; Aoyagi, Y.; Fujita, M.; Yamane, H.; Doi, Y.; Suzuki, Y.; Takeuchi, A.; Uesugi, K. Processing of a strong biodegradable poly [(R)-3-hydroxybutyrate] fiber and a new fiber structure revealed by micro-beam X-ray diffraction with synchrotron radiation. *Macromol. Rapid Commun.* **2004**, *25*, 1100–1104. [[CrossRef](#)]
265. Antipov, E.; Dubinsky, V.; Rebrov, A.; Nekrasov, Y.P.; Gordeev, S.; Ungar, G. Strain-induced mesophase and hard-elastic behaviour of biodegradable polyhydroxyalkanoates fibers. *Polymer* **2006**, *47*, 5678–5690. [[CrossRef](#)]
266. Krins, B. Effect of PHA-material structure on yarn and filament spinning. In Proceedings of the 2nd PHA-Platform World Congress, Cologne, Germany, 22–23 September 2021.
267. Perret, E.; Reifler, F.A.; Gooneie, A.; Chen, K.; Selli, F.; Hufenus, R. Structural response of melt-spun poly (3-hydroxybutyrate) fibers to stress and temperature. *Polymer* **2020**, *197*, 122503. [[CrossRef](#)]
268. Perret, E.; Reifler, F.A.; Gooneie, A.; Hufenus, R. Tensile study of melt-spun poly (3-hydroxybutyrate) P3HB fibers: Reversible transformation of a highly oriented phase. *Polymer* **2019**, *180*, 121668. [[CrossRef](#)]
269. Perret, E.; Reifler, F.A.; Gooneie, A.; Chen, K.; Selli, F.; Hufenus, R. X-ray data about the structural response of melt-spun poly (3-hydroxybutyrate) fibers to stress and temperature. *Data Brief* **2020**, *31*, 105675. [[CrossRef](#)] [[PubMed](#)]

270. Perret, E.; Reifler, F.A.; Gooneie, A.; Hufenus, R. X-ray data from a cyclic tensile study of melt-spun poly (3-hydroxybutyrate) P3HB fibers: A reversible mesophase. *Data Brief* **2019**, *25*, 104376. [CrossRef]
271. Perret, E.; Sharma, K.; Tritsch, S.; Hufenus, R. WAXD, polarized ATR-FTIR and DSC data of stress-annealed poly (3-hydroxybutyrate) fibers. *Data Brief* **2021**, *39*, 107523. [CrossRef]
272. Krishnanand, K.; Deopura, B.L.; Gupta, B. Determination of intrinsic birefringence values of polycaprolactone filaments. *Polym. Int.* **2013**, *62*, 49–53. [CrossRef]
273. Selli, F.; Erdoğan, U.; Hufenus, R.; Perret, E. Mesophase in melt-spun poly (ϵ -caprolactone) filaments: Structure–mechanical property relationship. *Polymer* **2020**, *206*, 122870. [CrossRef]
274. La Mantia, F.; Ceraulo, M.; Mistretta, M.; Morreale, M. Effect of hot drawing on the mechanical properties of biodegradable fibers. *J. Polym. Environ.* **2016**, *24*, 56–63. [CrossRef]
275. La Mantia, F.P.; Ceraulo, M.; Mistretta, M.C.; Morreale, M. Effect of cold drawing on mechanical properties of biodegradable fibers. *J. Appl. Biomater. Funct. Mater.* **2017**, *15*, 70–76. [CrossRef]
276. Mujica-Garcia, A.; Hooshmand, S.; Skrifvars, M.; Kenny, J.M.; Oksman, K.; Peponi, L. Poly (lactic acid) melt-spun fibers reinforced with functionalized cellulose nanocrystals. *RSC Adv.* **2016**, *6*, 9221–9231. [CrossRef]
277. Persson, M.; Lorite, G.S.; Cho, S.-W.; Tuukkanen, J.; Skrifvars, M. Melt spinning of poly (lactic acid) and hydroxyapatite composite fibers: Influence of the filler content on the fiber properties. *ACS Appl. Mater. Interfaces* **2013**, *5*, 6864–6872. [CrossRef] [PubMed]
278. John, M.J.; Anandjiwala, R.; Oksman, K.; Mathew, A.P. Melt-spun polylactic acid fibers: Effect of cellulose nanowhiskers on processing and properties. *J. Appl. Polym. Sci.* **2013**, *127*, 274–281. [CrossRef]
279. Rizvi, R.; Tong, L.; Naguib, H. Processing and properties of melt spun polylactide–multiwall carbon nanotube fiber composites. *J. Polym. Sci. Part B Polym. Phys.* **2014**, *52*, 477–484. [CrossRef]
280. Gilmore, J.; Yin, F.; Burg, K.J. Evaluation of permeability and fluid wicking in woven fiber bone scaffolds. *J. Biomed. Mater. Res. Part B Appl. Biomater.* **2019**, *107*, 306–313. [CrossRef]
281. Kabe, T.; Tsuge, T.; Kasuya, K.-I.; Takemura, A.; Hikima, T.; Takata, M.; Iwata, T. Physical and structural effects of adding ultrahigh-molecular-weight poly [(R)-3-hydroxybutyrate] to wild-type poly [(R)-3-hydroxybutyrate]. *Macromolecules* **2012**, *45*, 1858–1865. [CrossRef]
282. Zhou, M.; Fan, M.; Zhao, Y.; Jin, T.; Fu, Q. Effect of stretching on the mechanical properties in melt-spun poly (butylene succinate)/microfibrillated cellulose (MFC) nanocomposites. *Carbohydr. Polym.* **2016**, *140*, 383–392. [CrossRef]
283. Naeimirad, M.; Krins, B. *Structure-Properties of Melt-Spun Bioplastic Fibers in Correlation with Their Biodegradation Behaviour and Mechanical Performance (PolyBioDeg-101110810)*; European Commission: Brussels, Belgium, 2023.
284. Iwata, T.; Tanaka, T.; Doi, Y. High-Strength Fiber of Biodegradable Aliphatic Polyester and Process for Producing the Same. U.S. Patent WO2006038373, 13 April 2006.
285. Iwata, T.; Hongo, C.; Tamura, M. Biodegradable Polyester Fiber Having Excellent Thermal Stability and Strength, and Method for Producing Same. U.S. Patent US2014/0088288, 27 March 2014.
286. Zhang, J.; Wang, L.; Sun, J.; Jiang, S.; Li, H.; Zhang, S.; Yang, W.; Gu, X.; Qiao, H. A novel hollow microsphere acting on crystallization, mechanical, and thermal performance of poly (3-hydroxybutyrate-co-4-hydroxybutyrate). *Polym. Cryst.* **2021**, *4*, e10204. [CrossRef]
287. Qian, J.; Zhu, L.; Zhang, J.; Whitehouse, R.S. Comparison of different nucleating agents on crystallization of poly (3-hydroxybutyrate-co-3-hydroxyvalerates). *J. Polym. Sci. Part B Polym. Phys.* **2007**, *45*, 1564–1577. [CrossRef]
288. Barham, P.; Keller, A. The relationship between microstructure and mode of fracture in polyhydroxybutyrate. *J. Polym. Sci. Part B Polym. Phys.* **1986**, *24*, 69–77. [CrossRef]
289. Shah, D.T.; Tran, M.; Berger, P.A.; Aggarwal, P.; Asrar, J.; Madden, L.A.; Anderson, A.J. Synthesis and properties of hydroxy-terminated poly (hydroxyalkanoate) s. *Macromolecules* **2000**, *33*, 2875–2880. [CrossRef]
290. Melo-Lopez, L.; Cabello-Alvarado, C.J.; Andrade-Guel, M.L.; Medellín-Banda, D.I.; Fonseca-Florido, H.A.; Avila-Orta, C.A. Synthetic Fibers from Renewable Sources. In *Handbook of Nanomaterials and Nanocomposites for Energy and Environmental Applications*; Springer: Berlin/Heidelberg, Germany, 2020; pp. 1–25.
291. Perret, E.; Hufenus, R. Insights into strain-induced solid mesophases in melt-spun polymer fibers. *Polymer* **2021**, *229*, 124010. [CrossRef]
292. Tanaka, T.; Yabe, T.; Teramachi, S.; Iwata, T. Mechanical properties and enzymatic degradation of poly [(R)-3-hydroxybutyrate] fibers stretched after isothermal crystallization near T_g. *Polym. Degrad. Stab.* **2007**, *92*, 1016–1024. [CrossRef]
293. Aminlashgari, N.; Pal, J.; Sanwaria, S.; Nandan, B.; Srivastava, R.K.; Hakkarainen, M. Degradation product profiles of melt spun in situ cross-linked poly (ϵ -caprolactone) fibers. *Mater. Chem. Phys.* **2015**, *156*, 82–88. [CrossRef]
294. Stevens, E. *Green Plastics, Plastics and the Environment*; Princeton University Press: Princeton, NJ, USA, 2001.
295. Gonsalves, K.; Chen, X.; Cameron, J. Degradation of nonalternating poly (ester amides). *Macromolecules* **1992**, *25*, 3309–3312. [CrossRef]
296. Aaliya, B.; Sunooj, K.V.; Lackner, M. Biopolymer composites: A review. *Int. J. Biobased Plast.* **2021**, *3*, 40–84. [CrossRef]
297. Available online: <https://www.senbis.com/sustainable-products/> (accessed on 20 August 2023).
298. Miranda, C.S.; Ribeiro, A.R.; Homem, N.C.; Felgueiras, H.P. Spun biotextiles in tissue engineering and biomolecules delivery systems. *Antibiotics* **2020**, *9*, 174. [CrossRef]

299. Fan, X.; Keynton, R.S. Fabrication and characterization of biopolymer fibers for 3D oriented microvascular structures. *J. Microeng. Microeng.* **2019**, *29*, 083003. [[CrossRef](#)]
300. Koller, M. Biodegradable and biocompatible polyhydroxy-alkanoates (PHA): Auspicious microbial macromolecules for pharmaceutical and therapeutic applications. *Molecules* **2018**, *23*, 362. [[CrossRef](#)]
301. Andriano, K.P.; Pohjonen, T.; Törmälä, P. Processing and characterization of absorbable polylactide polymers for use in surgical implants. *J. Appl. Biomater.* **1994**, *5*, 133–140. [[CrossRef](#)]
302. Naeimirad, M. Marine degradable fishing net protection. *Technical Textiles*, 4 May; 2023.
303. Li, J.; Lemstra, P.J.; Ma, P. Can high-performance fibers be (come) bio-based and also biocompostable? *Adv. Ind. Eng. Polym. Res.* **2022**, *5*, 117–132. [[CrossRef](#)]
304. Manfra, L.; Marengo, V.; Libralato, G.; Costantini, M.; De Falco, F.; Cocca, M. Biodegradable polymers: A real opportunity to solve marine plastic pollution? *J. Hazard. Mater.* **2021**, *416*, 125763. [[CrossRef](#)] [[PubMed](#)]
305. Naeimirad, M.; Krins, B. Melt-spun high-tenacity marine-degradable filament yarns. In Proceedings of the European Bioplastics Conferece (EBC-23), Berlin, Germany, 12–13 December 2023.
306. Eck, M.; Schwab, S.T.; Nelson, T.F.; Wurst, K.; Iberl, S.; Schleheck, D.; Link, C.; Battagliarin, G.; Mecking, S. Biodegradable High-Density Polyethylene-like Material. *Angew. Chem.* **2023**, *135*, e202213438. [[CrossRef](#)]
307. Liu, Y.; Mecking, S. A synthetic polyester from plant oil feedstock by functionalizing polymerization. *Angew. Chem. Int. Ed.* **2019**, *58*, 3346–3350. [[CrossRef](#)] [[PubMed](#)]
308. Ortmann, P.; Mecking, S. Long-spaced aliphatic polyesters. *Macromolecules* **2013**, *46*, 7213–7218. [[CrossRef](#)]
309. Cristina, J.; de Ilarduya, A.M.; Abdelilah, A.; Yi, J.; Katja, L.; Muñoz-Guerra, S. Copolyesters Made from 1, 4-Butanediol, Sebacic Acid, and d-Glucose by Melt and Enzymatic Polycondensation. *Biomacromolecules* **2015**, *16*, 868–879.
310. Fodor, C.; Golkaram, M.; Woortman, A.J.; van Dijken, J.; Loos, K. Enzymatic approach for the synthesis of biobased aromatic-aliphatic oligo-/polyesters. *Polym. Chem.* **2017**, *8*, 6795–6805. [[CrossRef](#)]
311. Jiang, Y.; Loos, K. Enzymatic synthesis of biobased polyesters and polyamides. *Polymers* **2016**, *8*, 243. [[CrossRef](#)]
312. Biodegradation of biopolymeric fibers. *Man Made Fibers Int.* **2023**, *73*, 13.
313. Ghosh, K.; Jones, B.H. Roadmap to biodegradable plastics—Current state and research needs. *ACS Sustain. Chem. Eng.* **2021**, *9*, 6170–6187. [[CrossRef](#)]

Disclaimer/Publisher’s Note: The statements, opinions and data contained in all publications are solely those of the individual author(s) and contributor(s) and not of MDPI and/or the editor(s). MDPI and/or the editor(s) disclaim responsibility for any injury to people or property resulting from any ideas, methods, instructions or products referred to in the content.